Performance of Wireless Sensor Networks with Radio-Frequency Recharging of Sensor Nodes

by

Mohammad Shahnoor Islam Khan
M.Sc. in Computer Science, Ryerson University, Toronto, Canada, 2012
B.Sc. in Computer Engineering and Engineering, Bangladesh University of Engineering and Technology
Dhaka, Bangladesh, 2001

A dissertation
presented to Ryerson University

in partial fulfillment of the
requirements for the degree of
Doctor of Philosophy
in the Program of
Computer Science

Toronto, Ontario, Canada, 2016

Author's Declaration

I hereby declare that I am the sole author of this dissertation. This is a true copy of the dissertation, including any required final revisions, as accepted by my examiners.

I authorize Ryerson University to lend this dissertation to other institutions or individuals for the purpose of scholarly research.

I further authorize Ryerson University to reproduce this dissertation by photocopying or by other means, in total or in part, at the request of other institutions or individuals for the purpose of scholarly research.

I understand that my dissertation may be made electronically available to the public.

Performance of Wireless Sensor Networks with Radio-Frequency Recharging of Sensor Nodes

Radio-frequency (RF) recharging of sensor nodes is a promising way to minimize maintenance and prolong the operational life of wireless sensor networks. This thesis investigates several aspects of RF recharging that affect the performance of such networks, such as the interplay between RF recharging and data communications, the need for reliable recharging, the impact of service policy, and some techniques for extending the network lifetime by zoning. We first consider a Medium Access Control (MAC) protocol that uses polling in conjunction with a 1-limited and E-limited service policies. To evaluate the network lifetime, we have developed a probabilistic model of the energy depletion process within the proposed round-robin MAC protocol, while packet delays and throughput are evaluated through a queuing model. Our results indicated that the period between consecutive recharging pulses is limited by the distance between the most distant sensor node and the master node or station which sends out recharging pulses. To increase this period, we propose a zoning scheme in which nodes are logically grouped into circular zones centered at the master, so that nodes in a given zone send their data to their neighbors in the next closer zone which act as relays. A probabilistic analysis of this scheme confirms that zoning extends the time interval between recharge pulses and leads to equalization of node lifetimes, but also limits the available data transmission bandwidth. Finally, we have discussed a simple yet efficient algorithm for dividing the nodes into zones, and evaluated its computational complexity.

Acknowledgments

There are many people to whom I owe credit for this thesis. Without the support and encouragement of these wonderful people it would not be possible to finish this work.

I dedicate this thesis to my family: my wife Farzana and my son Farhaan, and my parents who supported me unconditionally and have been the source of motivation and inspiration for me and made my time more enjoyable during these years.

To my beloved wife and son for their support and encouragement.

Contents

List of Figures

List of Tables

Chapter 1

Introduction

1.1 The problem

Wireless sensor networks (WSNs) are often expected to perform for prolonged periods of time without human intervention which is costly and tedious, and sometimes even impossible [31]. As one of the most frequent reasons for maintenance is replacement or manual recharging of batteries, automatic recharging of node batteries can significantly extend the WSN lifetime [36].

Recharging may be accomplished using energy harvesting from the network surrounding [12], which is unreliable since there is no guarantee that the environment will be capable of supplying the required amount of energy when needed. Alternatively, node batteries may be recharged through radio frequency (RF) pulses [1] emitted by the network coordinator or base station [36, 37], which results in more predictable operation since the energy increment provided by a single recharging pulse depends only on the attenuation of wireless signal between the coordinator and the node.

In this case, recharging may occur in periodic intervals or on demand, when one or more sensor nodes report that their energy source is depleted beyond a predefined threshold. Such recharging is more reliable (provided that the coordinator's power source is reliable and, preferably, not dependent on recharging itself), and the energy increment ob-

tained in this manner can be tailored to the needs of individual nodes; in fact, it mostly depends on the attenuation of the wireless signal between the coordinator and the nodes in the network. However, if network nodes are equipped with a single antenna (which is often done for simplicity and cost effectiveness) network operation is not possible during the recharging process regardless of the RF bands in which normal operation and recharging are performed. As the result, the interplay between normal operation and recharging must be investigated in detail. In particular, achieving both maintenance-free operation and the desired level of communications performance necessitates a carefully designed and thoroughly evaluated medium access control (MAC) protocol.

1.2 Thesis contents and contributions

The focus of this thesis can be succinctly stated as the design and performance analysis of polling based MAC protocols for wireless sensor networks that allow in-band recharging of nodes in an adaptive, on-demand fashion. We will use probabilistic analysis and queuing theory in order to accurately model and evaluate the behavior of a number of MAC protocols. We will investigate the behavior of MAC protocols in a number of different scenarios that focus on strategies for reducing the energy consumption and increasing the interval between successive recharge pulses which disrupt regular data communications. These strategies include different service policies (1-limited and E-limited) [33], coordinated node sleep [21], and zoning and relaying [28].

The main contributions can be listed as follows:

1. Design and performance analysis of a round-robin MAC protocols with 1-limited and E-limited service policies, taking into account the duration of recharging pulse and varying network load.

2. Performance analysis of polling based MAC protocol with on-demand recharging, with provisions for relaying recharge requests in order to achieve reliable recharging.

3. Performance analysis of polling based MAC protocol in the wireless sensor network where nodes sleep for prolonged periods of time in order to save energy.

4. Performance analysis of a MAC protocol that uses zoning and relaying in order to balance the energy consumption of nodes at different distances from the coordinator node.

5. Finally, algorithms to achieve the allocation of nodes into zones in order to make the zoning and relaying algorithm possible.

Many of those contributions are published, or accepted for publication, in reputable international journals, or presented at various conferences. A list of my papers can be found before the main bibliography.

1.3 Thesis organization

The thesis is structured as follows.

Chapter 2 presents related work.

Chapter 3 discusses the simple poling-based MAC protocol and presents the probabilistic model that allows us to evaluate its performance.

Chapter 4 discusses the performance of the MAC protocol under E-limited scheduling.

Chapter 5 discusses the operation of the MAC protocol in the scenario in which nodes transmit their packets and then go to sleep for a prolonged period of time in order to conserve energy.

Chapter 6 presents a modified MAC protocol in which nodes are divided into circular zones, and packets are relayed form one zone to the next closer one, instead of directly from a node to the coordinator.

Chapter 7 discusses efficient algorithms for dividing the sensor network into a specified number of zones.

Finally, Chapter 8 concludes the thesis.

A list of our papers precedes the main bibliography.

Chapter 2

Related Work

2.1 Related Work

The MAC protocols proposed so far can be categorized in two large groups: variants of CSMA protocols, on the one hand, and polling based protocols, on the other [5]. ALOHA-like protocols with continuous energy harvesting have been proposed as well [9]. General treatment of energy replenishment which includes battery replacement or generic recharging was presented in [15]. A MAC protocol that explicitly requests energy replenishment through a subsequent RF pulse has been reported in [26]. Finally, a MAC protocol in which recharging is done through a high power RF pulse but in a different band so that data transmission is never interrupted, was described and analyzed in [22].

Generic mathematical model of energy replenishment which includes battery replacement or generic recharging was presented in [15]. The work focuses on generic concepts of 'battery replacement' or 'recharging' which occurs at a certain replenishment rate, rather than on harvesting the energy from the environment or recharging through RF pulses.

Energy harvesting offers a theoretically infinite but, at the same time, unreliable power source [8], and energy allocation must be carefully planned and optimized to ensure uninterrupted operation of the network.

A number of MAC protocols for WSNs have been designed for energy harvesting from

the environment, for example using solar batteries or fluorescent lamps, both of which offer nearly continuous energy replenishment [24]. Energy harvesting is usually assumed to occur independently of data communications, although some approaches do allow for the possibility of the interplay between wireless communication protocols and RF energy transfer.

A comparative analysis of a number of energy harvesting algorithms, including practical measurements, was reported in [7].

Another detailed study of a number of medium access protocols, including TDMA, framed-ALOHA and Dynamic Framed ALOHA, for networks with continuous energy harvesting was reported in [9]. The paper assumes that the power sources of individual sensor nodes use continuous energy harvesting from ambiental sources such as sunlight, fluorescent lamps, and even the heat from heat sinks of CPUs in desktop computers.

While RF energy transfer does extend the useful lifetime of sensor networks almost to the point of making them 'immortal' [36], regular data communications in a wireless sensor network will be affected to some extent by the activities related to energy transfer [26]. Yet detailed studies of the interaction between the two are still scarce, and more work is needed to decide on the optimal scheduling of energy transfers and the adjustment of network parameters needed to account for these interactions. This interaction may be avoided if recharging uses a different RF band from data communications, sometimes referred to as 'heterogeneous frequency harvesting' [27], but this solution is more expensive due to the need for two RF transceivers and two antennas.

A number of CSMA- and polling-based medium access protocols have been analyzed and compared using both analytical modeling and simulation in [5], and a polling-based protocol was found to offer better performance than its CSMA-based counterparts.

Sleep-wake policies that minimize a hybrid performance measure based on the mean queue length and mean data loss rate are discussed in [11].

We note that our earlier work in this area has considered another polling MAC in which recharging occurs in a different RF band and, thus, does not interfere with data commu-

nications [22]. A generic model for energy replenishable sensor nodes which include battery replacement or generic recharging was presented in [15]. The work mainly focuses on generic recharging that happens at a certain replacement rate, rather than on energy harvesting from the environment or through RF recharging. More often than not, energy harvesting and data communication occur independently but some approaches consider the interplay between them as well [29]. Energy harvesting draws from a theoretically infinite power source but it is unreliable [8] due to its dependence on ambient conditions. This means that energy expenditure and subsequent use must be planned and carefully optimized in order to guarantee uninterrupted network operation. A comparative analysis of different energy harvesting techniques, including practical measurements, has been outlined in [7].

2.2 Related work

Generic mathematical model of energy replenishment which includes battery replacement or generic recharging was presented in [15]. The work focuses on generic concepts of 'battery replacement' or 'recharging' which occurs at a certain replenishment rate, rather than on harvesting the energy from the environment or recharging through RF pulses.

Energy harvesting offers a theoretically infinite but, at the same time, unreliable power source [8], and energy allocation must be carefully planned and optimized to ensure uninterrupted operation of the network.

A number of MAC protocols for WSNs have been designed for energy harvesting from the environment, for example using solar batteries or fluorescent lamps, both of which offer nearly continuous energy replenishment [24]. Energy harvesting is usually assumed to occur independently of data communications, although some approaches do allow for the possibility of the interplay between wireless communication protocols and RF energy transfer.

A comparative analysis of a number of energy harvesting algorithms, including practical measurements, was reported in [7].

Another detailed study of a number of medium access protocols, including TDMA, framed-ALOHA and Dynamic Framed ALOHA, for networks with continuous energy harvesting was reported in [9]. The paper assumes that the power sources of individual sensor nodes use continuous energy harvesting from ambiental sources such as sunlight, fluorescent lamps, and even the heat from heat sinks of CPUs in desktop computers.

While RF energy transfer does extend the useful lifetime of sensor networks almost to the point of making them 'immortal' [36], regular data communications in a wireless sensor network will be affected to some extent by the activities related to energy transfer [26]. Yet detailed studies of the interaction between the two are still scarce, and more work is needed to decide on the optimal scheduling of energy transfers and the adjustment of network parameters needed to account for these interactions. This interaction may be avoided if recharging uses a different RF band from data communications, sometimes referred to as 'heterogeneous frequency harvesting' [27], but this solution is more expensive due to the need for two RF transceivers and two antennas.

A number of CSMA- and polling-based medium access protocols have been analyzed and compared using both analytical modeling and simulation in [5], and a polling-based protocol was found to offer better performance than its CSMA-based counterparts.

Sleep-wake policies that minimize a hybrid performance measure based on the mean queue length and mean data loss rate are discussed in [11].

We note that our earlier work in this area has considered another polling MAC in which recharging occurs in a different RF band and, thus, does not interfere with data communications [22].

RF recharging may extend the lifetime of sensor nodes to effectively render them 'immortal' [25], but normal data operation can be affected to a large extent by the actions related to energy transfer as they require a temporary suspension of data communication activities – i.e., a vacation period [35]. Vacation period has significant impact on the queuing delay as well [39]. To reduce mean queue length and data loss, a MAC-based sleep-awake policy was proposed in [11]. However, more work is required to figure out the optimal

scheduling of energy transfers and the adjustment of different parameters accountable for these interactions.

Several CSMA-based MAC protocols have been proposed to prolong battery lifetime for WSNs [38] [10]. These protocols mainly focus on energy conservation by enabling sleeping of one node while others are transmitting data. However, such MAC protocols can't guarantee per-node fairness and may result in higher latency time for some of the nodes. On the other hand, polling-based MAC protocols improve real time performance and provide fairness among nodes by implementing different types of scheduling [40].

Evaluation of MAC protocols with provisions for recharging has been done mostly for energy harvesting using solar batteries or fluorescent lamps which offer continuous energy replenishment. Several analytical and simulation-based models have been described for both CSMA- and polling-based MAC protocols [5][16]. ALOHA-like protocols with continuous energy harvesting have been proposed as well [9]. these results show that polling-based MAC protocols outperform CSMA-based ones in terms of network performance.

Periodic recharging of sensor nodes is a promising way to minimize maintenance and prolong the operational life of wireless sensor networks (WSNs) [5]. Recharging can use energy from the environment in a process commonly referred to as 'energy harvesting' [12], or it can be performed via high energy pulses from the network master or base station [26]. The former approach does not require an external power source with appropriate capacity, but the latter offers greater reliability and controllability as it does not depend on the availability of sufficient energy in the environment to replenish the nodes' power source when needed. On account of this, RF recharging is gaining acceptance in recent years [36, 37].

Two main issues determine the performance of RF recharging. First, it may take place periodically, in regular intervals determined beforehand, or on-demand, i.e., when a sensor node reports that its available energy has dropped below a predefined threshold value. The former approach is simpler, but the frequency of recharging may be difficult to adjust: doing it too frequently may be inefficient, while doing it too seldom can incur death of

some nodes due to depletion of their power source.

Second, RF recharging and regular data communications can use the same RF band or two different RF bands. The use of a single RF band is attractive on account of hardware simplicity, but careful tailoring of the protocol and detailed analysis of its performance are needed to assess the impact of the interplay between recharging and data communications. However, using different bands requires two antennas and two RF transceivers [26] but allows uninterrupted data communications throughout recharging [22].

Performance analysis of MAC protocols along with recharging has focused on CSMA approach and its many variants [5], although ALOHA-like protocols with continuous energy harvesting have been developed and analyzed as well [9]. General treatment of energy replenishment including battery replacement or conventional recharging was presented in [15]. A MAC protocol that explicitly requests energy replenishment through a subsequent RF pulse has been studied in [26]. Performance analysis for MAC protocol has been investigated for uninterrupted transmission in which recharging is done through a high power RF pulse in separate band [22].

Zoning was first described in an analysis of distance-dependent energy exhaustion of nodes in a sensor field [28]; however, the paper did not elaborate on the MAC protocol. Zoning was also proposed in the context of separation of local and global traffic [14], but without considering the impact of distance on energy consumption or replenishment rate of nodes in different zones.

Chapter 3

Performance Networks with RF Recharging of Nodes

In this chapter we begin our analysis of polling-based MAC protocols for wireless sensor networks with RF recharging. We consider the protocol that uses round robin, 1-limited service policy. It allows nodes to explicitly request recharging when their energy level drops below a predefined threshold. As nodes are equipped with a single antenna, recharging will interrupt data communications since both occur in the same RF band, similar to the solution described in [26]. However, the sensing process is active all the time and data packets are being collected even while recharging. The performance of the network using this protocol is then evaluated through probabilistic analysis and a dedicated queuing model, with a focus on the evaluation of the battery depleting process and the impact of recharging interval on data communications in the network.

3.1 Polling MAC and recharging

3.1.1 MAC protocol

We assume the network consists of m nodes, one of which – hereafter referred to as the coordinator – is equipped with a suitable power source that allows it to emit RF recharging pulses. The remaining $m - 1$ nodes are identical nodes with a built-in sensor unit used to sense and generate data which are then sent to the coordinator; they are also equipped with a RF transceiver that can recharge the on-board battery from the recharging pulse.

We consider a round robin polling MAC protocol where the coordinator polls each node sequentially by sending a polling (POLL) packet, similar to the MAC used in Bluetooth [20]. The MAC address of the recipient is tagged in the header of the POLL packet. Occasionally, the coordinator will send a downlink data (DDATA) packet instead of a POLL one; such packets may be sent to a specific node, or to all nodes as a broadcast. Each node listens to all POLL or DDATA packets to check whether it is the recipient, in which case it replies with an uplink DATA packet or, if it has no data to send, an empty (NULL) packet. When polled, each node is allowed to send a single packet of unit time length. We will refer to the time elapsed between two successive visits to any node in the target network as the polling cycle.

The network layout is depicted in Fig. 3.1; note that different nodes are located at different distances from the coordinator.

Bit and packet errors are quantified by their respective probabilities p_{BER} and $p_{PER} = 1 - (1 - p_{BER})^S$, where S is the total number of bits in a packet. If a DATA packet is correctly received, a dedicated field of the next POLL or DDATA packet header towards the same recipient node will contain an acknowledgement. In the absence of acknowledgement, the node will repeat the last packet sent, up to n_{rt} times.

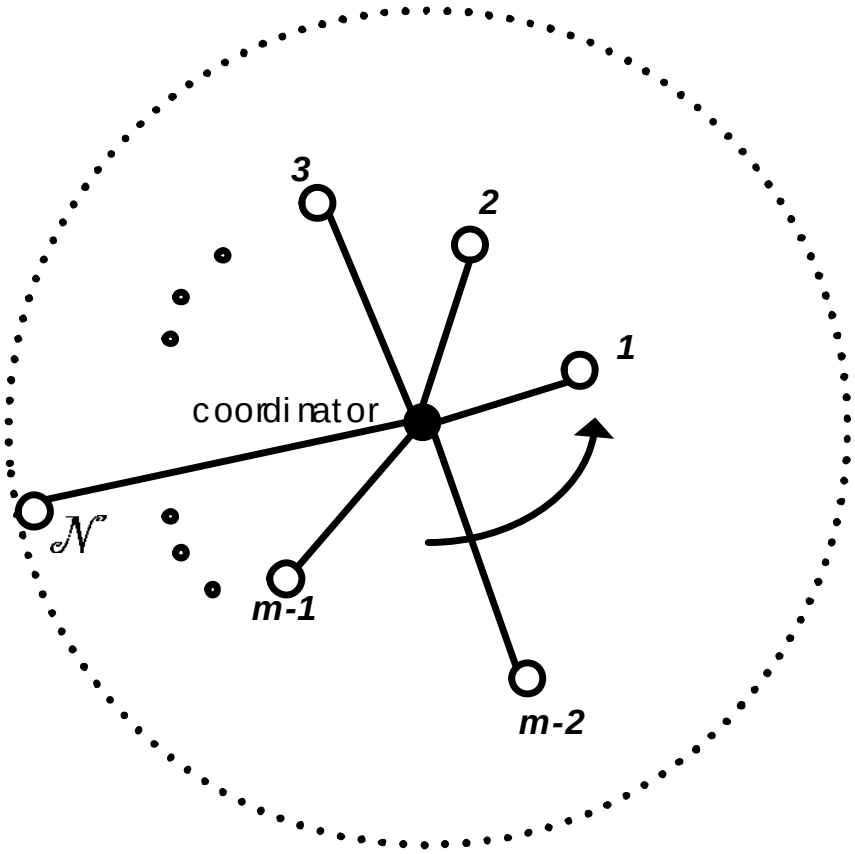

Figure 3.1: Logical representation of the network.

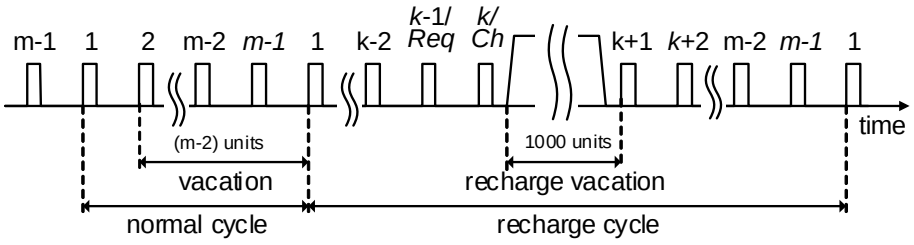

Figure 3.2: Format of network operation and recharging.

3.1.2 Recharging process

We assume that each node has the same initial energy level of E_{max}, equal to its battery capacity, which can't be exceeded when recharged. During data communications period,

energy is used to support sensing, listening to and/or receiving POLL and DDATA packets, and transmitting (and, possibly, retransmitting) DATA and NULL packets. The rate of energy expenditure will depend on packet generation rate λ, retransmit limit n_{rt}, bit error rate p_{BER}, and size of the network, i.e., the number of nodes m.

When the available energy has dropped below a predefined threshold, the node requests a recharge via a dedicated information field in the header of its DATA or uplink NULL packet. The coordinator will then announce the upcoming recharge pulse in its next POLL or DDATA packet. The recharging pulse follows the announcement after a suitable timeout which allows the nodes to activate the recharging circuitry. Upon recharging, the network resumes normal operation. This process is schematically depicted in Fig. 3.2.

The recharging pulse has a power P_c and lasts for T_c time units. The received RF power at node i is calculated using the Friis' transmission equation : $P_{ri} = \eta G_{ri} G_t \left(\frac{\lambda_w}{4\pi R_i}\right)^2 P_c$, where η is the coefficient of efficiency of RF power conversion, G_{ri} and G_t are the antenna gains at the receiver (i.e., node) and transmitter (i.e., coordinator), respectively, λ_w is the wavelength, and $R_i \gg \lambda_w$ is the distance between the coordinator and node i [6][30]. The maximum possible energy increment for node i is, then, $\Delta E_i = P_{ri} \cdot T_c$, and the node energy level will be replenished to the level $\min(E_{max}, E_{th} + \Delta E_i)$. This process is schematically shown in Fig.3.3(a).

Let us now investigate the behavior of the network between two successive recharging events. Under uniformly distributed traffic load, fixed network size and constant reliability, the energy expenditure rate will vary due to randomness of packet retransmission, but the mean time to reach the energy threshold will be the same for each node. The first recharging request will be issued by the node which has done the maximum number of transmission cycles. Upon first recharging, the energy level of node i will be $\min(E_{max}, E_{th} + \Delta E_i)$. The node at the greatest distance from the coordinator, labelled with $\mathcal{N}$, will get minimum energy due to the maximum path loss of the RF signal strength. This node will be recharged minimally during each of the upcoming recharging periods. Traffic load is uniformly distributed among the nodes. Energy expenditure for transferring DATA and NULL packets

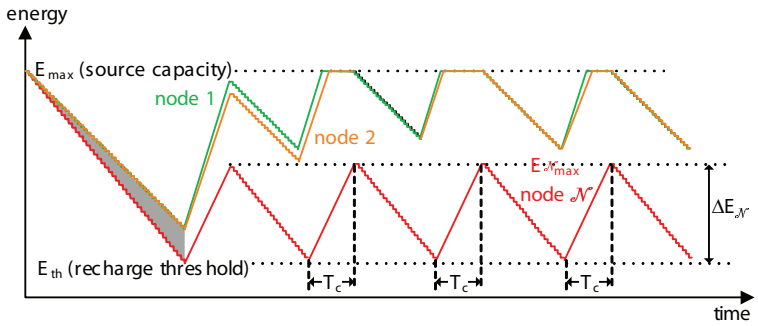

(a) Energy levels during recharging and normal operation.

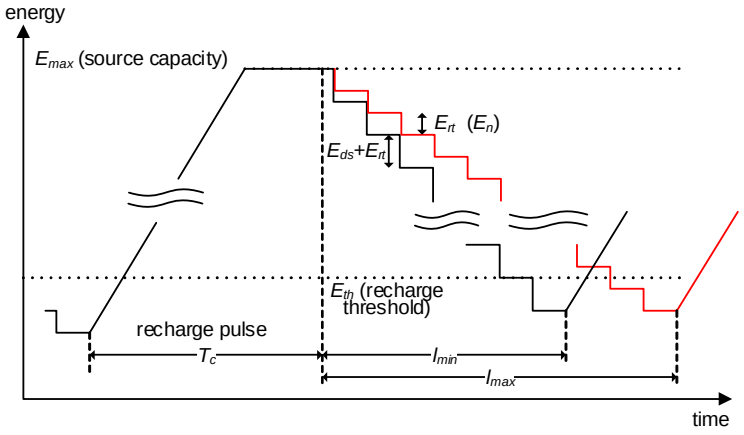

(b) Energy levels – initial detail.

Figure 3.3: Pertaining to energy expenditure and replenishment.

will be almost similar for each node over longer period of time. But all the nodes are not recharged equally as they are located in different distances from the coordinator. As the maximum distant node gets minimum energy, its energy will be used up and the node will suffer energy outage first compared to the other nodes.

In the second and subsequent recharging cycles, node $\mathcal{N}$ will be the one to issue recharging requests. Other nodes will receive larger energy increments in the recharging process: not only their energy will never fall to the threshold value, they will be recharged to capacity in each recharging cycle.

The initial operation cycle is shown in more detail in Fig. 3.3(b). Due to the randomness of packet loss, period between two successive recharging is a random variable which can

be described with a suitable probability distribution. Energy expenditure for a polling cycle will be obtained by counting the number of cycles needed for the farthest node $\mathcal{N}$ to use up its energy budget. Consequently, we need to find the joint probability distribution of the number of polling cycles and consumed energy during this period.

3.2 Recharging model

Table 3.1 shows notation used in this section to describe the different equations and algorithm. Energy consumption corresponding to atomic activities of a node are listed in Table 3.2. Using these values we can calculate the energy consumption of a node during a polling cycle; this value depends on the type of activity that the node engages in a given cycle.

- Upon receiving a POLL packet, the node may have data in its buffer, which occurs with the probability of ρ_b, hereafter referred to as the effective utilization of the node (its actual value will be calculated later).

- Transmission of a DATA packet uses up energy E_{poll} to receive the POLL packet and energy E_{dt} for the actual transmission.

- If the data has been sensed in the current polling cycle, E_{ds} of energy was used to sense that data, otherwise the data still resides in the buffer from a previous polling cycle.

- If the node has no data to send (which occurs with the probability of $1 - \rho_b$), it did not use energy for sensing, and will use up energy E_{poll} to receive the POLL packet and energy E_{nt} for the actual transmission of a NULL packet.

- Finally, the term $(m-2)E_h$ corresponds to the fact that, in each cycle, the node must listen to the headers of POLL packets addressed to $m-2$ other nodes (i.e., all nodes except itself and the coordinator).

Table 3.1: Table of Notations.

Symbol	Definition
p_{PER}	probability of error in a received packet.
E_{max}	maximum energy capacity of a node
E_{th}	threshold energy level of a node below which a node sends energy request.
$\Delta E_i(i)$	Energy gain of a node i after single recharging by the coordinator
$sum_{mini}(i)$	coefficient of $x^i\sigma^j$ including equivalent energy units conversion.
$sum_{small}(i)$	coefficient of x^i including equivalent energy units conversion.
$E_{X_p(x,y,\sigma,t)}$	Joint PGF function for different energy units (sensing packet, transmitting DATA and NULL packets) time cycles with in a single re-charging period.
$E_{Xv(v,t)}$	PGF function after converting energy variables x, y and σ into a single unit v.
τ_{max}	maximum number of packets sent between successive re-charging points.
τ_{min}	minimum number of packets sent between successive re-charging points.
η_Δ	representing floating point energy value $\Delta E_{\mathcal{N}}$ to the nearest integer value which is multiples of E_{ds}.
η_{rt}	ratio of DATA packet transmission energy and DATA sensing energy.
η_n	ratio of NULL packet transmission energy and DATA sensing energy.
$T(t)$	PGF of polling cycles for which energy expenditure of a node is exceeded.
$E[T]$	mean number of polling cycles between consecutive recharging points.
$V_{prd}(x)$	vacation a node enjoys while other $(m-2)$ nodes are in service.
$V_{rcg}(x)$	vacation while the coordinator sends recharging pulse.
$V(x)$	total vacation period enjoyed by a node.
$E[V]$	average vacation period.
ρ_b	total offered load.
$\Pi(x)$	number of packets left in the queue after the departing packet without reliability.
$\Pi_g(x)$	number of packets left in the queue after the departing packet with reliability.
$W*(s)$	Packet waiting time in the queue.

Energy consumption of a single node during a polling cycle is summarized in Table 3.3.

Table 3.2: Energy consumption of atomic activities.

Activity	Variable
data sensing	E_{ds}
receiving a POLL packet	E_{poll}
listening to the header of a POLL packet	E_h
transmission of a DATA packet	E_{dt}
transmission of a NULL packet	E_{nt}

Table 3.3: Energy consumption at the level of the polling cycle.

Node activity in the cycle	Amount
first attempt to transmit a DATA packet	$E_t = E_{ds} + E_{poll} + (m-2)E_h + E_{dt}$
attempt to re-transmit a DATA packet	$E_{rt} = E_{poll} + (m-2)E_h + E_{dt}$
transmitting a NULL packet	$E_n = E_{poll} + (m-2)E_h + E_{nt}$

We are now equipped to develop the analytical model of recharging period along with the delay model at the node queue. For simplicity, we will assume uniform distribution of load among the nodes.

Probability generating function (PGF) for the energy consumption along with the number of polling cycles required for a single DATA packet transmission is

$$Ep(x,y,t) = \frac{xyt\sum_{k=0}^{n_{rt}}(xt)^k {p_{PER}}^k}{\sum_{k=0}^{n_{rt}}{p_{PER}}^k} \tag{3.1}$$

where variables y, x, and t refer to energy consumption for data sensing, transmission of a DATA packet, and the polling cycle of the network, respectively. Numerator in Eq. (3.1) explains that a DATA packet consumes 1 unit of sensing energy (y) and 1 unit of transferring energy (x) in 1 period of time (t) with $(1 - p_{PER})$ probability value for successful transmission. For unsuccessful attempt, first re-transmission will be initiated successfully at

$t = 2$ time cycle with $((1 - p_{PER})p_{PER})$ probability value. But this time only transmission energy x will be used up as sensing is not required any more for re-transmission. If the first re-transmission attempt is unsuccessful, second successful re-transmission will take place at $t = 3$ time with $((1 - p_{PER})p_{PER}^2)$ probability value. This process of re-transmission attempts will be repeated for every unsuccessful attempt till number of re-transmission for a single packet reaches n_{rt} value. Then the packet will be dropped. Denominator in (3.1) normalizes (summation of all probabilities values is equal to 1) the PGF function. This PGF function is a combination of energy units and time unit.

To account for the cycles where a NULL packet is sent instead of a DATA one, the above PGF must be modified to read

$$E_{all}(x, y, \sigma, t) = \rho_b Ep(x, y, t) + (1 - \rho_b)\sigma t \tag{3.2}$$

where the additional variable σ denotes the energy consumption for the transmission of a NULL packet.

Upon recharge, the energy of the furthest node $\mathcal{N}$ will be well above the threshold value: $E_{max}^{\mathcal{N}} = E_{th} + \Delta E_{\mathcal{N}}$. Due to stochastic character of data sensing and the impact of noise and interference on packet transmission and retransmission, the energy of this node will drop to the threshold level at a random time between $\tau_{min} = E_{max}^{\mathcal{N}}/(E_{ds} + (n_{rt} + 1)E_{rt})$ and $\tau_{max} = E_{max}^{\mathcal{N}}/E_n$ packet transmissions. The above limits depend on the intensity of traffic, transmission errors which lead to retransmission, and maximum number of retransmission attempts allowed. The lower limit, τ_{min}, corresponds to the case where the node has some data to send at all times and each of the packets takes a maximum number n_{rt} retransmissions to be successfully sent, whereas the upper limit, τ_{max}, is reached when the node buffer is empty throughout the recharge cycle, so that the node sends only NULL packets. We note that the probability of reaching either of the limits is small but non-zero nevertheless. Total number of packet transmissions within two consecutive charging point varies $(\tau_{max} - \tau_{min} + 1)$ different ways.

The next step is to combine the possible numbers of DATA and NULL packet transmissions, as well as DATA packet retransmissions, to form a joint probability distribution of total energy expenditure and required number of polling cycles between successive recharging pulses. The resulting PGF is

$$E_{X_p(x,y,\sigma,t)} = \frac{\sum_{k=\tau_{min}}^{\tau_{max}} E_{all}(x,y,\sigma,t)^k}{\tau_{max} - \tau_{min} + 1} \tag{3.3}$$

In (3.3) we have applied convolutions (range of the convolution is from τ_{min} to τ_{max}) on PGF of single packet transmission k times where k is total number of transmitted packets in a re-charging period. These convolutions (range between τ_{min} and τ_{max}) are uniformly distributed.

To simplify the link to energy consumption values from Tables 3.2 and 3.3, it is convenient to normalize the energy for transmitting a DATA or NULL packet to the amount needed for sensing a single data value, i.e.,

$$\eta_{rt} = E_{rt}/E_{ds} \tag{3.4}$$

$$\eta_n = E_n/E_{ds} \tag{3.5}$$

and map $x = y^{\eta_{rt}}$ and $\sigma = y^{\eta_n}$ in (3.3). Since data packet transmission (described by the variable x) requires the highest energy value, all the coefficients of energy units are collected, combined and finally rounded up to the next integer value for obtaining greater accuracy; the new combined energy unit, dimensionally equal to y, will be labeled v. The actual process of merging the energy variables x, σ and y into variable v is shown in Algorithm 1.

The final PGF $E_{Xv(v,t)}$ contains a single energy variable v with an integer multiple of E_{ds} as its power, and a cycle variable t. Minimum and maximum degrees of v in $E_{Xv(v,t)}$ are expressed as d_v^{min} and d_v^{max}, respectively. As described earlier, for uniform traffic

Algorithm 1: Energy transformation for each time unit within the PGF function.

Data: $E_{Xp(x,y,\sigma,t)}$, transmission ratios η_{rt} and η_n

Result: PGF of combined energy usage, in units of E_{ds}, and the number of polling cycles between successive recharging periods.

Calculate minimum d_x^{min} and maximum d_x^{max} degree of variable x in $E_{Xp(x,y,\sigma,t)}$;
for $i \leftarrow d_x^{min}$ **to** d_x^{max} **do**
    Get coefficient $x(i)$ of x^i in $E_{Xp(x,y,\sigma,t)}$ ($x(i)$ is a polynomial on y, σ and t excluding the variable x) ;
    Evaluate minimum d_σ^{min} and maximum d_σ^{max} degree for variable σ in $x(i)$;
    for $j \leftarrow d_\sigma^{min}$ **to** d_σ^{max} **do**
        Get coefficient $x\sigma(i,j)$ for σ^j in $x(i)$ ($x\sigma(i,j)$ is polynomial on y and t) ;
        Find minimum d_y^{min} and maximum d_y^{max} degree of variable y in $x\sigma(i,j)$;
        for $k \leftarrow d_y^{min}$ **to** d_y^{max} **do**
            Find coefficient $x\sigma y(i,j,k)$ of y^k in $x\sigma(i,j)$ ($x\sigma(i,j)$ is a polynomial on t only);
            Combined coefficient of energy x, σ and y consumption;
            $E_{com}(i,j,k) = \lceil i \cdot \eta_{rt} + j \cdot \eta_n + k \rceil$;
            form new element of new polynomial as $x\sigma y(i,j,k) v^{E_{com}(i,j,k)}$
        Third level summation on unified energy units
        $sum_{mini}(i,j) \leftarrow \sum_{k=d_y^{min}}^{d_y^{max}} x\sigma y(i,j,k) u^{E_{com}(i,j,k)}$;
    Second level summation $sum_{small}(i) \leftarrow \sum_{j=d_\sigma^{min}}^{d_\sigma^{max}} sum_{mini}(i,j)$;
New PGF for on combined energy unit as $E_{Xv(v,t)} \leftarrow \sum_{i=d_x^{min}}^{d_x^{max}} sum_{small}(i)$;

distribution, recharging requests will be triggered by the node $\mathcal{N}$ that is farthest away from the coordinator. Energy increment can be expressed through the ratio $\eta_\Delta = \Delta E_\mathcal{N}/E_{ds}$, similar to (3.4) and (3.5).

The condition that the energy resource is exceeded can be described with the polynomial

$$Tr(t) = \sum_{i=\eta_\Delta}^{d_v^{max}} f_t(i) \tag{3.6}$$

where $f_t(i)$ (which is polynomial in t) denotes the coefficients of the PGF $E_{Xv(v,t)}$ associated with energy variable v and its power i:

$$f_t(i) = \text{coeff}(E_{Xv(v,t)}, v, i) \tag{3.7}$$

Since variable t denotes the number of polling cycles, $Tr(t)$ represents the conditional PGF for the number of polling cycles required for which energy expenditure of the furthest node will be exceeded. To qualify as a probability distribution of the number of polling cycles between two successive recharging requests, $Tr(t)$ must be unconditioned to

$$T(t) = \frac{Tr(t)}{Tr(1)} \tag{3.8}$$

Mean number of polling cycles between two successive recharging requests is, then, $E[T] = T'(1)$. Since the proposed 1-limited MAC protocol supports only single packet transmission in a polling cycle, the probability of recharge is as $P_r = \frac{1}{E[T]}$.

3.3 Queuing and vacation model

The MAC protocol described above utilizes round robin scheduling of nodes with 1-limited service policy. Therefore, it can be modeled as a M/G/1 gated limited system with vacations [33].

In this scenario, the vacation has two components. First of them, cyclical or periodical vacation, is due to the transmission and reception of packets by other nodes in a polling cycle. This vacation consists of service times of the other $m-2$ nodes, i.e., it excludes the target node and the coordinator, and its PGF is

$$V_{prd}(x) = (\rho_b G_{up}(x)x + (1-\rho_b)x^2)^{m-2} \tag{3.9}$$

Second type of vacation is the vacation caused by recharging (during which no data trans-

mission can take place), and its PGF is

$$V_{rcg}(x) = P_{rt}x^{T_c} + (1 - P_{rt}) \tag{3.10}$$

Combined PGF of the total vacation can be calculated as

$$V(x) = V_{rcg}(x)V_{prd}(x) \tag{3.11}$$

Mean and standard deviation of the total vacation are

$$E[V] = V'(1) \tag{3.12}$$

$$V_{sd} = \sqrt{(V''(1) - (V'(1))^2 + V'(1))} \tag{3.13}$$

We assume that POLL, DATA, and NULL packets last for one unit time slot each. Data packets are generated by sensing at a rate of λ per node, following a Poisson process. PGFs for uplink (DATA and NULL) packets and downlink (POLL) packets are $G_{up}(x)$ and $G_{dp}(x) = x$, respectively. Total mean packet time for a node (total denoting both uplink and downlink together) is $G'_{up}(1) + G'_{dp}(1)$. Offered load for each node is, then, $\rho = \lambda(G'_{up}(1) + G'_{dp}(1))$. However, the actual load will be higher due to vacations:

$$\rho_v = \rho + \lambda E[V] \tag{3.14}$$

where $E[V]$ represents the average duration of the vacation period. The use of retransmissions to achieve reliable transmission effectively converts a single packet transmission into a burst with the PGF of

$$G_b(x) = \frac{x\sum_{k=0}^{n_{rt}} x^k {p_{PER}}^k}{\sum_{k=0}^{n_{rt}} {p_{PER}}^k}; \tag{3.15}$$

and its mean value is $E[G_b] = G_b'(1)$.

Hence, the total offered load in the uplink is

$$\rho_b = (\rho + \lambda_u E[V])E[G_b] \tag{3.16}$$

As total offered load depends on mean vacation time while cyclical vacation depends on total offered load, we need to simultaneously solve equations (3.16) and (3.12) to get these two values.

Assuming a FIFO servicing discipline, we can model 1-limited M/G/1 queues without transmission errors by considering a packet followed by a vacation as a virtual packet with the PGF of $B_1(x) = G_{up}(x)G_{dp}(x)V(x)$. This allows us to use the standard expression for the number of packets left after the departing uplink packet as

$$\Pi(x) = \frac{(1-\rho_v)(1-V^*(\lambda-\lambda x))B_1^*(\lambda-\lambda x)}{\lambda E[V](B_1^*(\lambda-\lambda x)-x)} \tag{3.17}$$

$$= (1-\lambda(E[G_{up}]+E[G_{dp}]+E[V]))(1-V^*(\lambda-\lambda x)) \cdot \frac{G_{up}^*(\lambda-\lambda x)G_{dp}^*(\lambda-\lambda x)V^*(\lambda-\lambda x)}{\lambda E[V](G_{up}^*(\lambda-\lambda x)G_{dp}^*(\lambda-\lambda x)V^*(\lambda-\lambda x)-x)} \tag{3.18}$$

where we have converted the PGFs for packet time and vacation time into Laplace-Stieltjes Transforms (LST) by replacing variable x with e^{-s}. For simplicity, each node is assumed to have a buffer of infinite size; the error introduced by this approximation is negligible at small to moderate load.

In the presence of transmission errors and retransmissions, each packet becomes a burst of random length. If the number of retransmissions is limited to n_{rt}, as assumed above, the PGF for the burst size is given by (3.15), and the overall PGF for the distribution of packets left after a single departing packet is

$$\Pi_g(x) = \frac{(1-\rho_b)(1-V^*(\lambda-\lambda x))G_b(B_1^*(\lambda-\lambda x))}{\lambda E[V]G_b(B_1^*(\lambda-\lambda x)-x)} \tag{3.19}$$

where $G_b(B_1^*(\lambda - \lambda x)$ represents the PGF of a burst where argument x is replaced with $B_1^*(\lambda - \lambda x)$, which is further replaced with $B_1^*(\lambda - \lambda x) = G_{up}^*(\lambda - \lambda x)G_{dp}^*(\lambda - \lambda x)V^*(\lambda - \lambda x)$.

Probability distribution of the number of packets left after a packet departure can be converted into the probability distribution of packet delay. This is usually accomplished by observing that the number of packets left after a packet departure is equal to the number of packets that have arrived during the time the departing packet was in the system. If response time for a packet is T_r, the last observation can be expressed as

$$\Pi_g(x) = T_r^*(\lambda - \lambda x) \tag{3.20}$$

In the presence of transmission errors and re-transmissions, the response time for a packet consists of waiting time until that packet is transmitted correctly. Waiting time includes waiting for all previous packets as well as the time needed for unsuccessful transmissions of the target packet. Therefore the probability distribution of waiting time can be described with

$$\Pi_g(x) = W^*(\lambda - \lambda x)G_{up}^*(\lambda - \lambda x) \tag{3.21}$$

Upon substitution $s = \lambda - \lambda x$, the probability distribution of the packet delay becomes

$$\begin{aligned} W^*(s) &= \frac{1}{G_{up}^*(s)}\Pi_g(1 - \frac{s}{\lambda}) \\ &= \frac{(1-\rho_b)(1-V^*(s))G_b(G_{up}^*(s)G_{dp}^*(s)V^*(s))}{\lambda E[V](G_b(G_{up}^*(s)G_{dp}^*(s)V^*(s)) - 1 + s/\lambda)G_{up}^*(s)} \\ &= \frac{(1-\rho_b)(1-V^*(s))G_b(G_{up}^*(s)G_{dp}^*(s)V^*(s))}{G_{up}^*(s)E[V](\lambda G_b(G_{up}^*(s)G_{dp}^*(s)V^*(s)) - \lambda + s)} \end{aligned} \tag{3.22}$$

Moments of packet delay can be obtained as $(-1)^k W^{*(k)}(0)$ where k denotes the order of the moment (e.g. first moment has $k = 1$, second moment has $k = 2$ etc) and (k) denotes the k-th derivative of the LST $W^*(s)$. However, multiple applications of l'Hôpital's rule

are necessary to obtain higher moments. In most cases, it suffices to find first moment (mean) and second central moment (standard deviation); the latter is obtained as

$$W_{sd} = \sqrt{(W^{*(2)}(0) - W^{*(1)}(0)^2)} \tag{3.23}$$

3.4 Performance results

We consider the network with $m = 3$ to 11 nodes. Ordinary nodes generate packets at a rate of $\lambda = 0.007 \,..\, 0.019$ with an increment value of 0.002 packets per time unit per node. Bit error rate is assumed to be constant with a probability of $p_{BER} = 10^{-5}$. The packet retransmission limit was set to $n_{rt} = 3$. Both downlink (POLL) and uplink (DATA or NULL) packets last for one time slot. When requested, the coordinator sends a recharging pulse of power 0.1W that lasts for 1000 slots. All the nodes are located within a disc at the distance of $1 \,..\, 10$ meters from the coordinator. In our experiment, we have considered energy consumption values for different events, i.e., sensing packets, transmitting, according to the [2].

Our first set of experiments shows the main performance descriptors of network load and recharging as functions of packet generation rate λ and network size m.

Fig. 3.4(a) shows the total offered load from (3.16). As can be seen, the offered load is approximately linearly dependent on the packet generation rate and network size, as described by (3.9).

Mean recharging period expressed in polling cycles and recharging probability are shown in Figs. 3.4(b) and 3.4(c), respectively. As can be seen, larger network size leads to faster battery depletion, since all nodes have to listen to all POLL packets and the duration of the polling cycle is directly proportional to network size. The packet arrival rate is small enough throughout the observed range, hence the probability of having no data to send (i.e., of sending a NULL packet) is very high when m is small. As a NULL packet requires less power to transmit than a DATA one, the recharging period is higher at smaller

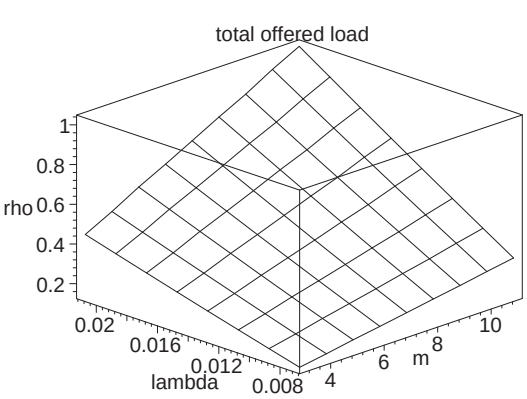

(a) Total offered load.

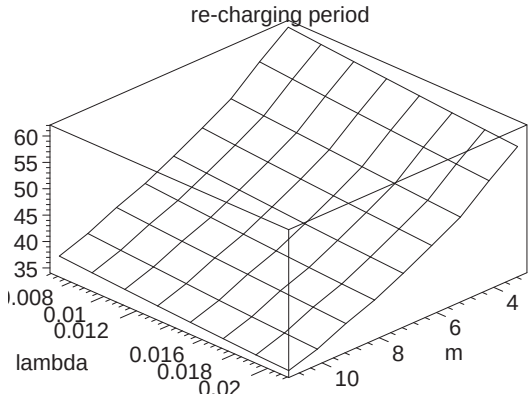

(b) Number of polling cycles per recharging period.

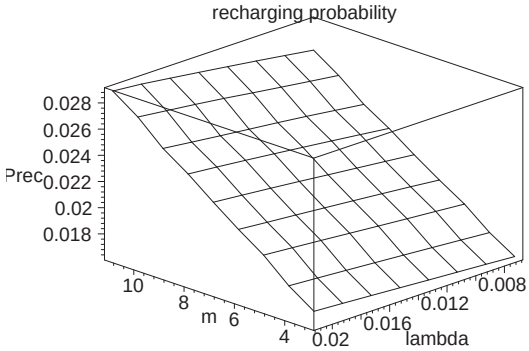

(c) Recharging probability.

Figure 3.4: Descriptors of load and recharging.

values of m. On the other hand, larger network size leads to a longer vacation time during which more packets arrive, hence the probability that the node queues are empty decreases. Fewer NULL packets decrease the recharging period as well.

The packet generation rate λ has both a positive and negative impact on the recharging period. Namely, higher packet rate results in more DATA packets and fewer NULL packets, which leads to a shorter recharging period. At the same time, higher packet rate triggers more packet retransmissions which requires slightly less energy than regular packet transmissions (E_{rt} vs. $E_{rt} + E_{ds}$) which has the opposite effect. Energy difference between DATA packet and NULL packet is not huge margin in our model as DATA packet size is

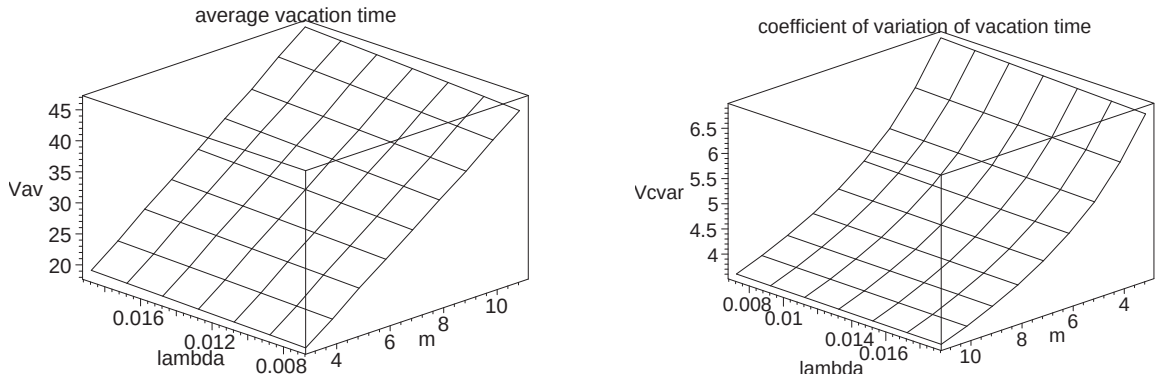

(a) Mean value.

(b) Coefficient of variation.

Figure 3.5: Descriptors of vacation time.

small. Moreover most of the energy of a node is consumed for longer vacation period. According to Fig. 3.4(b), recharging period is reduced at a snail's pace for higher traffic rate. Traffic has slower impact on recharging period and probability compared to the network size.

As the result, the impact of the packet generation rate λ on both recharging period and recharging probability is rather small.

Descriptors of total vacation time are shown in Fig. 3.5. Mean vacation time increases with the network size due to an increase in cyclic vacation component, while mean vacation time increases only slightly with packet generation rate due to the slow increase in recharging probability. Coefficient of variation exhibits similar behavior, except that the dependency on network size is exponential as per (3.9). As the standard deviation of vacation time is smaller than the mean, the behavior of the distribution is hypo-exponential.

Probability distribution of the number of polling cycles between two successive recharging points derived in (3.8) is evaluated for varying packet generation rate; the results are shown in Fig. 3.6 where diagrams on the left correspond to a network with $m = 3$ nodes while those on the right correspond to a network with $m = 11$ nodes. Top and middle rows show the distributions for the lowest ($\lambda = 0.007$ per node per time slot) and highest packet generation rate ($\lambda = 0.019$) considered, while the bottom row shows the ensembles

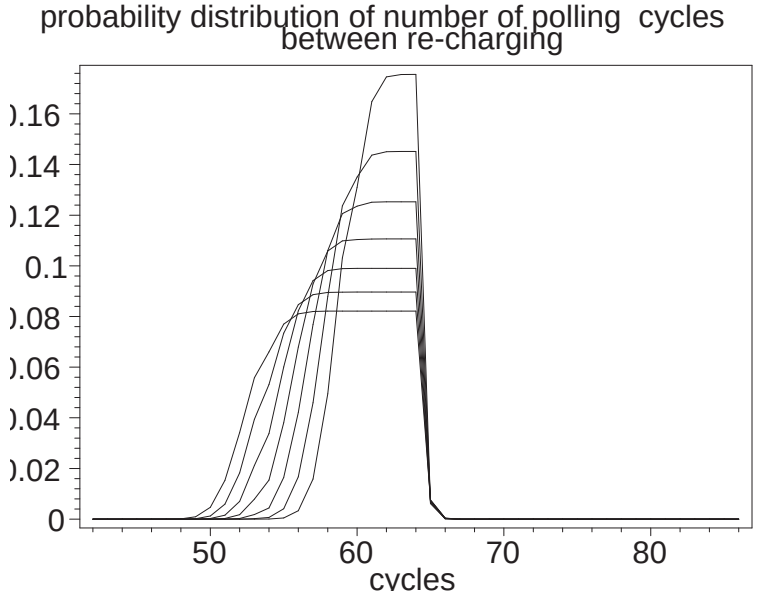

(a) Ensemble of cycle distributions for packet generation rate from $\lambda = 0.007$ (topmost curve) to 0.019 (bottommost curve), in steps of 0.002, at $m = 3$.

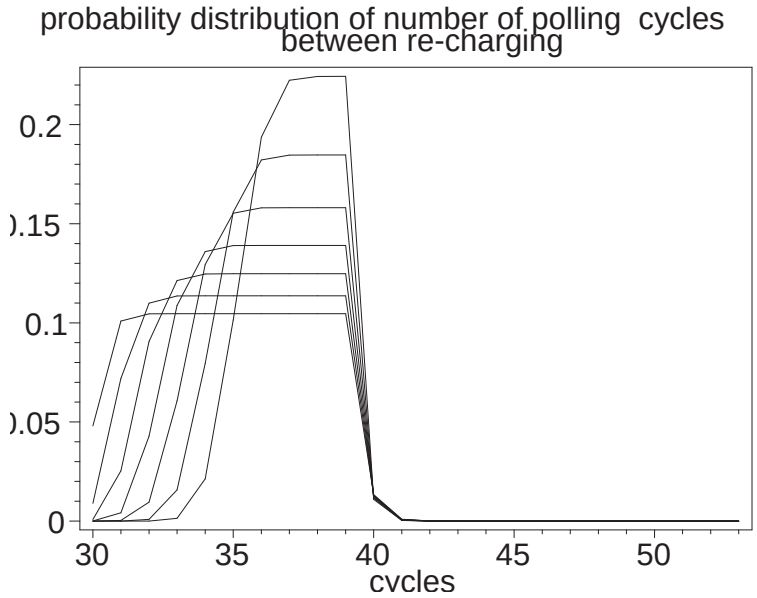

(b) Ensemble of cycle distributions for packet generation rate from $\lambda = 0.007$ (topmost curve) to 0.019 (bottommost curve) in steps of 0.002, at $m = 11$.

Figure 3.6: Distributions of the number of polling cycles between two successive recharging pulses.

of cycle distributions for packet arrival rates between lowest and highest value in steps of $\Delta\lambda = 0.002$.

As can be seen, lower packet generation rate results in probability distribution of the number of recharging cycles with a narrower shape. Higher packet generation rate increases packet retransmission which requires slightly less power, and by extension the lower bound of the recharging period distribution decreases. On the other hand, increased packet generation rate leads to an increase in DATA packet transmission and retransmission, but decreases the number of NULL packets; as the result, the upper bound of the distribution remains largely unaffected by this increase.

The probability distributions for $m = 11$ (right column), both the lower and upper bound of the distribution are smaller by about 25 than their counterparts for $m = 3$ ((left column). The difference is caused by the prolonged polling cycle at higher value of m. In both cases, the probability appears to be nearly flat (i.e., uniform) throughout the width of the main lobe of the distribution.

Finally, the diagrams in Fig. 3.7 show the first two moments of the packet waiting time at the node, as calculated from the probability distribution of (3.22). In small networks (i.e., low values of m), mean waiting time increases linearly with packet generation time and vice versa. However, the increase soon becomes exponential, as more nodes and higher packet generation rate are responsible for higher rate of packet arrivals, and packets have to wait much longer. Note that recharging (with a pulse that lasts 1000 unit time slots) also contributes to this waiting time, as data is still being sensed even during recharge. The waiting time might be reduced by increasing the power of the recharging pulse which would allow for a reduction in its duration. Standard deviation of the waiting time, Fig. 3.7(b), exhibits much the same pattern. Note that the ratio of standard deviation to mean value remains close to 1 at higher values for both m and λ: the ratio is lower (i.e., hypo-exponential) for moderate offered loads but gets closer to 1 at higher values (the range of independent variables in the diagrams corresponds to total offered load up to about $\rho_b = 0.75$).

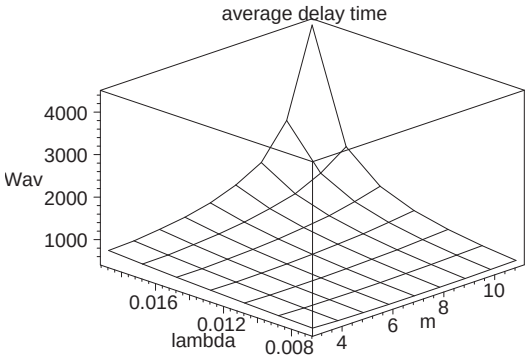

(a) mean waiting time

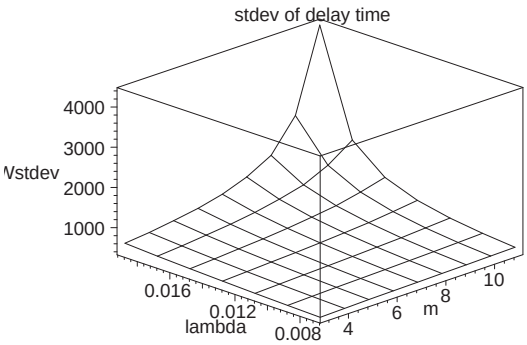

(b) standard deviation of waiting time

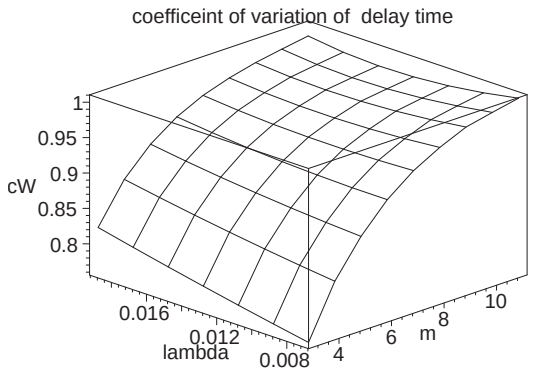

(c) coefficient of variation of waiting time

Figure 3.7: Descriptors of packet waiting time.

Chapter 4

Performance of Wireless Recharging under E-limited Scheduling

4.1 Introduction

The MAC protocol in the previous chapter used a polling mechanism in which individual nodes are serviced using 1-limited service policy. In other words, each node was allowed to send at most a single data packet to the coordinator when polled. While this service policy ensures fairness and leads to best performance at very high loads [3, 17], it is unsuitable for scenarios where traffic load is not too high and/or different nodes have different mean packet arrival rates. In particular, the interleaving of data communications and recharging periods imposed by in-band RF recharging limits the traffic load that a WSN with RF recharging can handle.

In this chapter, we extend the MAC protocol so as to allow nodes to send up to M data packets when polled. This policy, known as E-limited service [33], leads to better performance in terms of offered load, vacation time and queueing delay, compared to 1-limited service policy [32]. As before, we evaluate the performance of this protocol using probabilistic analysis and a dedicated uplink queueing model which focuses on the battery depleting process and models the impact of the recharging interval on data communication

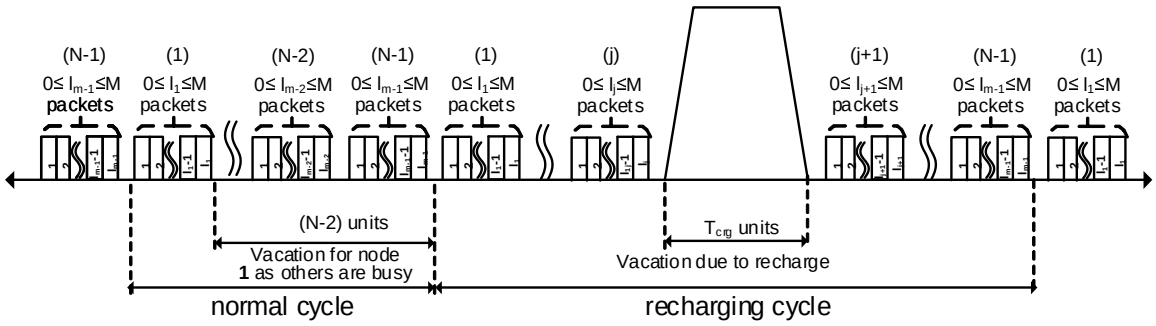

Figure 4.1: Packet Transmissions of nodes in a polling cycle.

performance.

4.2 MAC Protocol

The network consists of $N-1$ sensor nodes and a coordinator. Each of the nodes has a sensing unit to collect sensing data which is then delivered to the coordinator. The coordinator sequentially polls each sensor node in a round robin fashion by sending POLL packets which may or may not contain data, similar to Bluetooth [20].

Upon receiving a POLL packet, the sensor node sends a DATA or NULL packet, depending on whether it has data to send or not, in the uplink to the coordinator. After receiving a DATA packet, the coordinator will send a new POLL packet to the same sensor node. After receiving a NULL packet, or after receiving a total of M DATA packets, the coordinator will move on to poll the next sensor node. This service policy corresponds to E-limited policy [33] which is non-gated, as the data sensed during the delivery of a DATA packet can be included, as long as the maximum of M packet is not exceeded.

All sensor nodes are listening to the header part of each POLL packet in order to find out which node is to respond. We define a *polling cycle* as the time interval between two consecutive visits to the same node. Therefore, in a polling cycle shown in Fig. 4.1, each node gets the opportunity to send at most M DATA packets to the coordinator.

We assume that the packet arrival rate follows Poisson distribution with mean arrival rate λ for all nodes. Packets are assumed to have a fixed size of L bits; the corresponding probability generating function (PGF) will be $G_p(z) = z^L$, and its Laplace-Stieltjes transform will be $G_p^*(s) = e^{-sL}$.

Our analysis will follow the theory of $M/G/1$ queuing systems with vacations. The number of packets at the uplink queue of a sensor node can be modelled with set of embedded Markov points that correspond to the moments when a node vacation is terminated due to the arrival of data, and the moments when a packet from a node is served in its entirety.

Let q_i be the joint probability that a Markov point in the uplink transmission from a sensor node is a vacation termination time and there are $i = 0, 1, 2 \ldots$ packets in the uplink queue of a node. Variables a_i and f_i represent the probability of i packet arrivals during the service time of a single packet and during each vacation period, respectively, while π_i^m denotes that the number of packets in the system after the completion of the m^{th} packet service, $m = 1 \,..\, M$, is i. The following equations then hold:

$$\pi_i^1 = \sum_{k=0}^{i+1} q_k a_{i-k+1} \tag{4.1a}$$

$$\pi_i^m = \sum_{k=0}^{i+1} \pi_k^{m-1} a_{i-k+1}, \qquad m = 2 \,..\, M \tag{4.1b}$$

$$q_i = \left(\sum_{m=1}^{M-1} \pi_0^m + q_0 \right) f_i + \sum_{k=0}^{i} \pi_k^M f_{i-k}, i = 0, 1, \ldots \tag{4.1c}$$

The PGFs for number of packets after each packet service and queue are

$$\Pi_m(z) = \sum_{i=0}^{\infty} \pi_i^m z^i \quad m = 1 \,..\, M \tag{4.2a}$$

$$Q(z) = \sum_{i=0}^{\infty} q_i z^i \tag{4.2b}$$

During the service period of one node, the other $N - 2$ nodes are forced to undertake a vacation. The PGF and LST of vacation time are denoted with $V(z)$ and $V^*(s)$, respec-

tively, while the number of packets arrival during a single vacation period is $V(\lambda - \lambda z)$. Then, the PGF of packet arrivals during a vacation is

$$V(\lambda - \lambda z) = \sum_{i=0}^{\infty} a_i z^i \tag{4.3}$$

Using (4.1) and (4.3), we can simplify the PGFs from (4.2) to

$$\Pi_1(z) = \frac{[Q(z) - q_0]B^*(\lambda - \lambda z)}{z} \tag{4.4a}$$

$$\Pi_m(z) = \frac{\Pi_{m-1}(z) - \pi_0^{m-1}B^*(\lambda - \lambda z)}{z}, \;\; m = 2 \,..\, M \tag{4.4b}$$

$$Q(z) = \left[\sum_{m=1}^{M-1} \pi_0^m + q_0 + \Pi_M(z)\right] V^*(\lambda - \lambda z) \tag{4.4c}$$

The impact of noise and interference is often measured through bit error rate ER_b, or the equivalent packet error rate $\sigma = 1-(1-ER_b)^L$ (since the data packet has a fixed size of L bits). Transmission reliability is implemented through Automatic Repeat Request (ARQ) protocol which retransmits corrupted packets up to n_{ret} times. Taking retransmissions into account, we can revise the PGF $Q(z)$ to

$$\begin{aligned} Q_\sigma(z) = & \frac{(1-\sigma)\sum_{i=0}^{n_{ret}}(\sigma z)^i \left(\sum_{m=1}^{M-i-1} \pi_0^m + q_0 + \Pi_{M-i}(z)\right)}{(1-\sigma)\sum_{i=0}^{n_{ret}} \sigma^i} \\ & \cdot V^*(\lambda - \lambda z) \end{aligned} \tag{4.5}$$

The PGF $Q_\sigma(z)$ must be normalized by dividing it into $Q_\sigma(1) = 1 - \Pi(1)$.

Overall, the operation of the network can be expressed through the $M(N-1)$ equations above; by solving these equations, we can derive probability values in the normalized PGF $\frac{Q\sigma(z)}{Q(1)}$.

The uplink transmission is terminated after sending M packets or when the queue is

empty. The PGF for the duration of uplink service period (including NULL packets) is

$$\begin{aligned} S^u(z) =& \frac{1}{Q_\sigma(z)}\Bigg[z + \sum_{i=M}^{\infty} q_i (G_p(z))^M \\ &+ z(G_p(z))^M \sum_{i=1}^{M-i} q_i \\ &+ \sum_{i=1}^{M-1} q_i \sum_{l=1}^{M-k} (z - z(G_p(z))^l) \psi^*_{M-l,i}(G_p(z))\Bigg] \end{aligned} \tag{4.6}$$

where

$$\psi^*_{l,i}(z) = \frac{iw^l}{l(l-i)!} \cdot \frac{d^{l-i}}{dy^{l-i}} (zG^*_p(\lambda - \lambda z))^{2n} \tag{4.7}$$

In the downlink, the coordinator sends only POLL packets, to each of which the sensor responds by a single uplink DATA or NULL packet. Let S denote the service time for a downlink and uplink transmission. The corresponding PGF may be written as

$$\begin{aligned} S(z) =& \frac{1}{Q_\sigma(z)}\Bigg[z + \sum_{i=M}^{\infty} q_i (zG_p(z))^M \\ &+ z(zG_p(z))^M \sum_{i=1}^{M-i} q_i \\ &+ \sum_{i=1}^{M-1} q_i \sum_{l=1}^{M-k} (z - z(zG_p(z))^l) \psi^*_{M-l,i}(zG_p(z))\Bigg] \end{aligned} \tag{4.8}$$

Probability of sending a NULL packet in the uplink is

$$s^u_0 = S^u(0) \tag{4.9}$$

while the PGF for the service time spent transmitting DATA packets is

$$S^u_+(z) = S^u(z) - s^u_0 \tag{4.10}$$

4.3 Recharging model

We assume that all nodes are initially charged to the maximum battery capacity of E_{max} which can't be exceeded. Energy is used to sense, process, send and resend data, including NULL packets, but also to listen to POLL packets sent to the node in question as well as to all other nodes. Table 4.1 represents units for energy expenditures for various events considered in the model.

When the energy level of a node drops below a predefined threshold E_δ, the node sends a recharge request by piggybacking the appropriate message onto a DATA or NULL packet it sends to the coordinator. Upon receiving such a request, the coordinator sends a special POLL packet informing all the nodes about a pending recharge RF pulse. This packet also contains the information about the power of the recharging pulse and its duration, P_{crg} and T_{crg}, respectively.

While recharging is initiated by the node with the energy below the threshold, all nodes will benefit from it and replenish their energy sources. As different nodes are located at different distance from the coordinator, the amount of energy they will receive from the recharge pulse will be proportional to the path loss LP_i between the coordinator and the node i as per Friis' transmission equation, $LP_i^r = \eta G_i^r G_t \left(\frac{\lambda_w}{4\pi r_i}\right)^2 P_{crg}$, where η is the coefficient of efficiency for RF power conversion, G_i^r and G_t are antenna gains for the receiver (sensor node) and the transmitter (coordinator), respectively, λ_w is the wavelength of the RF signal, and r_i is the distance between the receiver and transmitter [6]. The energy level of node i is, then, changed to $\min(E_{max}, E_{delta} + P_{crg} T_{crg} LP_i$.

At the end of recharging operation, normal data communication resumes, with the coordinator polling the next node in the round robin sequence. Although, a particular node i sends energy request when its energy falls bellow E_δ but all the nodes are recharged simultaneously while the coordinator sends charging pulse. Due to the different path loss values, the nodes will possess different energy level after the recharging operation.

It is worth noting that the initial recharging request can be triggered by any sensor node

Table 4.1: Elementary energy consumption units.

Energy expenditure	label
Data sensing	E_{ds}
Listening to the POLL packet	E_{poll}
Listening to the header of POLL packet	E_{pa}
Data packet transmission	E_{dt}
Null packet transmission	E_{nt}

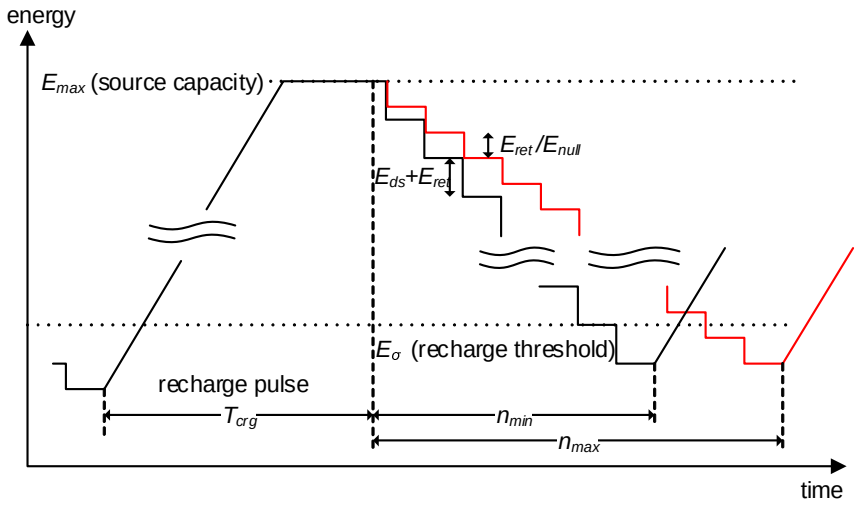

Figure 4.2: Details of energy consumption rate and its variation [23].

as all nodes experience data traffic with the same probability distribution. However, after a few cycles, energy requests will always be issued by the node at the largest distance from the coordinator, as its energy will be replenished the least due to path loss [23].

Table 4.2: Energy consumption units at polling cycle level.

Energy expenditure	label
cycle with no data packet	$E_{null} = E_{poll} + (m-2)E_{pa} + E_{null}$
cycle with first transmission attempt	$E_{tr} = E_{ds} + E_{poll} + (m-2)E_{pa}/\overline{S_+^u}(z) + E_{dt}$
cycle with packet re-transmission	$E_{ret} = E_{poll} + (m-2)E_{pa}/\overline{S_+^u}(z) + E_{dt}$

The energy expenditure of a node during a time period between successive recharge pulses will fluctuate due to randomness of traffic arrivals and data packet retransmissions. As the result, the time intervals between two recharging points is a random variable. Fig. 4.2 shows two possible energy consumption processes of a node starting from maximum energy level E_{max}.

To analyze the impact of recharging on data performance, let us find the total number of polling cycles along with energy expenditure for the farthest node starting from a recharge point until its energy level falls below E_δ. To this end, we need the joint probability distribution of consumed energy for E-limited system along with the required time. Table 4.1 shows the total energy needed to transmit a DATA packet (which includes sensing, listening to a POLL packet, and actual transmission); a NULL packet (in which case sensing is not needed, and the actual transmission is presumably shorter than for a full DATA packet); and to retransmit a previously corrupted DATA packet (which also does not require new data sensing).

Let us now calculate the PGF for energy consumption along with the required number of time units for successful transmission of packets by a node in a polling cycle. Let v and w denote the energy units for transmitting or retransmitting a data packet, respectively, and let t denote the time unit. By replacing $z = (v^{\frac{1}{\sum_{i=0}^{n_{ret}} \delta^i}} \cdot w \cdot t^L)$ in (4.10), we obtain the PGF for the combined energy expenditure and time as

$$E_{data}(w, v, t) = S_u^+(v^{\frac{1}{\sum_{i=0}^{n_{ret}} \sigma^i}} \cdot w \cdot t^L) \tag{4.11}$$

Let Φ denote the energy unit for transmitting a NULL packet. Note that, under E-limited service policy, only one NULL packet is sent in a polling cycle. Then, the complete PGF for sending DATA and NULL packets can be expressed as

$$E_{all}(w, v, \phi, t) = E_{data}(w, v, t) + (1 - s_0^u)\phi t \tag{4.12}$$

where $s_0^u = 1 - \rho_{tot}$ is the probability that the node buffer is empty, and ρ_{tot} denotes the

total offered load (effective utilization) of a node.

Let us consider that the farthest node Y has the energy consumption budget of Δ_Y after it is recharged. By inspecting dynamics of DATA and NULL packet transmission, we conclude that Δ_Y amount of energy consumption is finished between $n_{min} = \Delta_Y/((n_{ret} + 1)E_{ret} + E_{ds})$ and $n_{max} = \Delta_Y/(E_{null})$ packet transmissions. The minimum number of packet transmissions corresponds to the scenario where a node has packets all the time and each packet needs n_{ret} attempts to be sent successfully, while the maximum number corresponds to the scenario in which the node queue is always empty and only NULL packets are sent. The probability of sending packets between these two boundaries has non zero values.

Now, we need model the joint probability distribution of energy consumption along with time duration in order to send all the combinations of DATA and NULL packets between two charging points. The PGF $EEp(w, v, \phi, t)$ considering all possibilities can be written as

$$EEp(w, v, \phi, t) = \frac{\sum_{j=n_{min}}^{n_{max}} E_{all}(w, v, \phi, t)^j}{n_{max} - n_{min} + 1} \tag{4.13}$$

As our model requires to determine total energy expenditure, we require to combine all the energy consumption units. According to Tables 4.1 and 4.2 we define translation ratios between re-transmission and NULL packet transmission energies with sensing energy as

$$nT = E_{null}/E_{ds}$$
$$rT = E_{ret}/E_{ds}$$

Further we need to use these ratios to map $w = v^{rT}$ and $\phi = v^{nT}$ in (4.13). However since variable v already appears with high powers, it is possible to collect the coefficients, round the powers and combine them in joint energy consumption variable u (which is equivalent to v by dimension but we have considered different variable name for clarity).

Algorithm 2: PGF for combined energy unit and time unit.

Data: $EE_{all}(w, v, \phi, t)$, conversion ratios nT and rT
Result: PGF for energy consumption representing in E_{ds} quanta along with number of polling cycles between two consecutive charging points.

Find minimal min_w and maximal max_w exponent of variable w in $EE_{all}(w, v, \phi, t)$;
for $i \leftarrow min_w$ **to** max_w **do**
    Derive coefficient w_{cof}[i]of w^i (polynomial on v, ϕ and t) ;
    Find minimal min_ϕ and maximal max_ϕ exponent of variable ϕ in $w_{cof}[i]$;
    for $k \leftarrow min_\phi$ **to** max_ϕ **do**
        Calculate coefficient $\phi w[i, k]$ of ϕ^k in w_{cof}[i] (polynomial on v and t) ;
        Find minimal min_v and maximal max_v exponent of variable v in $\phi w[i, k]$;
        for $j \leftarrow min_v$ **to** max_v **do**
            Find coefficient $v\phi w[i, k, j]$ of v^k in ϕw[i,k] (polynomial on t);
            calculate combined integer energy consumption coefficient a $exp[i, k, j] = \lceil i \cdot rT + k \cdot zT + j \rceil$;
            form new element of new polynomial as $v\phi w[i, k, j]u^{exp[i,k,j]}$
        Sum third level sum_{mini}[i,k] $\leftarrow \sum_{jj=min_\phi}^{\max_\phi} v\phi w[i, k, jj]u^{exp[i,k,j]}$;
    Sum second level sum_{small}[i] $\leftarrow \sum_{kk=min_\phi}^{max_\phi} sum_{mini}$[i, kk] ;
form new PGF as $EE_u(u, t) \leftarrow \sum_{ii=min_w}^{max_w} sum_{small}$[ii] ;

The algorithm 2 shows merging the variables w, ϕ, v into variable u (which has same unit as v).

After combining all energy units, the new PGF $EE_u(u, t)$ has only one energy unit u with an integer multiple of E_{ds} in its exponent. Minimum and maximum exponent value of variable u in $EE_u(u, t)$ are expressed as min_{exp} and max_{exp}, respectively. As explained earlier, recharge is initiated by the furthest node Y from the coordinator. Node Y gains Δ_Y of energy during recharge, and when its energy level reaches E_δ due to energy consumption new recharging request is sent. We will express the energy budget in multiples of sensing energy quantum, $n_{ds} = \frac{\Delta_Y}{E_{ds}}$, so as to have it match the matches unit of variable u in the PGF $EE_u(u, t)$.

Let $u_{cef}(i)$ be the coefficient of u^i in $EE_u(u, t)$. In that case, $u_{cef}(i)$ will be a polynomial function in t. Then, the polynomial conditioned to the event that energy consumption

is exceeded can be derived as

$$T_r(t) = \sum_{i=n_{ds}}^{max_{exp}} u_{cef}(i) \tag{4.14}$$

Since t represents the time for polling cycles, polynomial $T_r(t)$ is the conditional PGF for polling cycle numbers for which energy budget of a node is exceeded. $T_r(t)$ has to be unconditioned in order to become a complete probability distribution for the number of polling cycles.

$$T(t) = \frac{T_r(t)}{T_r(1)} \tag{4.15}$$

The mean number of polling cycles between two consecutive recharging appeals is, then, $\overline{T} = T'(1)$.

A node i will be in outage if it needs more energy than the available Δ_i. The probability of this event is $p_{out} = \frac{1}{T}$, which will be referred to as outage probability or even recharging probability $p_{rec} = p_o$, since the node requests a recharge before the onset of an outage.

4.4 Vacation model

A node is forced to undertake vacation (during which it can't perform data transmit/receive operation) when other nodes are transmitting packets or when it receives recharging pulse from the coordinator. Let us now find the probability distribution of this vacation period. We assume that time is expressed in basic slots, with POLL and NULL packets consuming one slot each while a DATA packet consumes L time slots. $S(z)$ presents the node service time: the time for sending packets in the uplink and receiving POLL messages in the downlink.

The node receives uplink packet with λ arrival rate. Without the impact of vacation, a node's offered load will be $\rho = \lambda \cdot \overline{S}$. However, a node may be required to undergo a

vacation. Let $V(z)$ be the PGF of the vacation period and $\overline{V}$ be the average vacation time. During the vacation period, the node is not allowed to send data but it continues to receive traffic at the rate of λ which increases the load to

$$\rho_{tot} = \rho + \lambda\overline{V} \tag{4.16}$$

The total vacation period can be split into two components:

1. Cyclical vacation consists of service times of other $N-2$ nodes and its PGF is

$$V_{cyc}(z) = (S(z))^{m-2} \tag{4.17}$$

2. Recharging vacation is the duration of the recharge pulse, and its PGF is

$$V_{rec}(z) = P_{out}z^{T_{crg}} + (1 - P_{out}) \tag{4.18}$$

PGF for the total vacation time is

$$V(z) = V_{rec}(z)V_{cyc}(z) \tag{4.19}$$

and its mean and standard deviation can be found as

$$\overline{V} = V'(1) \tag{4.20}$$

$$V_{stdev} = \sqrt{(V''(1) - (V'(1))^2 + V'(1))} \tag{4.21}$$

Note that total offered load depends on the mean vacation period, while the cyclical vacation depends on total offered load. Therefore, (4.16) and (4.20) need to be solved together as a system.

4.5 Queuing model

The PGF (4.5) contains $\Pi_M(z)$ and π_O^k, $1 \leq k \leq M-1$, values, and we need to decompose this compound PGF (i.e., a PGF that has other PGFs as elements) into simpler, separate PGFs. Note that under E-limited service, after serving a packet a node with a non-empty queue may or may not undergo a vacation, depending on how many packets have been served. Therefore, the beginning of a vacation period is a function of the number of packets served by the node. We can model the E-limited system as a $M/G/1$ system with Bernoulli scheduling, where service continues with the probability of $p_s = 1 - p_v$ (where p_v is the vacation probability). In this case, q_i can be re-written as

$$q_i = (q_0 + \pi_0) f_i + p_v \sum_{k=1}^{i} \pi_k f_{i-k} \quad i = 1, 2, \cdots \tag{4.22a}$$

$$\pi_i = \sum_{k=1}^{i+1} q_k a_{i-k+1} + p_s \sum_{k=1}^{i+1} \pi_k a_{i-k+1} \quad i = 0, 1, \cdots \tag{4.22b}$$

$$\sum_{i=0}^{\infty} (q_i + p_i) = 1 \tag{4.22c}$$

while the PGFs for the queue and the number of packets remaining after service can be written as

$$Q(z) = [q_0 + p_s \pi_0 + p_v \Pi(z)] V * (\lambda - \lambda z) \tag{4.23a}$$

$$\Pi(z) = [Q(z) + p_s \Pi(z) - (q_0 + p\pi_0)] \frac{S_u(z)}{z} \tag{4.23b}$$

$$Q(z) + \Pi(z) = 1 \tag{4.23c}$$

From (4.23a), (4.23b), we obtain separate PGFs as

$$Q(z) = \frac{(q_0 + p_s\pi_0)[(z - S_u(\lambda - \lambda z)]V^*(\lambda - \lambda z)}{z - [p_s + p_v V * (\lambda - \lambda z)]S_u(\lambda - \lambda z)} \tag{4.24a}$$

$$\Pi(z) = \frac{(q_0 + p_s\pi_0)[(V^*(\lambda - \lambda z) - 1]S_u(\lambda - \lambda z)}{z - [p_s + p_v V^*(\lambda - \lambda z)]S_u(\lambda - \lambda z)} \tag{4.24b}$$

$$q_0 + p_s\pi_0 = \frac{1 - \rho_{tot} - p_s\lambda\overline{V}}{1 - \rho_{tot} - \lambda\overline{V}} \tag{4.24c}$$

At this time, p_v value can easily be calculated as other terms in (4.24c) are known. In particular, the number of the packets in the queue is

$$Q\sigma(z) = [(1 - \sigma) + \sigma z]Q(z) \tag{4.25}$$

$\frac{Q\sigma(z)}{Q(1)}$ and $\frac{\Pi(z)}{\Pi(1)}$ are normalized PGF functions.

Let us now find the probability distributions of packet delay from the probability distribution of the number of packets left after a packet has been served. If $T^*(s)$ is the LST of the time during which a packet is in the system, the number of packet arrivals during that time is

$$\frac{\Pi(z)}{\Pi(1)} = T^*(\lambda - \lambda z) \tag{4.26}$$

Packet waiting time, the LST of which is denoted with $W^*(s)$, includes waiting for all previous packets, as well as for previous unsuccessful transmissions of that same packet; its probability distribution can be written as

$$\frac{\Pi(z)}{\Pi(1)} = W^*(\lambda - \lambda z)S_u(\lambda - \lambda z) \tag{4.27}$$

Finally, we can substitute $s = \lambda - \lambda z$ or equivalently $z = 1 - \frac{s}{\lambda}$ to calculate the value of

$W^*(s)$. The probability distribution of packet delay becomes

$$W^*(s) = \frac{s(1-2\lambda\overline{S})}{s-\lambda+\lambda(G_p^*(s))^2} \cdot \frac{1-V^*(s)}{s\overline{V}} \cdot \frac{q_0^u}{Q\sigma(1)V^*(s)} \tag{4.28}$$

Mean value of the queuing delay is obtained as

$$\overline{W} = \frac{\lambda(\overline{L^2}+\overline{L}^2)}{1-2\lambda L} \cdot \frac{\overline{L}}{1-2\lambda\overline{L}} + \frac{\overline{V^2}}{2\overline{V}} - \overline{V} + \frac{Q'(1)}{\lambda Q(1)} \tag{4.29}$$

4.6 Performance results

We have assumed that individual sensor nodes are randomly located within a circle of 10 metre radius, with the coordinator in its centre. Network size N is varied between 3 to 9 nodes including the coordinator. We have assumed free space loss (i.e., path loss coefficient was set to 2). The bit error rate was fixed at $ER_b = 10^{-5}$. For E-limited service policy, a sensor node was allowed to transmit up to $M = 2$ packets, while the number of retransmissions for a corrupted packet was $n_{ret} = 3$.

The mean packet arrival rate per node λ was varied between 0.008 and 0.022 in 0.002 step increments. In the downlink, the network has only POLL packets. Packet transmission time is constant and equal to one time slot while the duration of the charging pulse duration was 1000 slots. Using these values, we have solved the system of equations described above using Maple 16 from Maplesoft, Inc. [19].

Fig. 4.3(a) presents total offered load, as defined by (4.16). AS can be seen, the offered load increases with both network size N and traffic arrival rate λ. The later relationship is self-explanatory, as higher packet arrival rate will obviously lead to higher load. On the other hand, more nodes in the network mean that a given node is given less time and, consequently, less chance to send data. Moreover, it undergoes longer vacation period due to longer cyclical vacation component, as per (4.17). At the same time, new packets keep coming during the vacation period. As the result, the effective offered load per node

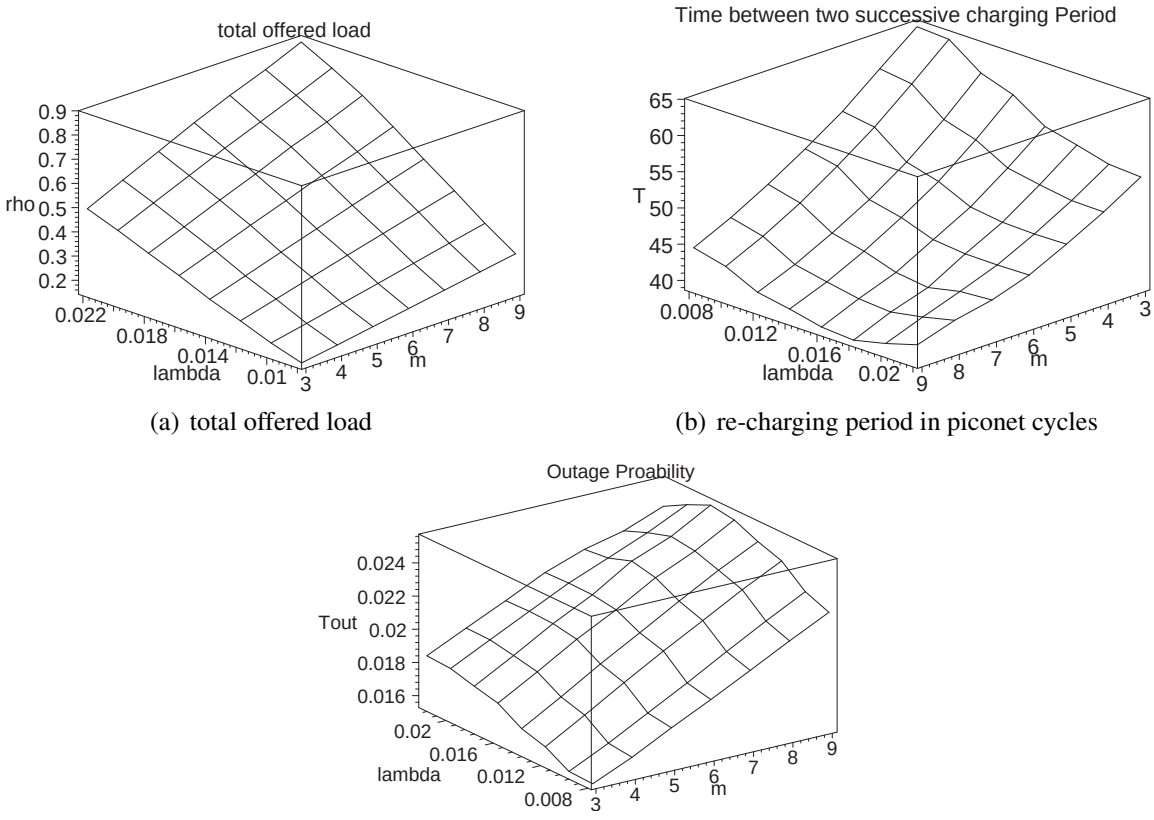

(a) total offered load

(b) re-charging period in piconet cycles

(c) Outage probability

Figure 4.3: Descriptors of load and recharging performance.

increases.

Mean recharging period is shown in Fig. 4.3(b). At first, it may look counter-intuitive to have the mean recharging period decrease with the number of nodes as each node actually receives a smaller fraction of active time. Note that a larger network translates into a longer vacation time for an individual sensor node. Larger network size also leads to faster depletion of energy since all the nodes have to listen to all POLL messages, both their own and other nodes' ones. On account of this, mean recharging period is inversely proportional to network size.

At the same time, recharging period decreases at higher traffic intensity as more energy is required to send a DATA packet compared to a NULL packet. The recharging probability

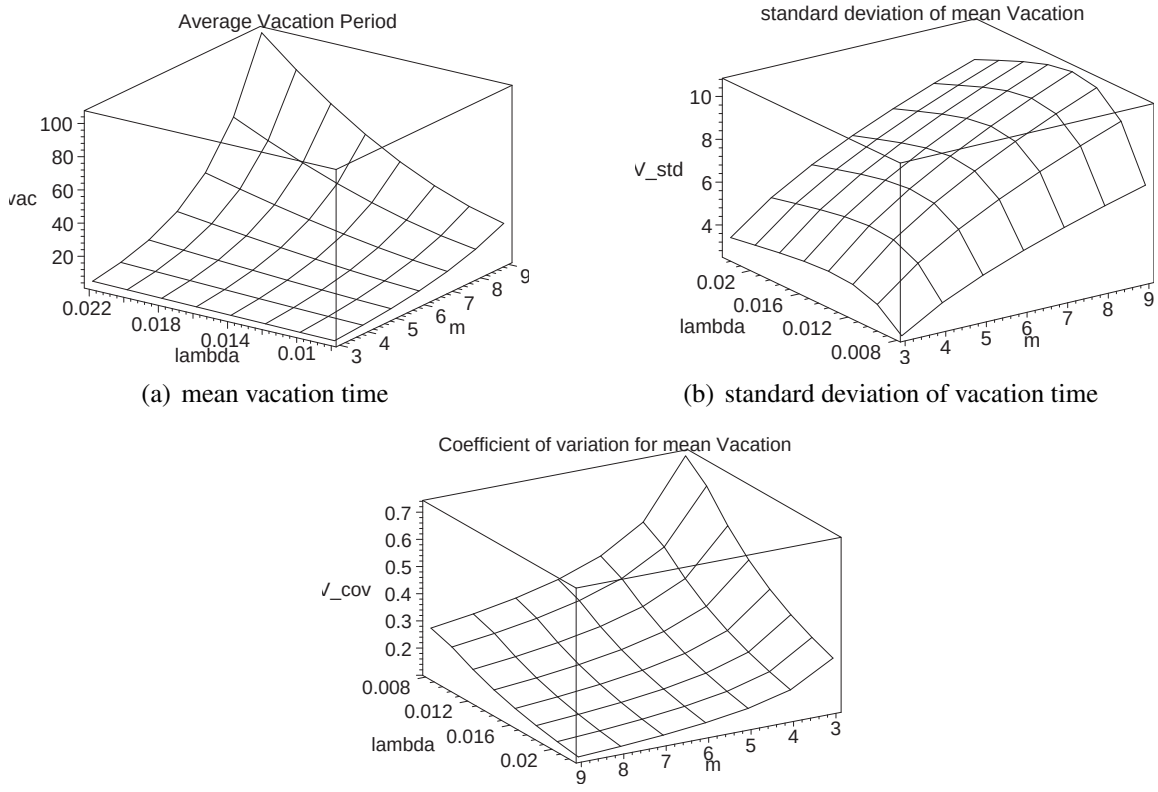

(a) mean vacation time

(b) standard deviation of vacation time

(c) coefficient of variation of vacation time

Figure 4.4: Descriptors of vacation time.

shown in Fig. 4.3(c) is the inverse of recharging period, and its behaviour is exactly opposite to that of the recharging period.

Descriptors of vacation time are shown in Fig. 4.4. Mean vacation time increases gradually with increasing traffic intensity, since a node consumes energy at a faster rate. On account of higher energy consumption, recharging probability also increases – i.e., more frequent recharging vacation V_{rec} occurs. On the other hand, larger network size N lead to longer cyclical vacation V_{cyc} which is an exponential function of the network size. In turn, longer V_{cyc} increases the total vacation time.

Standard deviation of mean vacation time exhibits similar behavior but at a somewhat reduced rate, on account of the fact that higher arrival rates decrease the number of NULL

packets. Standard deviation also increases more rapidly with the number of nodes as this injects more variability in the transmission process. For this reason, the coefficient of variation of the vacation time, $V_{stdev}/\overline{V}$, decreases with higher packet arrival rate but grows with increasing network size. It is worth noting that the coefficient of variation of the vacation time is above one, i.e., vacation time exhibits hyper-exponential behavior.

Ensembles of probability distribution of polling cycle periods between two successive recharging pulses are shown in Fig. 4.5(a) for the network of size $N = 4$. Both the boundary limits ('lower' and 'upper') of distribution space have smaller values at higher traffic intensity. Namely, higher traffic arrival rate increases packet retransmission probability, and packet retransmission requires less power consumption. As a result 'lower boundary' starts from smaller value range and 'upper boundary' ends up with a smaller value, compared to the analogous curve obtained at a lower traffic arrival rate.

Fig. 4.5(b) is shifted to the left (i.e., towards lower values) for larger network size, compared to the diagrams in Fig. 4.5(a). Namely, when the network size increases, nodes consume more power as they need to listen to a larger number of POLL packets targeting other nodes in the network.

Finally, Fig. 4.6 shows the mean packet waiting time. Initially, this waiting time increases slowly with the packet arrival rate λ and network size N. However, at larger values of N and/or λ, a steeper increment in mean packet waiting time is observed due to the simultaneous impact of high traffic intensity and large vacation period. Note that this waiting period includes the recharging vacation, i.e., the component of vacation time due to the recharging pulse.

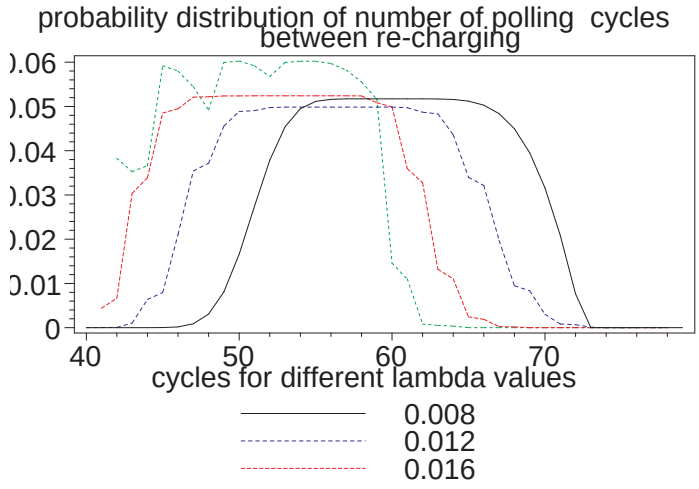

(a) Ensemble of cycle distributions for $\lambda = 0.008 \cdots 0.020$ when $N = 4$

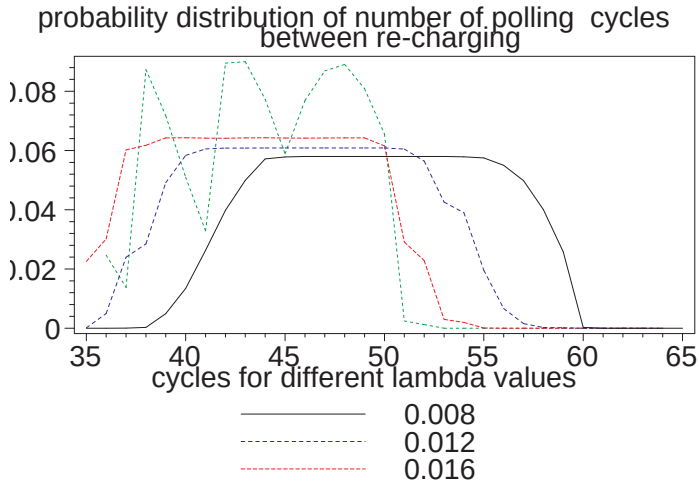

(b) Ensemble of cycle distributions for $\lambda = 0.008 \cdots 0.020$ when $N = 7$

Figure 4.5: Probability distributions of number of polling cycles between two successive re-charging for different network sizes.

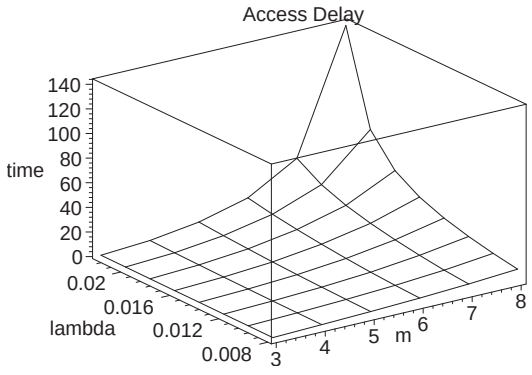

Figure 4.6: Descriptor of waiting time in piconet with wireless charging.

Chapter 5

Networks with RF Recharging and Coordinated Node Sleep

5.1 Introduction

In this chapter, we propose a simple MAC protocol in which the master sequentially polls ordinary sensor nodes and performs in-band recharging when explicitly requested by a sensor node. Polling is done in a round robin fashion and each node is allowed to send a single data packet upon polling (i.e., a 1-limited service policy is used). Furthermore,

5.2 The operation of the polling MAC

Let us consider a sensor network consisting of N nodes as shown in Fig. 5.1. A special node, hereafter referred to as the master, is equipped with a power source that can emit RF recharging pulses upon request. The remaining $N-1$ nodes are equipped with sensor units and a RF transceiver capable of data communications as well as recharging.

We assume that the master node sequentially polls each node via POLL messages, each of which targets a specific node, similar to a Bluetooth network [20]. Each node must listen to the header part of each POLL message but only the addressed node responds: it sends

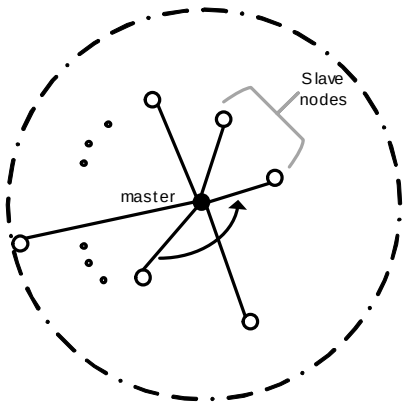

Figure 5.1: Logical presentation of the network.

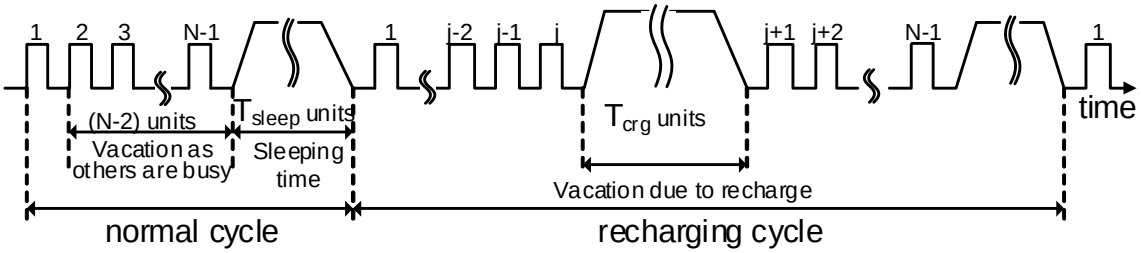

Figure 5.2: Format of the polling cycle in recharging process.

back a single DATA or NULL packet, depending on whether it has data to send or not. After serving all $N-1$ nodes sequentially, the master instructs all nodes to go to sleep for a fixed duration of T_{sleep} cycles by broadcasting a special POLL message. A polling cycle consists of $N-1$ POLL and DATA/NULL packets, followed by a sleep interval, as shown in Fig. 5.2. The time elapsed between two consecutive visits to any node in the target network will be referred to as a polling cycle.

A DATA packet reception may fail due to noise and interference with the probability of $p_{err} = 1-(1-p_{ber})^n$, where p_{ber} stands for bit error rate (BER) and n is the total number of bits in the packet including headers. Packets that were successfully received are acknowledged in the POLL packet sent by the master node in the next polling cycle; if the reception was not successful, the node will resend the packet up to n_{ret} times before

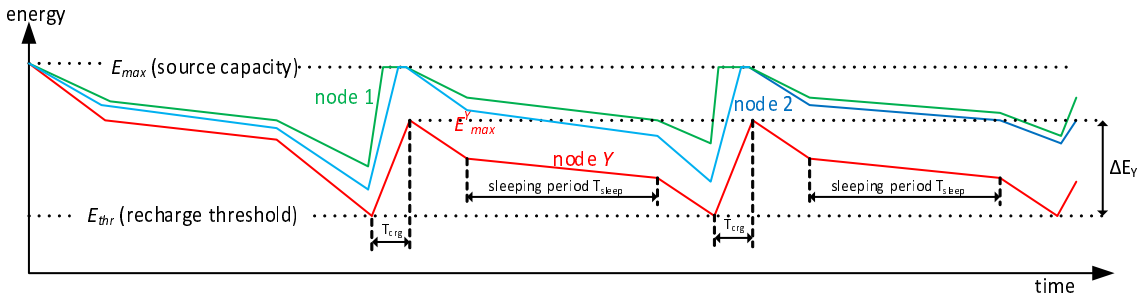

Figure 5.3: Energy expenditure and recharging periods.

dropping the packet in question.

Initially, all the nodes are charged to the maximum energy level E_{max}. Nodes consume energy for data sensing and processing, listening to POLL packets, and transmitting DATA and NULL packets, as per rates listed in Table 5.1.

When a node energy goes bellow a predefined threshold value E_{thr} – a condition referred to as energy outage – the node waits until polled and sends a recharge request to the master node by enabling the appropriate bit in the header field of its next DATA or NULL packet. The energy threshold should be sufficient to allow the current DATA packet to be transmitted with up to n_{ret} retransmission attempts:

$$E_{thr}(N) \geq (E_t + E_{poll} + (N-2)E_h)(n_{ret}+1) \tag{5.1}$$

Upon receiving a recharge request, the master node broadcasts a special POLL packet informing all the nodes about the pending recharge pulse. This pulse is sent immediately after the announcement; its power is P_{crg} and its duration is T_{crg} cycles. The received RF power for node j at a distance R_j from the master is calculated based on Friis' transmission equation: $P_{(r,j)} = \eta G_t G_r \left(\frac{\lambda_{RF}}{4\pi R_j^2}\right) P_{crg}$, where η is the coefficient of efficiency for RF power conversion, G_t and G_r are antenna gains for the transmitter and receiver, respectively, and λ_{RF} is the RF wavelength [6]. (For simplicity, we set the path loss coefficient to 2 – i.e., free space loss is assumed). Maximum possible energy gain for the node j can be $\Delta E_j =$

Table 5.1: Energy consumption of a node.

Basic tasks	
sensing a DATA packet	E_s
listening a POLL packet	E_{poll}
listening to POLL packet	E_h
transmitting a DATA packet	E_{td}
transmitting a NULL packet	E_{tn}
High level tasks	
NULL packet	$E_n = E_{poll} + 2(N-2)E_h + E_{tn}$
DATA packet initial	$E_t = E_s + E_{poll} + (N-2)E_h + E_{td}$
DATA packet retransmission	$E_{rt} = E_{poll} + (N-2)E_h + E_{td}$

$P_{(r,j)}T_{crg}$, but the actual node energy level after recharge will be $min(E_{max}, E_{thr}+\Delta E_j)$, as the rated battery capacity E_{max} can't be exceeded. The process of charging and discharging of node battery through regular operation is schematically shown in Fig. 5.3.

As the same RF band is employed for both recharging process and data communication, the latter will be interrupted by the former. For clarity, a polling cycle interrupted by the recharge pulse will be referred to as a recharge polling cycle.

As noted above, noise and interference can damage a DATA packet transmission and cause up to n_{ret} retransmissions (which may still fail). Unsuccessful transmission of a packet with recharge request may cause the node to exhaust its energy in which case it is effectively lost for all subsequent network activities.

5.3 Modeling the recharging process

Energy expenditure of a given node will differ from one polling cycle to another due to unpredictability of packet arrivals and packet retransmissions, although the mean time to consume the energy increment $E_{max} - E_{thr}$ will be same for each node. Moreover, the node at the greatest distance from the master (node Y) will receive the least amount

of energy at the time of recharging. Initially, the recharge request may come from any node; but in the long run, node Y will always be the one to initiate the recharge process and, consequently, determine the time period between two consecutive recharge requests (and ensuing recharge pulses). This time period is a random variable and its probability distribution needs to be derived. Focusing on energy expenditure of the most distant node, we may calculate the time interval between two recharge requests in units of polling cycles. Hence, we need to find the joint probability distribution of the number of polling cycles and energy consumed in each polling cycle.

The probability generating function (PGF) of the energy and time cycles needed for successful transmission of a DATA packet is

$$E_d(s,r,t) = \frac{srt\sum_{k=0}^{n_{ret}}(rt)^k p_{err}^k}{\sum_{k=0}^{n_{ret}} p_{err}^k} \tag{5.2}$$

where variables s and r stand for sensing and transmitting a DATA packet, respectively, and parameter t is used for counting polling cycles. Note that data sensing is required in the first attempt to transmit data only, but not in subsequent retransmission attempts, which is why the variable s is not considered in the retransmission part of (5.2).

However, a DATA packet is sent only when the node has data to send, otherwise the node sends a NULL packet. The probability of these events is ρ_{tot} and $1-\rho_{tot}$, respectively, where ρ_{tot} is the total offered load. Therefore, we use an additional variable, ϕ, for tracking power consumption during NULL packet cycles, which gives the updated PGF as

$$E_{d/n}(s,r,\phi,t) = \rho_{tot}E_d(s,r,t) + (1-\rho_{tot})\phi t \tag{5.3}$$

After the completion of packet transmissions from all nodes, the master node broadcasts a POLL message which instructs each node to sleep for T_{sleep} cycles. According to the data for a typical Bluetooth LE chipset [2], power consumption during sleep is negligibly low

compared to the power consumption during other activities shown in Table energy-cycle.

In the presence of transmission errors, PGF for the sleeping time upon a successful transmission of a packet is

$$E_{sleep}(s,r,\phi,t) = (1-p_{err})st^{T_{sleep}} \sum_{i=0}^{n_{ret}} (p_{per} st^{T_{sleep}})^i \tag{5.4}$$

However, the probability of occurrence of this sleep time is $\frac{1}{2(N-1)}$, and the PGF for energy consumption has to be normalized accordingly to become

$$E_s(s,r,\phi,t) = \frac{E_{sleep}(s,r,\phi,t)}{2(N-1)} + \left(1 - \frac{1}{2(N-1)}\right) \tag{5.5}$$

As retransmission is not required for sending NULL packets, the PGF for sleeping time when sending NULL packets is

$$E_{s/n}(s,r,\phi,t) = \frac{st^{T_{sleep}}}{2(N-1)} + \left(1 - \frac{1}{2(N-1)}\right) \tag{5.6}$$

Total PGF for successful transmission of a DATA or NULL packet, including the sleeping period, then becomes

$$\begin{aligned} E_{total}(s,r,\phi,t) =& \rho_{tot} Ep(s,r,t) E_s(s,r,\phi,t) \\ &+ (1-\rho_{tot})\phi t E_{s/n}(s,r,\phi,t) \end{aligned} \tag{5.7}$$

To compute the range of polling cycles between consecutive recharge points, we need to find the maximum and minimum number of transmitted packets. Maximum number of packet transmissions q_{max} occurs when there is no data to send at all during the entire polling cycle, hence only NULL packets are sent. Conversely, the number of packet transmissions is at its minimum q_{min} when the node has fresh DATA packets in each cycle and

each of these is retransmitted n_{ret} times. These numbers can be calculated as

$$q_{max} = \left\lceil \frac{E_{thr} + \Delta_Y}{E_n + \frac{s}{2(N-1)}} \right\rceil$$
$$q_{min} = \left\lfloor \frac{E_{thr} + \Delta_Y}{(n_{ret}+1)E_r + E_{sd} + s\frac{(n_{ret}+1)}{2(N-1)}} \right\rfloor \tag{5.8}$$

and the PGF for the number of packet transmissions sustained by the energy increment for the most distant node Y is

$$E_{S_p}(r, s, \phi, t) = \frac{\sum_{k=q_{min}}^{q_{max}} E_{total}(r, s, \phi, t)^k}{q_{max} - q_{min} + 1} \tag{5.9}$$

To find the total energy consumed in different time slots we need to convert different energy units to a single one – in this case the energy for sensing E_s, which is the smallest of all basic units listed in Table energy-cycle. Conversion is accomplished by defining the ratios of energy for DATA packet retransmission and NULL packet transmission to the data sensing energy unit as follows:

$$r_{rt} = E_{rt}/E_s \tag{5.10}$$
$$r_{\phi} = E_n/E_s \tag{5.11}$$

After mapping $r = z^{r_{rt}}$ and $\phi = z^{r_\phi}$ in (5.9) to use the ratios defined above, the updated PGF will use a single energy unit v only:

$$E_{S_v}(v, t) = E_{S_p}(r, s, \phi, t) \tag{5.12}$$

and the new PGF $E_{S_v}(v, t)$ will have only two variables: the exponent of variable v depicts the total energy used as multiples of s units, and the exponent of variable t represents the total number of time slots required to consume this energy.

The resulting PGF can be represented as

$$E_{S_v}(v,t) = \sum_{k=0}^{v^{(max)}} f_k(t) v^k \tag{5.13}$$

where the coefficients $f_k(t)$ are polynomials in t only. Let $v^{min} = \frac{\Delta E_Y}{E_s}$ be the minimum number of energy consumption unit(s) that causes the energy level to fall below E_{thr}, and let the maximum exponent $v^{(max)}$ of energy unit v in $E_{S_v}(v,t)$ correspond to the maximum energy consumption of a node during a single recharge cycle. The PGF for this scenario is

$$T_{(out/p,Y)}(t) = \sum_{k=v^{min}}^{v^{(max)}} f_k(t) \tag{5.14}$$

As $T_{(out/p,Y)}(t)$ contains only a part of sample space, it has to be normalized to become a proper PGF:

$$T_{(out,Y)}(t) = \frac{T_{(out/p,Y)}(t)}{T_{(out/p,Y)}(1)} \tag{5.15}$$

from which we can get the average number of polling cycles between two consecutive recharging requests sent from the same node as

$$\overline{T_{(out,Y)}} = T'_{(out,Y)}(t)|_{t=1} \tag{5.16}$$

Since a node can only send a single packet in any given polling cycle (i.e., the service discipline is 1-limited), the outage probability can be calculated as $p_{out} = \frac{1}{\overline{T_{(out,Y)}}}$.

5.4 Vacation Model

Assuming that the data packet arrivals follow a Poisson process with the arrival rate of λ, the MAC protocol described above can be modelled as a $M/G/1$ gated limited system

with vacations [34]. We assume that POLL, DATA, and NULL packets take one unit time slot each. Let the PGFs for uplink DATA/NULL packet and downlink POLL packets be defined as $G_u(z) = z$ and $G_d(z) = z$, respectively. Mean service time of a node in both directions (uplink and downlink) is obtained as $G_u(1) + G_d(1)$, while the offered load of a node is $\rho = \lambda(G'_u(z)|_{z=1} + G'_d(z)|_{z=1})$.

However, the actual offered load is $\rho_s = \rho + \lambda\overline{V}$ due to the presence of vacations ($\overline{V}$ is the mean vacation period). Furthermore, the use of packet retransmissions to achieve reliability transforms a single packet transmission into a burst with the PGF of

$$G_b(z) = \frac{z\sum_{k=0}^{n_{ret}} z^k p_{err}^k}{\sum_{k=0}^{n_{ret}} p_{err}^k} \tag{5.17}$$

and mean burst length of $\overline{G_b(z)} = G'_b(z)|_{z=1}$.

Therefore, the total scaled offered load becomes

$$\rho_{tot} = (\rho + \lambda\overline{V})\overline{G_b(z)} \tag{5.18}$$

In our model, vacation has two parts. The cyclical or periodic vacation occurs in each polling cycle due to the activity of other nodes and its duration is the sum of service times of the other $N - 2$ ordinary nodes, which results in the PGF of

$$V_{cyc}(z) = (\rho_{tot}G_u(z)z + (1 - \rho_{tot})z^2)^{N-2} \tag{5.19}$$

Another type of vacation is caused by the in-band recharge pulse during which there can be no data communication. The recharging vacation takes place when a node goes in energy outage; its probability of occurrence is p_{out} and it lasts for fixed T_{crg} time cycles. The PGF

for the duration of this vacation is

$$V_{rec}(z) = p_{out} z^{T_{crg}} + (1 - p_{out}) \tag{5.20}$$

The PGF of combined vacation periods can be obtained as

$$V(z) = V_{cyc}(z) V_{crg}(z) \tag{5.21}$$

Mean vacation period $\overline{V}$ and its standard deviation V_{sd} are

$$\overline{V} = V'(z)|_{z=1} \tag{5.22}$$

$$V_{sd} = \sqrt{V''(z)|_{z=1} + V'(z)|_{z=1} - (V'(z)|_{z=1})^2} \tag{5.23}$$

Note that the mean vacation period and total offered load are inter-dependent, which means that eqs. (5.18) and (5.22) have to be solved together as a system.

5.5 Queueing Model

We assume that packets are served according to a FIFO discipline. We can model 1-limited $M/G/1$ queues by considering a packet followed by a vacation as a virtual packet with the PGF of $B_v(z) = G_u(z) G_d(z) V(z)$ (when there is no transmission error). In this case, the PGF for the number of packets remaining in the queue upon a packet departure is

$$\Pi(z) = \frac{(1 - \rho_{tot})(1 - V^*(\lambda - \lambda z)) B_v^*(\lambda - \lambda z)}{\lambda \overline{V} (B_v^*(\lambda - \lambda z) - z)} \tag{5.24}$$

$$= (1 - \lambda(\overline{G_u(z)} + \overline{G_d(z)} + \overline{V}))(1 - V^*(\lambda - \lambda z)) \tag{5.25}$$

$$\cdot \frac{G_u^*(\lambda - \lambda z) G_d^*(\lambda - \lambda z) V^*(\lambda - \lambda z)}{\lambda \overline{V} (G_u^*(\lambda - \lambda z) G_d^*(\lambda - \lambda z) V^*(\lambda - \lambda z) - z)} \tag{5.26}$$

For computational simplicity, we assume that the queue buffer is of infinite size; the margin of error due to this approximation is negligible under small to moderate load. Tak-

ing into account that the use of packet retransmissions to achieve reliability effectively transforms a single packet transmission into a burst, the size of which is given by (5.17), the PGF for the number of packets in the queue upon a packet departure becomes

$$\Pi_b(z) = \frac{(1-\rho_{tot})(1-V^*(\lambda-\lambda z))G_b(B_v^*(\lambda-\lambda z))}{\lambda\overline{V}G_b(B_v^*(\lambda-\lambda z)-z)} \tag{5.27}$$

where $B_v^*(\lambda-\lambda z)$ from (5.24) is replaced by the burst service time $G_b(B_v^*(\lambda-\lambda z))$.

Probability distribution of the number of packets in the queue after the departure of a packet can be transformed into the probability distribution of packet delay. During the time interval when a single packet stays in the system (i.e., the queueing time and service time), the number of packet arrivals will be equal to the number of packets remaining in the queue after the departure of that packet. Thus, if the response time for a packet is $T_r(z)$, (5.27) can be rewritten as

$$\Pi_b(z) = T_r^*(\lambda-\lambda z) \tag{5.28}$$

Waiting time $W(z)$ includes the waiting for all earlier packets, as well as the time required for unsuccessful transmissions of the target packet, and its probability distribution is

$$\Pi_b(z) = W^*(\lambda-\lambda z)G_u^*(\lambda-\lambda z) \tag{5.29}$$

By substituting $s = \lambda - \lambda z$ in the above expression, we can express the probability distri-

bution of packet waiting time as

$$W^*(s) = \frac{1}{G_u^*(s)}\Pi_b(1 - s/\lambda) \tag{5.30}$$

$$= \frac{(1-\rho_{tot})(1-V^*(s))G_b(G_u^*(s)G_d^*(s)V^*(s))}{\lambda\overline{V}(G_b(G_u^*(s)G_d^*(s)V^*(s)) - 1 + s/\lambda)G_u^*(s)} \tag{5.31}$$

$$= \frac{(1-\rho_{tot})(1-V^*(s))G_b(G_u^*(s)G_d^*(s)V^*(s))}{G_u^*(s)\overline{V}(\lambda G_b(G_u^*(s)G_d^*(s)V^*(s)) - \lambda + s)} \tag{5.32}$$

The k^{th} moment of packet delay can be calculated as the k^{th} derivative of LST $W^*(s)$, $(-1)^k W^{*(k)}(0)$. Mean waiting time and standard deviation can be calculated as

$$\overline{W} = -W^{*(1)}(s)|_{s=0} \tag{5.33}$$

$$W_{sd} = \sqrt{W^{*(2)}(s)|_{s=0} - (W^{*(1)}(s)|_{s=0})^2} \tag{5.34}$$

5.6 Performance evaluation

To assess the performance of the proposed MAC protocol, we have used Maple 16 from Maplesoft, Inc. [19] to solve the system of equations outlined above. We have considered networks with $N = 3$ to 13 nodes located within a 1 to 10 meter distance from the master node. Packet arrival rate was $\lambda = 0.011$ packets per node per time unit, which was set to $100\mu s$. All packets (POLL, DATA, and NULL) are assumed to take one time unit. DATA packets have 50 bytes (400 bits) while the bit error rate was varied from 10^{-5} to 10^{-3}. Maximum number of packet retransmissions n_{ret} was three; unsuccessful packets were dropped afterwards. Recharging period T_{crg} has a fixed duration of 1000 time cycles while the recharging power was $1W$. Mandatory sleeping period T_{sleep} of 50 cycles was imposed at the end of each polling cycle. Energy levels for units listed in Table energy-cycle were taken from the Texas Instruments' CC2540 data [41].

Our first experiment involves variable number of nodes and bit error rate. Total offered load ρ_{tot} is shown in Fig. 5.4(a): it depends very much on the number of nodes (i.e., network

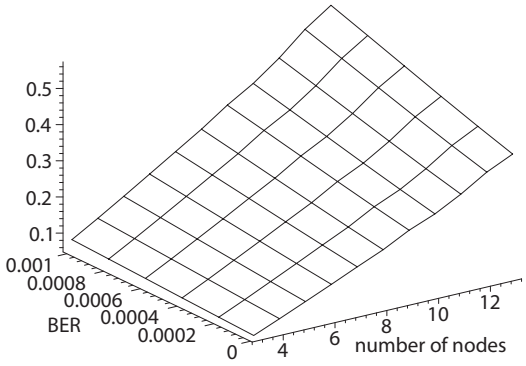

(a) Total offered load ρ_{tot}.

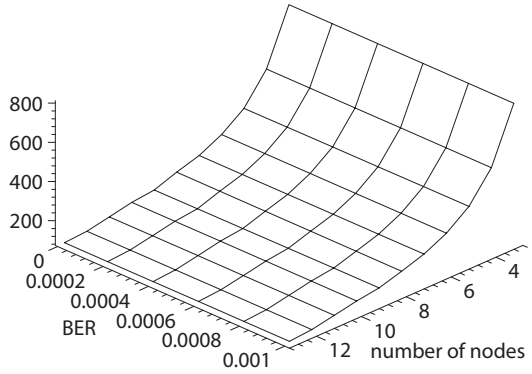

(b) Mean time between two consecutive recharging events.

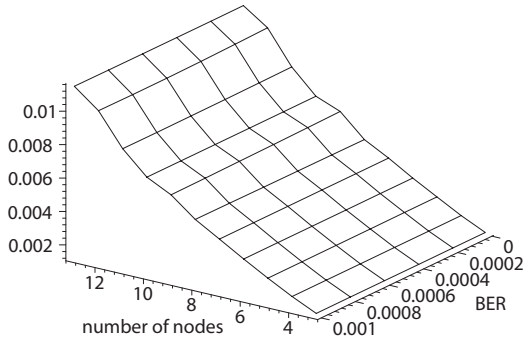

(c) Outage probability.

Figure 5.4: Representations of total offered load and recharging operation.

size) but only slightly on the bit error rate. Apart from the sheer increase in the number of packets, the number of nodes also indirectly affects the offered load through the duration of cyclic vacation which is an exponential function of the network size $N-2$, (5.19). Longer cyclic vacation results in more packet arrivals so any given node has proportionally less time to send data which eventually intensifies the offered load. On the other hand, increasing bit error rate causes a higher retransmission rate which subsequently increases the load, but the dependency is not as pronounced and the rate of increase is sub-exponential.

Mean number of cycles between consecutive recharging events is shown in Fig. 5.4(b). Again, the number of nodes is the major determining factor for these variables. With more nodes, any given node needs to listen to more POLL packet headers and, thus, consumes

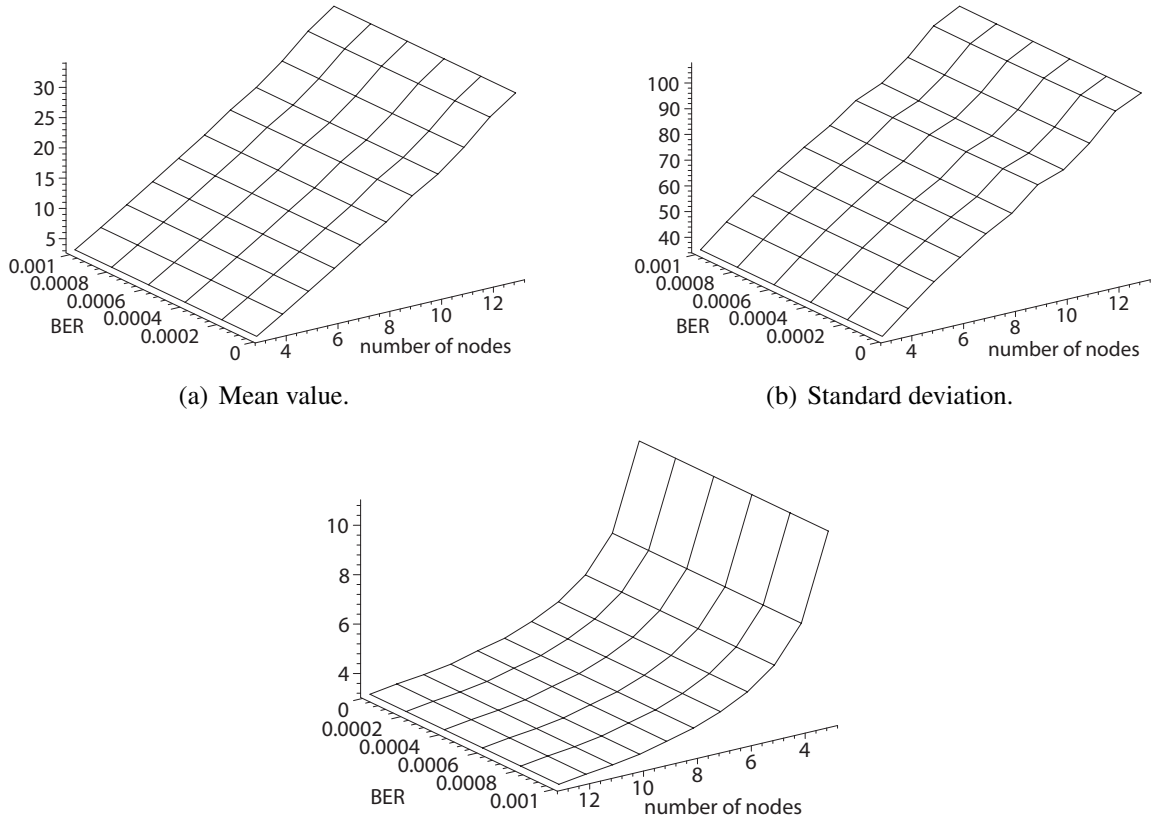

(a) Mean value.

(b) Standard deviation.

(c) Coefficient of variation.

Figure 5.5: Descriptors of vacation time.

more energy. As the result, the mean period between successive recharge points is inversely proportional to the network size N. By the same token, higher bit error rate causes more retransmissions, and DATA packets consume more energy than their NULL counterparts. Still, the dependency is not as pronounced, so that mean period decreases only slowly with BER. Energy outage probability shown in Fig. 5.4(c) is simply reciprocal of the mean period.

In the same setting, the descriptors of the vacation time are shown in Fig. 5.5. All three descriptors – mean, standard deviation, and coefficient of variation (defined as the ratio of the other two) – are strongly dependent on the number of nodes, as defined by (5.19); at the same time, they are virtually independent on the bit error rate. This last observation

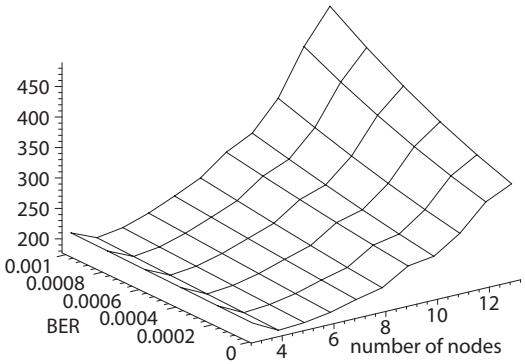

(a) Mean value.

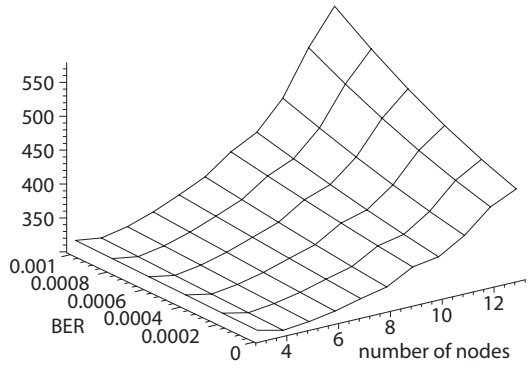

(b) Standard deviation.

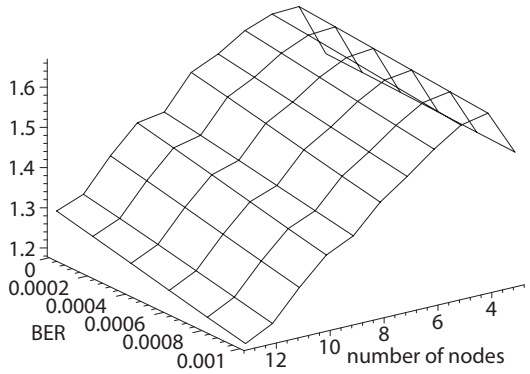

(c) Coefficient of variation.

Figure 5.6: Descriptors of packet queueing delay.

may be somewhat unexpected, as different intermediate variables are indeed affected by the bit error rate. However, one should keep in mind that the duration of both types of vacation periods in the MAC protocol are determined by the protocol itself rather than by the network and traffic parameters. We note that the coefficient of variation $V_{std}/\overline{V}$, shown in Fig. 5.5(c), decreases when the number of nodes increases, but shows strong hyper-exponential behavior throughout the observed range of parameter values.

The diagrams in Fig. 5.6 show the mean, standard deviation and coefficient of variation of the packet delay at the node queue. As could be expected, mean packet delay in Fig. 5.6(a) increases with the number of nodes as the polling cycle gets longer. It also increases with bit error rate, but only at larger network size where the impact of packet

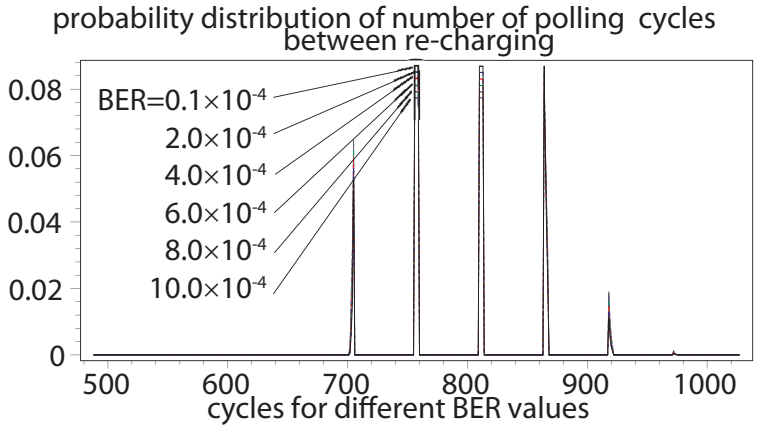

(a) Network with $m = 3$ nodes.

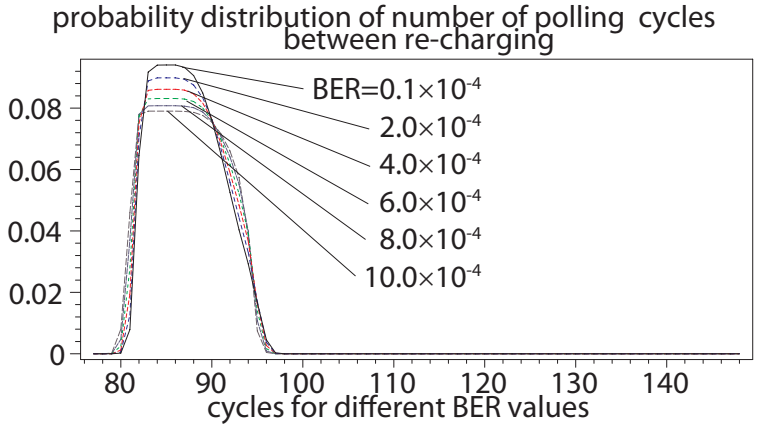

(b) Network with $m = 13$ nodes.

Figure 5.7: Probability distribution of the number of polling cycles between two consecutive recharging events.

retransmissions begins to show. Standard deviation of delay time, Fig. 5.6(b), exhibits similar behavior. However, coefficient of variation decreases when the number of nodes increases, as the variations in delay caused by different number of retransmissions from different nodes tend to cancel each other. It is worth noting that the value of the coefficient of variation is between 1.2 and 1.7 – i.e., mildly hyper-exponential – in the observed range of independent variables.

Probability distribution of the number of polling cycles between consecutive recharging pulses is shown in Fig. 5.7 as the function of bit error rate. When the network has three

nodes (master and two ordinary ones), the probability distribution, shown in Fig. 5.7(a), is characterized by discrete peaks caused by the mandatory sleep period imposed after each polling cycle which has four time units (two nodes, each with a POLL packet followed by a DATA or NULL packet). The impact of bit error rate is very small, making the peaks obtained at different values almost indistinguishable from each other. In this scenario, recharging occurs after about 700 to 900 cycles, which is quite good but the improvement is obtained at the expense of short cycles with higher sleeping probability.

When the network has 13 nodes (master and twelve ordinary ones), the probability distributions are spread over a wider range of values, as can be seen in Fig. 5.7(b). While the curves obtained for different values of bit error rate are still close to each other, the higher values result in slightly but noticeably wider distribution shape than lower ones. This is the consequence of longer polling cycles (24 time units) but the period between recharge pulses is much shorter than in the previous case: it occurs between 80 and 96 cycles. For networks of larger size, energy consumption is faster and recharging becomes more frequent, which means the corresponding distributions will be wider and shifted toward smaller cycle values.

Chapter 6

Zoning and relaying-based MAC protocol

We have seen in previous chapters that one of the most important problems with recharging through RF pulses is that the amount of energy obtained through recharging depends on distance: nodes which are farther away from the master receive smaller amounts of energy due to path loss. As the result, the period between successive recharge requests is determined by nodes farthest away from the master [13]. Closer nodes get recharged more often than necessary and their batteries never reach the energy threshold [23]. Path loss can't be eliminated, therefore the only feasible way in which network lifetime could be prolonged is by adapting the energy consumption so that nodes closer to the recharging source consume more energy whilst farther ones consume less. Equalization of energy consumption rate for different nodes is, thus, the key to extending the period between successive recharges and, consequently, increasing the network lifetime.

A promising way toward such equalization is to apply zoning to the sensor field. Zoning involves dividing the nodes into circular zones or coronas centered at the master. Nodes in the zone closest to the master transmit their packets directly, while nodes in the most distant zone perform no relaying. Nodes in other zones act as relays for the packets sent by their counterparts in the zones farther away from the master. Finally, nodes in the most

distant zone simply relay their packets to nodes in a closer zone.

The main benefit of this approach stems from the fact that transmissions need only reach a node in the closer zone rather than the master. As the result, transmitter nodes can reduce their transmission power which will reduce their energy consumption; this will provide the most benefit to the nodes in the most distant zone as they receive the least amount of energy during recharge [13].

Zoning also requires that nodes closer to the master receive and retransmit other nodes' packets which will increase their power consumption. However, this increase is less critical since the energy increment received during recharge by the nodes in closer zones is much higher due to shorter distance to the master. Moreover, those nodes will be able to reduce their transmission power which will offset the increase in consumption to some extent. Overall, this approach should result in a more balanced power consumption and an increase in the time interval between successive recharging pulses.

In this chapter we present a MAC protocol based on polling that fully supports zoning and relaying. We then evaluate its performance using the tools of probabilistic analysis and queuing theory. We also describe a network formation protocol that divides the nodes into zones.

6.1 The MAC protocol

We assume that sensor nodes are randomly positioned, following uniform spatial distribution, in a circle of diameter $2D$ centered at the master. Nodes are logically divided into n_z zones shaped as concentric disks or coronas centered at the master, as shown in Fig. 6.1(a). Assuming that the master is located in zone 0 with the radius of zero, the outer radius of each zone $j = 0 \,..\, n_z$ is d_j, where $d_0 = 0$ and $d_{n_z} = D$. Nodes in zone 1 send their packets directly to the master; nodes in zones $j > 1$ send their packets to a relay node in the next lower zone $j - 1$, as will be explained below.

To balance the load for nodes that act as relays, we assume that the sensor field is also

divided into logical sectors such that each sector contains at most one node for each zone. In this manner, each node has a contiguous path to the master through nodes in the same sector but in lower-numbered zones. This setup is schematically presented in Fig. 6.1(a) for a network with three zones and five sectors.

The setup described above requires that each zone contains approximately equal number of nodes. Given uniform spatial distribution of nodes, this can be achieved if zone areas are equal, as per following system of equations:

$$d_j^2 - d_{j-1}^2 = d_{j-1}^2 - d_{j-2}^2, \qquad j = 2 \,..\, n_z \tag{6.1}$$

6.1.1 Network formation

In order to establish zones and sectors, the master needs to conduct network formation algorithm. We assume that master knows the network diameter D, the number of zones n_z it wants to establish, and the outer radius of each zone which can be obtained from the system of equations above.

The algorithm consists of three phases: paging, zone establishment, and sector establishment.

In the *paging phase*, the master learns the IDs and approximate distances of m network nodes. To this end, the master transmits periodic beacon packets to which nodes reply with their IDs. Collisions may be minimized by using an appropriate random wait procedure. If nodes reply with constant power, master will be able to estimate their distance on the basis of received signal strength (RSS) [18].

In the *zone establishment phase*, the master groups the nodes into zones according to their distance. It transmits beacon packets containing tuples of node ID and zone number as well as estimated power level for that zone. Each zone $j \in 1 \,..\, n_z$ contains m_j nodes, hence $m = \sum_{j=1}^{n_z} m_j$. To ensure that the next phase, sector establishment, creates the required

contiguous packet paths towards the master, the following relations must hold:

$$m_{n_z} \leq m_{n_z-1} \ldots \leq m_2 \leq m_1 \tag{6.2}$$

$$m_1 = \left\lceil \frac{m}{n_z} \right\rceil \tag{6.3}$$

They should not be difficult to achieve in case of uniform spatial distribution of nodes.

Finally, in the *sector establishment phase*, the master helps nodes establish sectors. This phase consists of a total of n_z rounds, one per each zone, starting from the most distant one.

First, the master sends a special POLL packet with sector inquiry to each node in zone n_z, which then respond with a packet to their counterparts in the next lower zone $n_z - 1$. Alternatively, a single POLL packet may be used for the entire zone, in which case the nodes transmit according to a schedule derived from their IDs or after a suitable random delay.

The response packet is transmitted at the power level established in the previous phase for the zone n_z. It is received by one or more nodes in zone $n_z - 1$ which record the sender ID and the RSS of the packet.

In the next round, the master sends the sector inquiry to each node in zone $n_z - 1$. These node respond by forwarding the response packets received from nodes in the next higher zone and the corresponding RSS values; as before, the nodes in the next lower zone $n_z - 2$ record the received packets and corresponding RSS values.

This procedure is repeated for each zone in descending order. Upon receiving all forwarded packets from zone 1, the master can group nodes into m_1 sectors and inform them accordingly. Grouping is done so that each sector contains a connected path of n_z nodes, one from each zone, ending with the master. Within a given sector, a node in a given zone acts as the relay for the node in the next higher zone and, indirectly, for nodes in all higher zones. Note that some paths may not begin at the most distant zone, depending on the total number of nodes, but they must be contiguous nonetheless.

6.1.2 MAC operation: polling

Once zones and sectors are established, normal operation may commence. It consists of poll cycles conducted sequentially over sectors. In each polling cycle master sends one POLL packet per each sector which contains the sector number. All nodes listen to the header of the POLL packet: nodes that don't hear their sector number may go back to sleep immediately, while nodes that hear their sector number will calculate the times for their receive and transmit activities, as follows. Nodes in a given sector communicate only when their sector is polled and sleep at other times. However, they need to listen to headers of POLL packets for other sectors, as explained below.

After hearing the POLL packet, the node in the most distant zone n_z transmits a packet to a node in the next lower zone, and immediately goes to sleep. If there was data to send, the node sends a DATA packet to the node from the same sector but in the next lower zone $n_z - 1$; otherwise, it sends a NULL packet to that same node.

The designated relay node receives and subsequently retransmits the packet to a node in the next lower zone, followed by a DATA or NULL packet of its own. This process continues until the node in zone 1 sends all the packets from its sector to the master, which then proceeds to poll the next sector.

Note that NULL packets contain no data and, thus, can be shorter than DATA packets. While this can be used to shorten the data transmission, it also complicates scheduling as all nodes in a given sector would have to listen for longer time – from the sector POLL packet until receiving all packets from higher zones. In this work we have adopted a simpler solution in which the poll period is divided into fixed duration transmission/reception slots. Thus the node in zone $i = 1 \,..\, n_z - 1$ can turn its radio on after $(n_z - i - 1)(n_z - i)/2$ packet slots following the POLL packet. It can switch to transmission after listening to exactly $n_z - i$ packets, some of which may be NULL, and retransmit the received packets, followed by a packet of its own, to the next lower zone or the master, in case $i = 1$.

Consequently, the sector service time consists of POLL packet time and $n_z(n_z + 1)/2$ packet slots. The entire polling cycle contains m_1 sector service times.

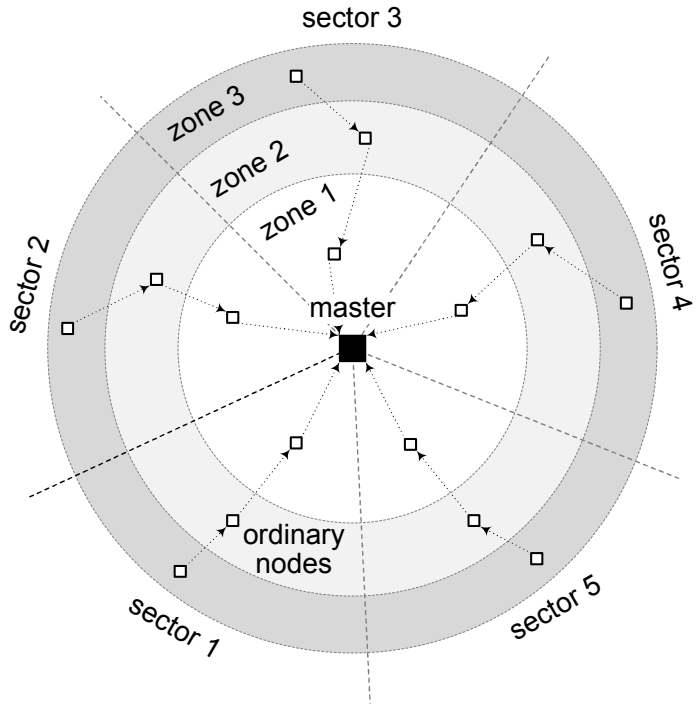

(a) Logical layout of the network with zones and sectors.

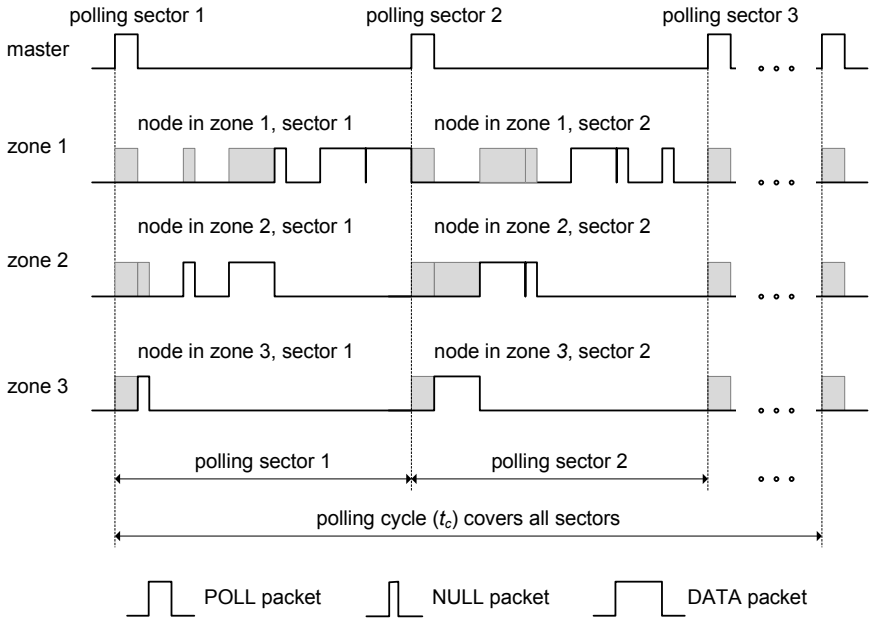

(b) Polling MAC operation. Shaded rectangles depict listening/receiving packets.

Figure 6.1: Pertaining to the principle of zoning and operation of the MAC protocol.

6.1.3 MAC operation: recharging

When a node detects that its energy has dropped below a certain threshold E_{thr}, it will request a recharge by appending the appropriate information to the header of its own DATA or NULL packet. Upon receiving such a request (which will be piggybacked on one of the packets relayed by the node in zone 1 of the current sector), the master completes the current sector poll and announces the upcoming recharge pulse in the next sector POLL packet. This is the reason why all nodes must listen to POLL packet regardless of the sector. Polling continues after the recharge pulse at the point it was interrupted.

Recharging is effected by the master through a pulse of power P_w and duration T_p. The energy increment received by a given node i is $\Delta_i = P_w T_p Pl_i$, where Pl_i is the path loss that is inversely proportional to the distance to the master raised to the power of path loss exponent, typically 2 to 4 [30].

Energy consumption of a node depends on its zone and the total number of zones. Nodes in zone j should adjust their transmit power so as to make sure their packets are correctly received by the relay nodes in zone $j-1$, which in the worst case amounts to the distance of $d_j - d_{j-2}$. On the other hand, receiving power is always the same and does not depend on distance [2, 41]. As the number of packets received and transmitted grows linearly as the zone index decreases, nodes close to the master spend more energy on packet relaying than nodes closer to the network edge.

The operation of the MAC protocol in a network with three zones is schematically shown in Fig. 6.1(b).

6.2 Modeling the MAC protocol

Let us now describe the analytical model for the MAC protocol, including both time and energy considerations. For simplicity, we will assume that all time intervals are expressed in multiples of the basic slot T, whereas all energy values are multiples of basic energy quantum E_u. Motivated by the data for a typical Bluetooth LE (low energy) chipset solution

[2], we will assume $T_s = 25\mu s$ and $E_u = 0.25\mu J$. Assuming packet sizes of 20, 40 and 80 bytes for NULL, sector POLL and DATA packet, respectively, that fit one, two and four slots, respectively, we obtain raw data rate of 6.4 Mpbs.

We assume that each data packet has length L_d in bits. If bit error rate is BER, packet error rate will be $PER = 1 - (1 - BER)^{L_d}$. MAC protocol has partial reliability implemented through Automatic Repeat Request (ARQ) technique with up to n_r retries for packet. To reduce energy consumption, DATA packets sent from a node are acknowledged by setting a dedicated field in the header of the POLL packet targeting that node in the next cycle.

During normal network operation, node uses its energy for data sensing, listening and transmitting. Listening consists of POLL/DATA packet reception and listening to the headers of other sector POLL packets. Transmission consists of relaying and transmission/retransmission of DATA and NULL packets. Energy consumption depends on the actual zone, total number of zones and sectors, traffic intensity, bit error rate, and maximum number of retries n_r. When the energy of node i drops to E_{thr}, the node will request recharging. When recharging is finished, the energy level will be $\min(E_c, E_{thr} + \Delta_i)$, where $E_c \approx E_{thr} + \max \Delta_i, i = 1 \ldots m$, is the battery capacity.

Energy budget for packet transmission depends on the maximum distance between adjacent zones i.e. on $d_j - d_{j-1}$, $j = 2 \ldots n_z$. Transmission power in all zones should be scaled such that signal in adjacent zone is received with same RSS and, consequently, same SINR. The reference RSS is the one measured after receiving POLL signal by nodes in zone n_z. If master transmits POLL packet with power P_{poll} and path loss exponent is l, then nodes in zone j should transmit with power $Pt_j = P_{poll} \frac{(d_j - d_{j-2})^l}{D^l}$.

Time between two consecutive recharging pulses is a random variable which depends on the number of zones and sectors, node traffic, and bit error rate. We assume uniform traffic load over all nodes. Obviously nodes in different zones will send recharging requests at different times due to different distances and relaying load. Our task is to analyze recharging periods in different zones and evaluate its impact on network capacity and packet delay.

6.2.1 Joint probability distribution of polling cycle time and consumed energy per cycle

In calculating the joint probability distribution of polling cycle time and consumed energy per cycle, we will use energy consumption variables, absolute and relative to the energy unit E_u, listed in Tables 6.1 and 6.2 for listening and transmission, respectively. (Note that the latter values depend on the zone in which the node resides.) In the development of the required Probability Generating Functions (PGFs), variable y will model the polling cycle, while variable z will denote energy consumption expressed in basic energy units; time periods (in base time slots) will be denoted with variable x.

PGF for the energy consumption of a single data packet sent from a node in zone j is

$$Epd(y,z) = \frac{z^{k_s} z^{k_{td,j}} y(1-PER) \sum_{i=0}^{n_r} y(z^{k_{td,j}})^i PER^i}{(1-PER) \sum_{i=0}^{n_r} PER^i} \tag{6.4}$$

For simplicity we have assumed that a NULL packet will be always decoded correctly; if this does not hold, the required model extension is straightforward. Mean value of $Epd(y,z)$ with respect to the number of cycles is $\overline{Epd_c} = \frac{d}{dy} Epd(y,z)\Big|_{y=1,z=1}$ which, for simplicity, will be written as $\overline{Epd_c} = \frac{d}{dy} Epd(1,1)$. From (6.4), we can find the probability of initial transmission attempt, including sensing, for a node in zone j as

$$Pf_j = 1/\overline{Epd_c} \tag{6.5}$$

If $Epn_j(z) = z^{k_{tn,j}}$ denotes the PGF for the transmission of a null packet in zone j and $\rho_{b,j}$ denotes the effective utilization of a node, the PGF for transmission energy for a single packet by the node in zone j becomes

$$Ep_j(y,z) = \rho_{b,j} z^{k_{td,j}} (Pf_j z^{k_s} + 1 - Pf_j) + (1-\rho_{b,j}) z^{k_{tn,j}} \tag{6.6}$$

Using (6.6) we can derive the PGF for energy expenditure for all activities of a node in

Table 6.1: Basic energy units for sensing and listening.

Energy expenditure	label	E_u multiple
energy unit	E_u	1
sensing	E_s	k_s
listening to the POLL packet	E_{lp}	k_{lp}
listening to the header of POLL packet	E_a	k_{la}
listening to data packet	E_{ld}	k_{ld}
listening to null packet	E_{ln}	k_{ln}

Table 6.2: Basic energy units for transmission in zone j.

Energy expenditure	label	E_u multiple
energy unit	E_u	1
transmitting null packet	$E_{tn,j}$	$k_{tn,j}$
transmitting data packet	$E_{td,j}$	$k_{td,j}$

zone j as

$$\begin{aligned} Ez_j(y,z) &= yz^{k_{lp}} z^{k_{la}(m_1-1)} \\ &\cdot(\rho_{b,j} z^{k_{ld}} + (1-\rho_{b,j}) z^{k_{ln}})^{n_z-j} \\ &\cdot(\rho_{b,j} z^{k_{td,j}} + (1-\rho_{b,j}) z^{k_{tn,j}})^{n_z-j} Ep_j(y,z) \end{aligned} \tag{6.7}$$

where m_1 denotes the number of sectors. Maximum and minimum energy expenditure of a node during sector poll in zone j are, then,

$$\begin{aligned} Ez_j^{(max)} &= k_{lp} + (m_1-1)k_{la} + k_{ld}(n_z-j) + k_s \\ &\quad + k_{td,j}(n_z-j+1) \\ Ez_j^{(min)} &= k_{lp} + (m_1-1)k_{la} + k_{ln}(n_z-j) \\ &\quad + k_{tn,j}(nz-j+1) \end{aligned}$$

This allows us to set the threshold for requesting recharging to a multiple of maximum energy expenditure of a node in zone 1 (closest to the master). Upon recharging, nodes in zone j will have energy budget of

$$Eb_j = E_{thr} + \Delta_j = E_{thr} + P_w T_p P l_i \tag{6.8}$$

The recharging request from this zone will be sent at a point in time between $l_{min,j} = \Delta_j / Ez_j^{(max)}$ and $l_{max,j} = \Delta_j / Ez_j^{(max)}$ polling cycles, depending on the zone, traffic intensity, error rate, and allowed number of retries. Shortest period between successive recharging requests occurs when each of the nodes in the sector has a new data packet at all times, while the longest period (and, consequently, maximum number of polling cycles) corresponds to the scenario where node buffers in the sector are always empty so that only NULL packets are transmitted.

Joint PGF of energy consumption when the number of polling cycles ranges between $l_{min,j}$ and $l_{max,j}$ is

$$SE_j(y,z) = \frac{\sum_{i=l_{min,j}}^{l_{max,j}} Ez_j(y,z)^i}{l_{max,j} - l_{min,j} + 1} \tag{6.9}$$

We can manipulate coefficients in the last expression in order to derive PGF of the recharging period in zone j, as shown in Algorithm 3.

Mean and standard deviation of the number of polling cycles between two successive recharging events in zone j are

$$\begin{aligned} \overline{T_{rec,j}} &= \frac{d}{dy} T_{rec,j}(1) \\ \sigma(T_{rec,j}) &= \sqrt{\frac{d^2}{dy^2} T_{rec,j}(1) - \overline{T_{rec,j}} + \overline{T_{rec,j}}^2} \end{aligned} \tag{6.10}$$

while the coefficient of variation is $Cv(T_{rec,j}) = \frac{\sigma(T_{rec,j})}{\overline{T_{rec,j}}}$. Finally, recharging probability

Algorithm 3: Creation of PGF for recharging period.

Data: $SE_j(y, z)$
Result: PGF for the recharging period (in polling cycles) in zone j

find minimal $Sminy_j$ and maximal $Smaxy_j$ degree of variable y in $SE_j(y, z)$;
for $i \leftarrow Sminy_j$ **to** $Smaxy_j$ **do**
    $cc[i, j](z) =$ coefficient$(SE_j(y, z), y, i)$;
    find minimal $minz_j$ and maximal $maxz_j$ degree of variable z in $cc[i, j](z)$;
    for $k \leftarrow minz_j$ **to** $maxz_j$ **do**
        $cic[k] =$ coefficient$(cc[i, j](z), z, k)$;
    form mass probability that energy resource will be exceeded in i-th cycle $Pm_{j,i} \leftarrow \sum_{k=E_{a,j}}^{maxz_j} cic[k]$;
form polynomial of recharging period as $T_{recp,j}(y) \leftarrow \sum_{i=miny_j}^{maxy_j} Pm_{j,i} y^i$;
form PGF of recharging period as $T_{rec,j}(y) \leftarrow T_{recp,j}(y)/T_{recp,j}(1) = \sum_{i=miny_j}^{maxy_j} P_{t(j,i)} y^i$;

can be calculated as

$$P_{r,j} = \frac{1}{\overline{\overline{T_{rec,j}}}} \tag{6.11}$$

6.2.2 Network cycle time

In the proposed MAC protocol, sectors are polled sequentially, while nodes within a sector transmit in the descending order of zones. Therefore, we need to model sector transmission time before following with the model of network cycle time.

Assuming that variable x denotes a basic time slot, packet sizes for NULL, sector POLL and DATA packets can be represented with PGFs $Gn(x) = x$, $Gp(x) = x^2$ and $Gd(x) = x^4(x)$, respectively. As both NULL and DATA packets are sent in a fixed-size transmission slot, duration of node service time in zone j can be calculated as

$$S_j(x) = Gd(x)^{2(n_z - j)+1} \tag{6.12}$$

The total sector service time is then

$$S(x) = Gp(x)Gd(x)^{(n_z(n_z+1)/2)} \tag{6.13}$$

and network cycle time is

$$T_{cyc}(x) = S(x)^{m_1} \tag{6.14}$$

The PGF of the recharging time was previously calculated as function of polling cycles in algorithm 3; its PGF expressed in slots is $T_{rec,j}(T_{cyc}(x))$.

6.3 Queueing model

In a single network cycle, a node can transmit at most one packet of its own; the remaining time is unavailable for service regardless of the zone in which the node resides. In terms of queueing theory, this constitutes a (cycle) vacation. As all nodes share the same network cycle, cycle vacation time will be the same for all of them: it consists of $m_1 - 1$ sector service times and all packet times in the target sector except the packet sent by target node, hence its PGF is

$$V_c(x) = S(x)^{(m_1-1)}Gp(x)Gd(x)^{n_z(n_z+1)/2-1} \tag{6.15}$$

Recharging vacation occurs during the recharging pulse when no transmission can take place; it is also common to all nodes in a given zone, say j, and its PGF is

$$V_{r,j}(x) = P_{r,j}x^{T_p} + (1 - P_{r,j}) \tag{6.16}$$

The total vacation experienced by a single node has the PGF of

$$V_j(x) = V_{r,j}(x)V_c(x) \tag{6.17}$$

and its mean value and standard deviation are

$$\overline{V_j} = \frac{d}{dx}V_j(1) \tag{6.18}$$

$$\sigma(V_j) = \sqrt{\frac{d^2}{dx^2}V_j(1) - (\overline{V_j})^2 + \overline{V_j}} \tag{6.19}$$

6.3.1 Offered load

As noted above, any given node can transmit at most one DATA or NULL packet in a polling cycle despite different relaying load across zones. As the network polling cycle is common to all nodes, this MAC scheme can be modeled using an approach similar to M/G/1 gated limited system with vacations [33]. For simplicity, we will assume that node buffer has infinite capacity; if needed, a finite buffer can be modeled without difficulty.

We assume that packets arrive to each node according to a Poisson process with rate λ. Basic offered load per node is $\rho = \lambda\overline{Gd}$; however, vacation after each packet transmission in zone j increases the offered load to

$$\rho_{v,j} = \rho + \lambda\overline{V_j} \tag{6.20}$$

where $\overline{V_j}$ denotes mean length of vacation period in zone j.

Packet retransmissions will also increase the offered load as they use bandwidth, and each retransmission is followed by a vacation as well. As the result, a single packet transmission is effectively changed into a burst transmission with the PGF of

$$Gb(x) = \frac{(1-PER)x\sum_{i=0}^{n_r} x^i PER^i}{(1-PER)\sum_{i=0}^{n_r} PER^i} \tag{6.21}$$

and mean value of $\overline{Gb} = \frac{d}{dx}Gb(1)$.

Thus, total effective offered load becomes

$$\rho_{b,j} = (\rho + \lambda\overline{V_j})\overline{Gb} \tag{6.22}$$

Note that offered load depends on mean vacation time, but the cyclical vacation depends on offered load; therefore, equations (6.4) up to (6.22) have to be solved together.

6.3.2 Waiting time

Since nodes in each zone modeled in isolation have vacations of different duration, waiting times for packets in each zone will be different. Assuming FIFO servicing discipline, we may use existing framework for limited M/G/1 queues with vacations but without transmission errors. To this end, we need to consider a packet followed by a vacation as a virtual packet with PGF of $B_{v,j}(x) = Gd(x)V_j(x)$. In that case, the number of packets left in the queue after a departing uplink packet can be expressed as

$$\Pi_j(x) = \frac{(1-\rho_{v,j})(1-V_j^*(\lambda-\lambda x))B_{v,j}^*(\lambda-\lambda x)}{\lambda\overline{V_j}(B_{v,j}^*(\lambda-\lambda x)-x)} \tag{6.23}$$

$$= (1-\lambda(\overline{Gd}+\overline{V_j}))(1-V_j^*(\lambda-\lambda x)) \cdot \frac{Gd^*(\lambda-\lambda x)V_j^*(\lambda-\lambda x)}{\lambda\overline{V_j}(Gd^*(\lambda-\lambda x)V_j^*(\lambda-\lambda x)-x)} \tag{6.24}$$

where PGFs for packet time and vacation time were converted into Laplace-Stieltjes Transforms (LSTs) by replacing variable x with e^{-s} (e.g., $V_j(x)$ was converted to $V_j^*(s)$).

As noted above, packet retransmissions will transform virtual packet into a packet burst with random length, the PGF of which is

$$Q_j(x) = Gb(B_{v,j}(x)) \tag{6.25}$$

and its LST becomes $Q_j^*(s) = Gb(B_{v,j}(e^{-s}))$. When this effect is included in the distribu-

tion of the number of packets left after departing packet we obtain the PGF of

$$\Pi_j(x) = \frac{(1-\rho_{b,j})(1-V_j^*(\lambda-\lambda x))Q_j^*(\lambda-\lambda x))}{\lambda\overline{V_j}(Q_j^*(\lambda-\lambda x)-x)} \tag{6.26}$$

Probability distribution of packet delay, expressed with LST of $W_j^*(s)$, can be found from the distribution of response time $T_j^*(s)$ and packet service time $Gd^*(s)$, since response time is the sum of waiting and packet service times, i.e., $T_j^*(s) = W_j^*(s)Gd^*(s)$. In stable state, the number of new packet arrivals during the response time of the target packet is equal to the number of packets left after the departure of the target packet, which may be written as

$$\Pi_j(x) = T_j^*(\lambda-\lambda x) \tag{6.27}$$

In the presence of transmission errors and retransmissions, response time for a packet consists of waiting time until the target packet is transmitted correctly; this includes waiting for all previous packets as well as for unsuccessful transmissions of the target packet. Therefore, the probability distribution of waiting time may be described with

$$\Pi_j(x) = W_j^*(\lambda-\lambda x)Gd^*(\lambda-\lambda x) \tag{6.28}$$

Since packet waiting time is a continuous random variable, we need to express it as a LST through the substitution $s = \lambda - \lambda x$, or, equivalently, $x = 1 - \frac{s}{\lambda}$. The probability distribution of the packet delay becomes

$$\begin{aligned} W_j^*(s) &= \frac{1}{Gd^*(s)}\Pi_j(1-\frac{s}{\lambda}) \\ &= \frac{(1-\rho_{b,j})(1-V_j^*(s))Q_j^*(s)}{\lambda\overline{V_j}Gd^*(s)(Q_j^*(s)-1+s/\lambda)} \\ &= \frac{(1-\rho_{b,j})(1-V_j^*(s))Q_j^*(s)}{Gd^*(s)\overline{V_j}(\lambda Q_j^*(s)-\lambda+s)} \end{aligned} \tag{6.29}$$

k-th moment of packet delay can be obtained as $(-1)^k W_j^{*(k)}(0)$. For example, standard deviation of waiting time is obtained as

$$W_{j,stdev} = \sqrt{W_j^{*(2)}(0) - W_j^{*(1)}(0)^2} \tag{6.30}$$

6.4 Performance results

We have varied the number of zones between $n_z = 2$ to $n_z = 5$. We assume that networks has $m = 25$ nodes including the master, except for the case when $n_z = 5$ where for simplicity we have adopted $m = 26$. Number of sectors is $m_1 = (m-1)/n_z$. Bit error rate is set to $BER = 10^{-5}$ and number of packet retransmissions is $n_r = 3$.

Charging pulse lasts for $T_p = 20ms$ (i.e., 800 slots) and its power is 1W. Network diameter is set to $D = 10$m. Path loss exponent is set to the free-space value of 2. Energy consumption data for reception and transmission are taken from [41, 2].

Uplink packet arrival rate was varied between 0.0009 and 0.0041 arrivals per node per unit slot; these values were chosen so that the maximum value of offered load is close to one. However, the value of 0.0041 packets per node per slot is not shown in all diagrams, for reasons to be explained below. Downlink traffic consists exclusively of sector POLL packets.

Our first set of diagrams depicts the performance of the recharging process. The corresponding results are shown in Fig. 6.2 to 6.5, for network with 2, 3, 4, and 5 zones, respectively, while columns depict total offered load per zone, mean time between successive recharging pulses (in milliseconds), and coefficient of variation of that time, respectively. The two last parameters were calculated for each zone in isolation, in order to be able to accurately evaluate their behavior.

As each zone has equal number of nodes, the offered load is nearly constant for each zone. It increases in a nearly linear fashion with packet arrival rate, as can be expected.

Mean recharging interval decreases with offered load, as more packets mean more en-

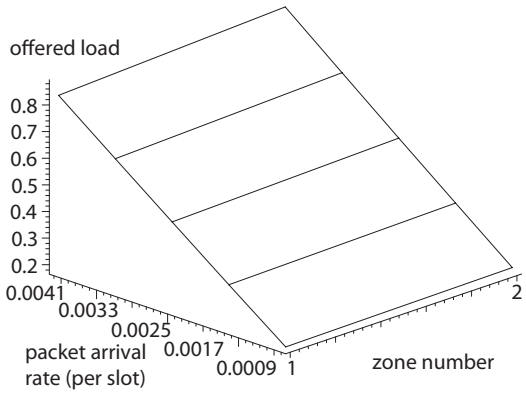

(a) Total offered load.

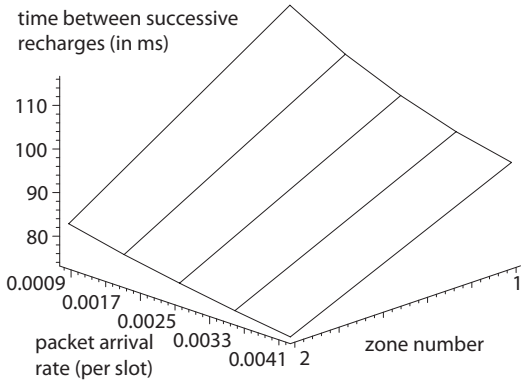

(b) Mean time between successive recharging pulsess.

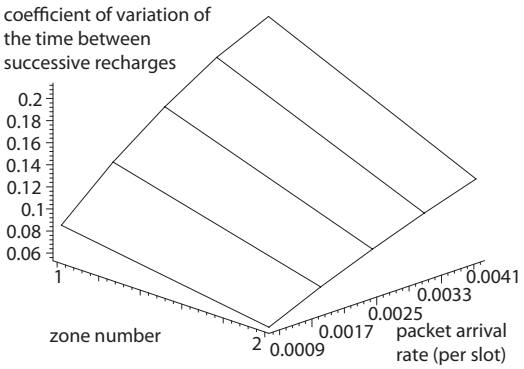

(c) Coefficient of variation of the time interval between successive recharging pulses.

Figure 6.2: Performance descriptors of the recharging process, network with $n_z = 2$ zones.

ergy consumption and require more frequent recharging. Mean recharging interval also depends on the actual zone as well as on the total number of zones. In general, nodes in the zone closest to the master (zone 1) enjoy the longest operational time due to the fact that they receive the highest amount of energy during recharge; by the same token, nodes located farthest from the master experience the shortest operational time.

However, relaying changes the picture since nodes in all zones but the highest-numbered one use energy for relaying as well, and nodes in closer zones have to relay more packets. As the result, shortest mean time between successive recharging pulses can be found in zone 2 in the network with two zones, but in zones 2 and 3 in the network with three zones,

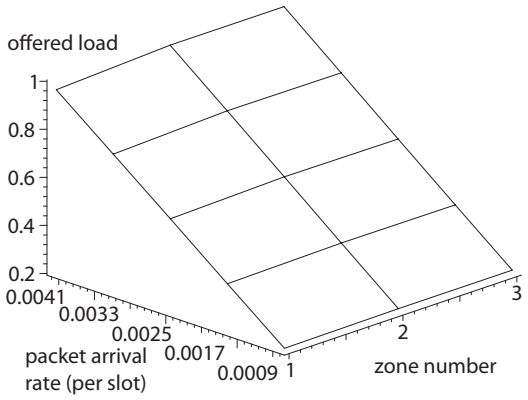

(a) Total offered loads.

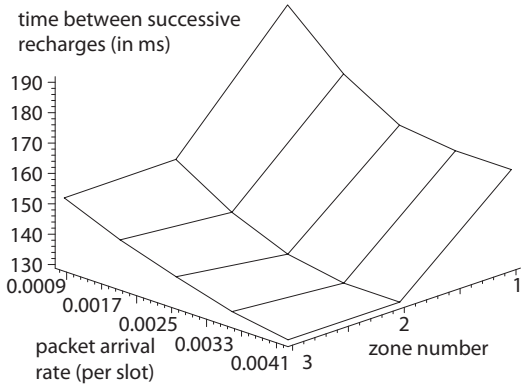

(b) Mean time between successive recharging pulses.

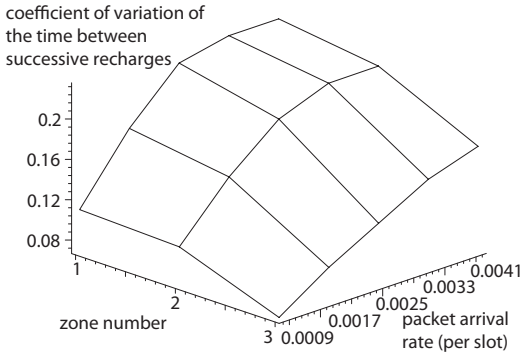

(c) Coefficient of variation of the time interval between successive recharging pulses.

Figure 6.3: Performance descriptors of the recharging process, network with $n_z = 3$ zones.

and in zone 3 in the network with four or five zones.

Coefficient of variation of the recharging interval ranges up to 0.2 to 0.3, depending on the number of zones. Due to the random character of node traffic, the first node to request recharge in a given polling cycle can be in (almost) any zone. To verify this observation, we have plotted the probability distribution of recharge interval in Fig. 6.6 for two different number of zones and three different values of packet arrival rate. In the network with two zones (top row), the two probability distributions are virtually disjoint at low arrival rates, Fig. 6.6(a). As the distribution for zone 2 occurs at lower values of the recharging interval than the one for zone 1, virtually all requests for recharging will come from zone

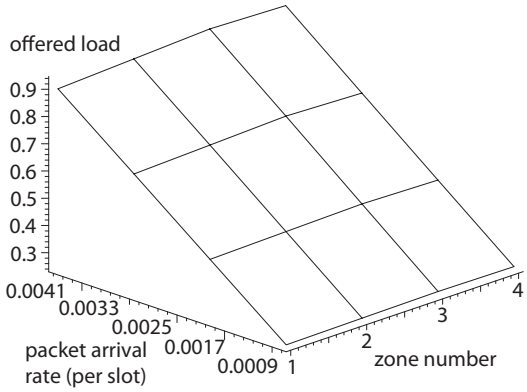

(a) Total offered load.

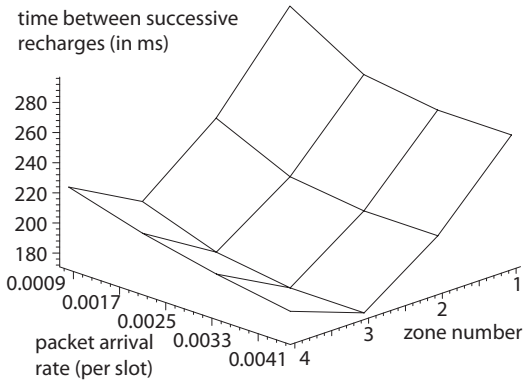

(b) Mean time between successive recharging pulses.

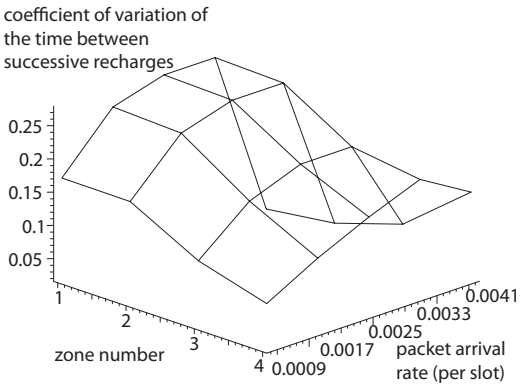

(c) Coefficient of variation of the time interval between successive recharging pulses.

Figure 6.4: Performance descriptors of the recharging process, network with $n_z = 4$ zones.

2. However, as the packet arrival rate increase, Figs. 6.6(c) and 6.6(e), the two distributions begin to show more and more overlap, which means there is increasing probability that a recharge request may originate from a node in zone 1 as well.

In the network with four zones (bottom row), probability distributions overlap in a large portion of the observed range of packet arrival rates. In this case, a recharge request may come from nodes in different zones, although the corresponding probabilities will differ, with nodes in the most distant zone most likely to send such a request.

Note that our model gives complete probability distribution of the time between successive recharge pulses, hence the actual probability that a node in zone n is more likely to

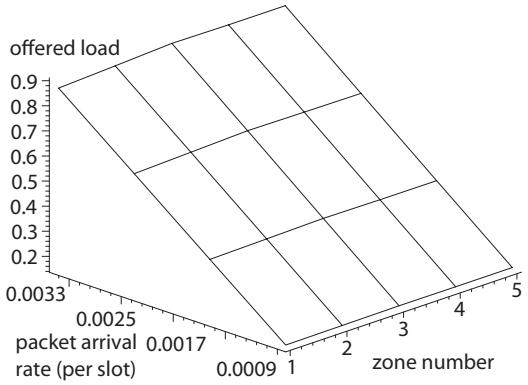

(a) Total offered load.

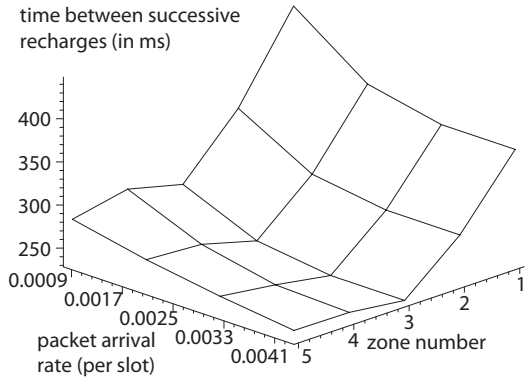

(b) Mean time between successive recharging pulses.

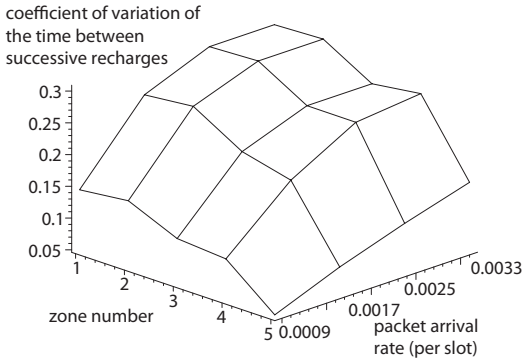

(c) Coefficient of variation of the time interval between successive recharging pulses.

Figure 6.5: Performance descriptors of the recharging process, network with $n_z = 5$ zones.

request recharge than a node in zone j may be calculated as

$$P(T_{rec,n} < T_{rec,j}) = \sum_{k=miny_j}^{maxy_j} P_{t(j,k)} \cdot \sum_{l=miny_n}^{k-1} P_{t(n,l)} \tag{6.31}$$

The final set of diagrams, Fig. 6.7 to 6.10, shows the mean, standard deviation, and coefficient of variation of packet delay. Delay is affected by the number of hops a packet has to pass before it reaches the master, which increases with the number of zones. However, packet delay is also extended by cycle and recharging vacations. As these last considerably longer than individual packet transmissions, mean packet delay does not differ much from

one zone to the next, as can be seen by comparing the diagrams in Figs. 6.7 to 6.10.

An unwanted consequence of the zoning approach is the reduced bandwidth due to the need that packets from all zones except zone 1 (the closest one) undergo several hops. In networks with more than two zones, the highest value of packet arrival rate (0.0041 packets per node per slot) leads to saturation and a drastic increase of packet delays, which is why the corresponding data points are not shown.

Standard deviation, as can be seen from the diagrams in Figs. 6.7 to 6.10, is rather close to the mean packet delay, but increases to higher values at high packet arrival rates. This increase is due to the fact that some packets are damaged and have to be retransmitted, as is the case with any packets that have arrived since the initial transmission of the damaged packet. As all packets must wait for the entire duration of the vacation period, even a small number of retransmissions increase both mean delay and its standard deviation.

This observation is further corroborated by the diagrams of the coefficient of variation of packet delay. In all cases, the coefficient of variation is well above one, which means that the actual distribution of packet delay values exhibits hyperexponential behavior.

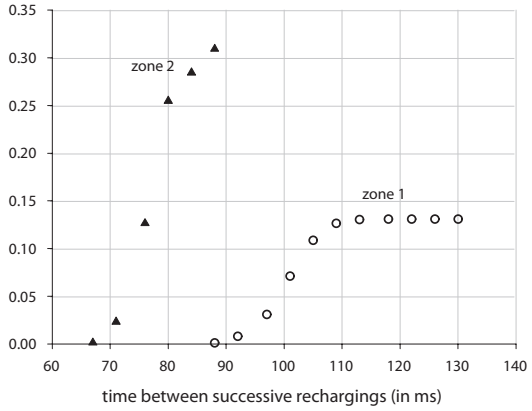

(a) Network with $n_z = 2$ zones, packet arrival rate $\lambda = 0.0009$ packets per node per slot.

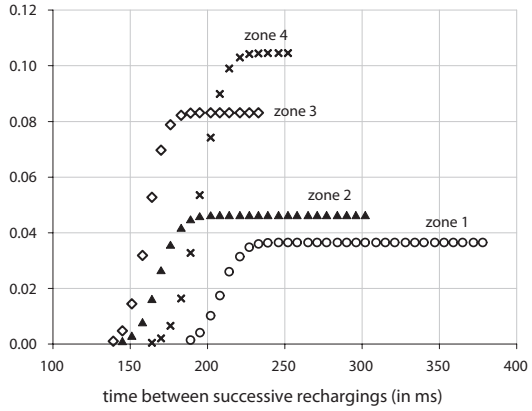

(b) Network with $n_z = 4$ zones, packet arrival rate $\lambda = 0.0009$ packets per node per slot.

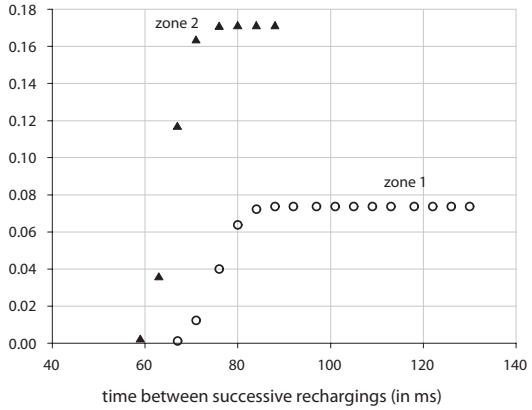

(c) Network with $n_z = 2$ zones, packet arrival rate $\lambda = 0.0025$ packets per node per slot.

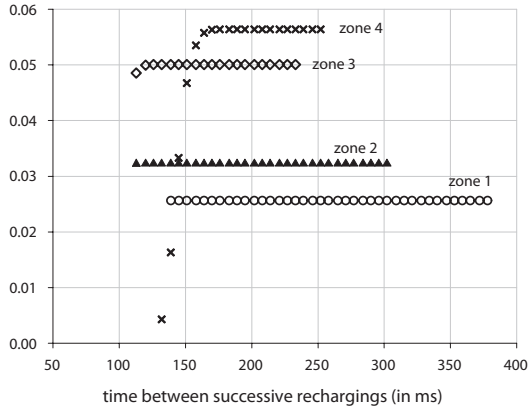

(d) Network with $n_z = 4$ zones, packet arrival rate $\lambda = 0.0025$ packets per node per slot.

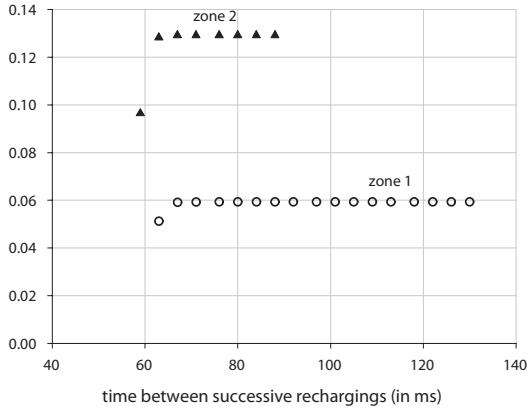

(e) Network with $n_z = 2$ zones, packet arrival rate $\lambda = 0.0041$ packets per node per slot.

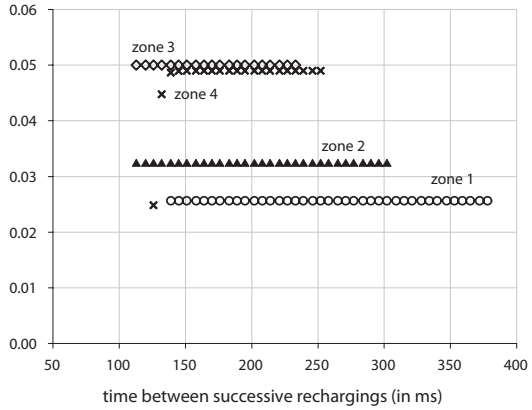

(f) Network with $n_z = 4$ zones, packet arrival rate $\lambda = 0.0033$ packets per node per slot.

Figure 6.6: Probability distribution of time interval between successive recharging pulses.

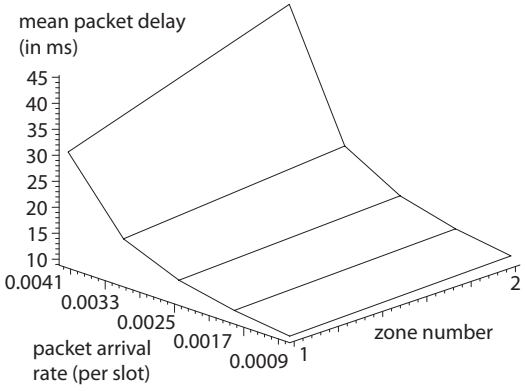

(a) Mean packet delay4.

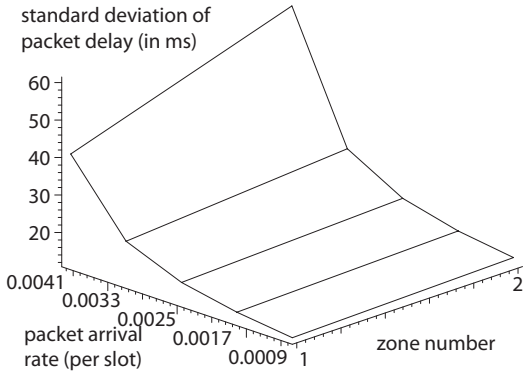

(b) Standard deviation of packet delay.

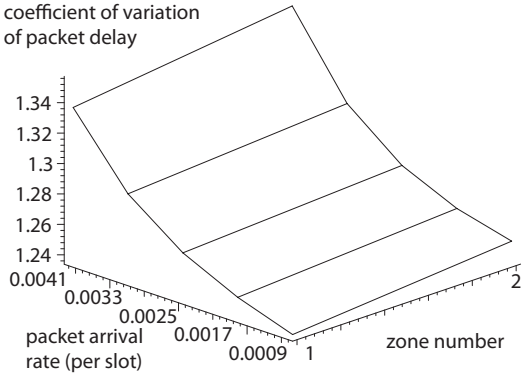

(c) Coefficient of variation of packet delay.

Figure 6.7: Performance of packet transmission, network with $n_z = 2$ zones.

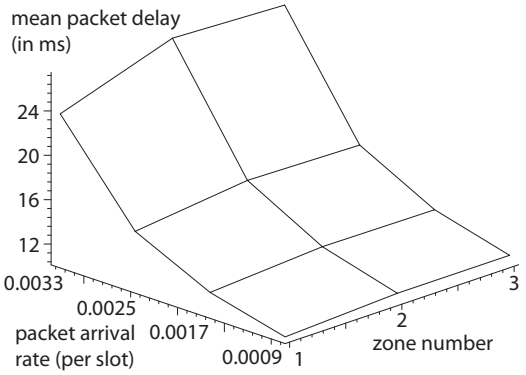

(a) Mean packet delay.

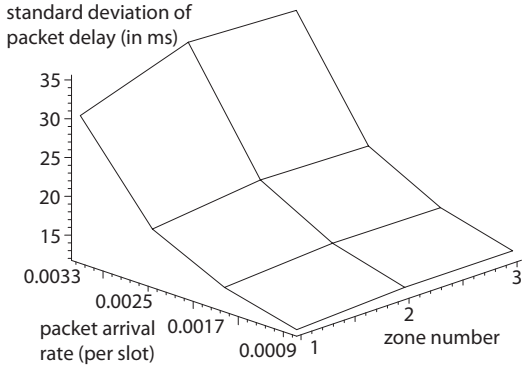

(b) Standard deviation of packet delay4.

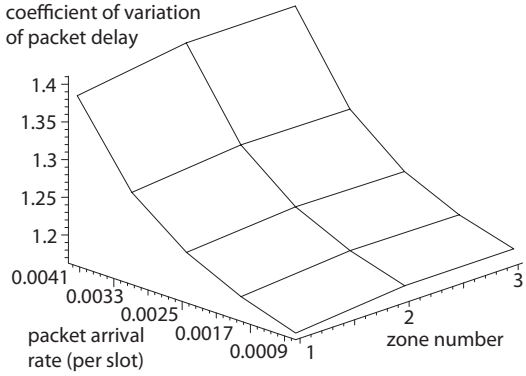

(c) Coefficient of variation of packet delay4.

Figure 6.8: Performance of packet transmission, network with $n_z = 5$ zones.

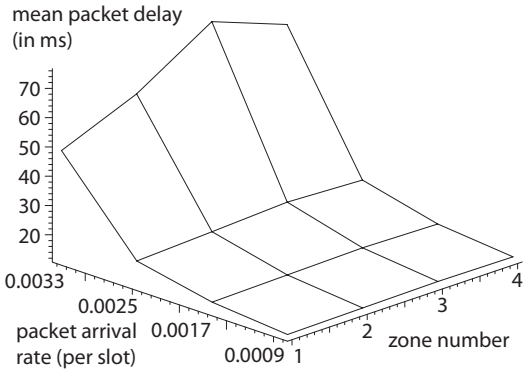

(a) Mean packet delay4.

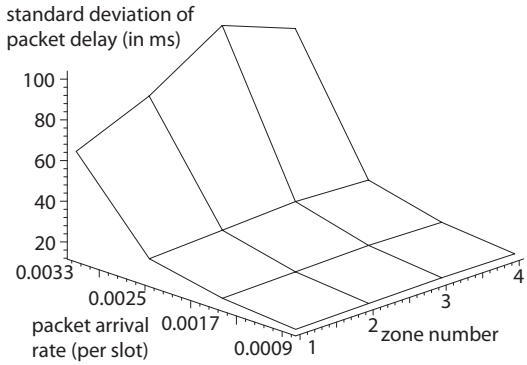

(b) Standard deviation of packet delay4.

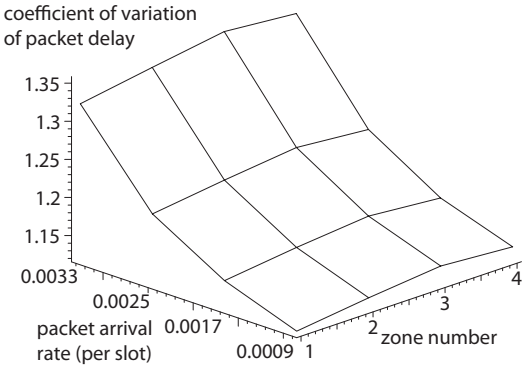

(c) Coefficient of variation of packet delay4.

Figure 6.9: Performance of packet transmission, network with $n_z = 4$ zones.

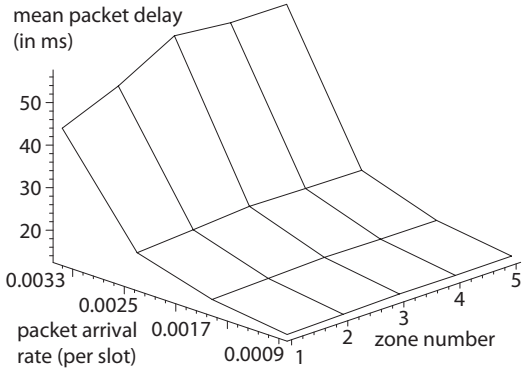

(a) Mean packet delay.

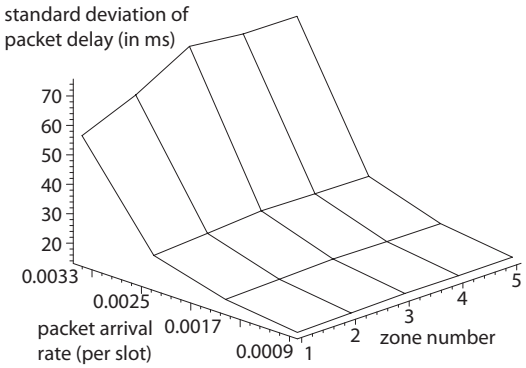

(b) Standard deviation of packet delay.

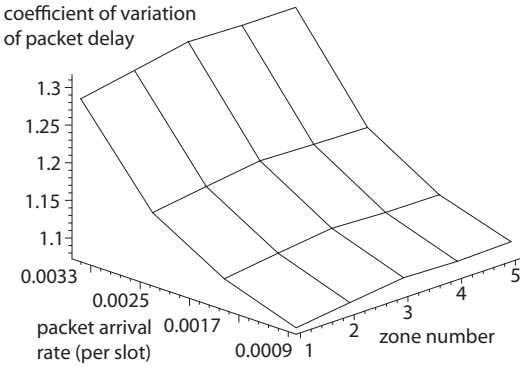

(c) Coefficient of variation of packet delay.

Figure 6.10: Performance of packet transmission, network with $n_z = 5$ zones.

Chapter 7

Optimum Zoning

In this chapter, we remove the assumption of different traffic volume and concentrate on the design of the relaying topology, with the goal of extending the time interval between successive recharge pulses. To this end, we propose a round robin, polling-based MAC protocol that uses 1-limited scheduling. The proposed protocol allows for efficient relaying with minimum overhead. We then try to find the optimum relaying topology that will extend the time interval between successive recharges as much as possible. The solution can be found by combinatorial analysis which is computationally infeasible in a sensor network, regardless of the computational capabilities of the master node. The extension of the recharge interval is achieved at the expense of the bandwidth available for data transfer. Then, we show that a computationally simpler approach which can be undertaken without interrupting the operation of the network is capable of extending the recharge interval without undue reduction in bandwidth.

The rest of the chaper is organized as follows. Section 7.1 introduces the polling MAC protocol, both the default single-zone version and the improved multi-zone one, while Section 7.2 presents energy expenditure incurred by both versions of this protocol. Section 7.3 presents the performance evaluation of the zoning approach. Finally, Section 7.4 presents the heuristic algorithm and its performance.

7.1 Zoning and the polling MAC protocol

We assume that the network consists of a master node equipped with an inexhaustible power supply, and a total of M sensor nodes powered by rechargeable power source. The sensors are randomly positioned in a circular area with the master node located at the center, as shown in Fig. 7.1. Each of the nodes senses the environmental variable of interest and attempts to send it to the master when polled. Sensing is performed at random or according to a predefined schedule; either way, sensing results are assumed to fit in a single packet.

While CSMA-CA schemes have been proposed for networks with RF recharging [5, 9], they suffer from a serious drawback. Namely, the node that is about to exhaust its energy reserve may not be able to ask for help due to a possible packet collision. Such nodes may even completely use up their energy and cease to operate, in which case network operation may be compromised. MAC protocols that use polling do not experience such problems, which is why we have chosen a polling-based MAC for our scheme.

In the default case, the master polls each node in sequence, from $i = 1$ to M, by sending suitably addressed POLL pulses in regular intervals, say t_p. When polled, the node responds with a single DATA packet, if there is sensing data to send, or a NULL packet, otherwise. The default configuration assumes a flat, single-zone structure in which each node sends its data directly to the master. In theory, the master could send a single POLL packet per polling cycle, and nodes could simply respond with their packets at predefined times afterwards. This would reduce the nodes' energy consumption since the number of packets they have to receive will be much reduced; again, nodes closer to the master would benefit more from this feature.

The flat structure described above leads to a large imbalance in power consumption between nearer and more distant nodes: while the latter will exhaust a large part of their energy reserve in each cycle, the former could well survive several cycles without recharging. As the result, recharge must be performed more often which introduces disruption in the data transmission schedule.

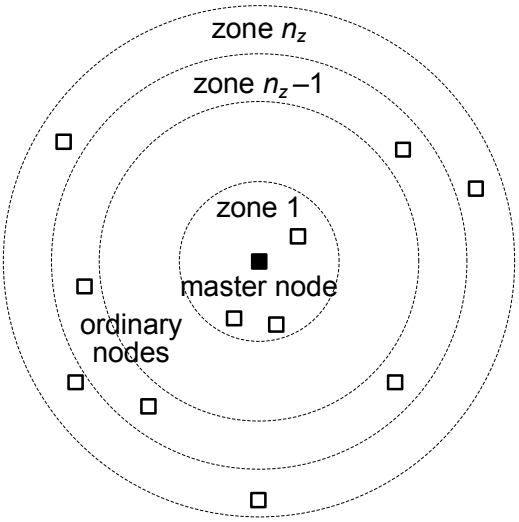

Figure 7.1: A wireless sensor network with rechargeable sensor nodes.

Zoning with relaying offers an attractive solution to this problem. In terms of topology, nodes are partitioned into a total of n_z circular zones centered at the master, as shown in Fig. 7.1. Zones may be of the same or different widths; the former solution was shown to offer better performance in [28], however they have considered an ideal case, rather than a specific topology. Partitioning is performed so that the zones are disjoint and include all nodes: $\sum_{i=1}^{n_z} m_i = M$. Nodes are logically divided into sectors, each of which is a tree rooted in one of the nodes in zone 1 that will ultimately deliver to the master packets from all the nodes in the sector.

In terms of scheduling, each node in zones $2..n_z$ simply delivers its packets to a suitable relay node in that same sector but in the next lower zone. If we label the nodes from 1 to M in descending order of distance to the master, this condition may be expressed in formal terms as the requirements that, for a source node s in zone $z = 2..n_z$, $\sum_{i=1}^{z-1} m_i < s < \sum_{i=1}^{z} m_i$, the corresponding relay node must be in zone $z-1$, i.e., $\sum_{i=1}^{z-2} m_i < r(s) < \sum_{i=1}^{z-1} m_i$.

In this setup, the master will send POLL packets sequentially to all nodes in zone 1. Upon hearing the POLL packet addressed to its sector nodes transmit their data sequen-

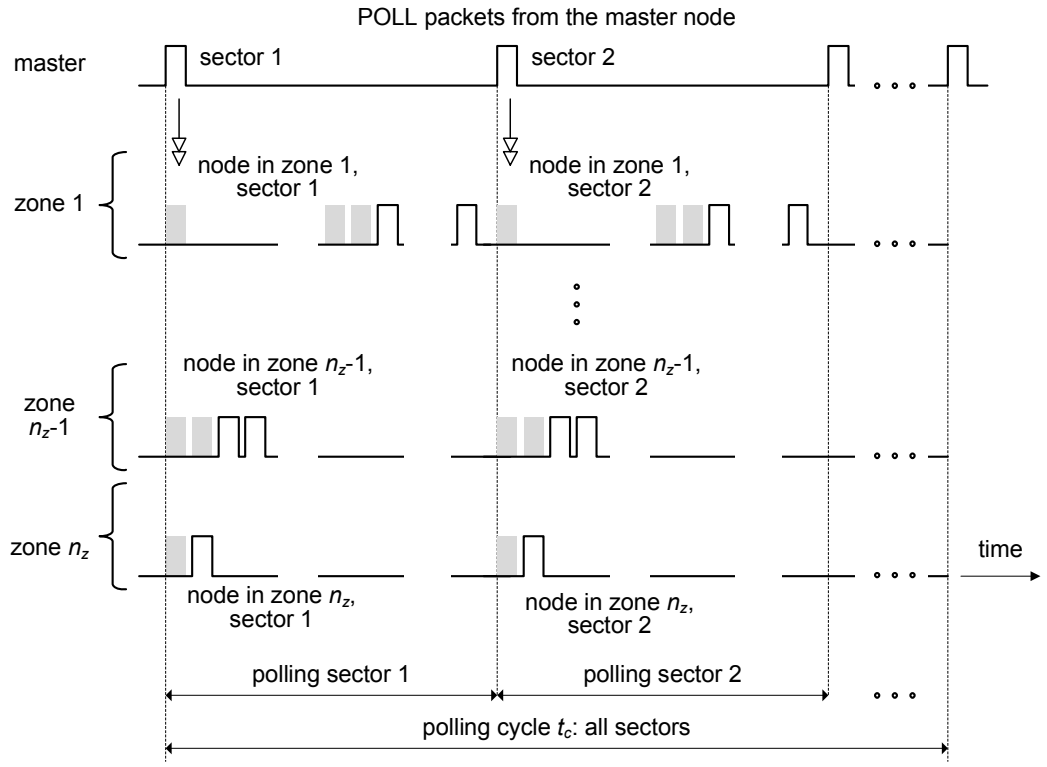

Figure 7.2: Polling-based MAC protocol.

tially, beginning with the node in the highest numbered zone. The designated relay receives that packet and re-sends it to its own relay before sending its own packet. The process continues until the node in the zone 1 sends all the relayed data, followed by its own data, to the master. The operation of the polling MAC is schematically shown in Fig. 7.2.

We note that packet transmission can be corrupted by noise and interference, which is why the master will acknowledge successfully received packets. To minimize the associated overhead, each successfully received data packet will be acknowledged through the POLL packet in the next polling cycle. If the acknowledgment is missing, the node will attempt packet transmission up to a certain number of times.

This scheme requires that each sector contains at least one node in every zone; however, a sector may contain more than one node in a given zone.

The duration of the polling cycle is, then,

$$\begin{aligned} T_c = &\quad m_1 T_{poll} + \sum_{i=1}^{M} h_i T_p \\ = &\quad m_1 T_{poll} + \sum_{j=1}^{n_z} j m_z T_p \end{aligned} \tag{7.1}$$

where T_{poll} and T_p are the durations of the POLL and DATA packets, respectively; m_i is the number of nodes in zone i; and h_i is the number of hops traversed by the packet sent from node i.

7.2 Energy expenditure

Nodes use energy to receive POLL packets from the master and DATA or NULL packets from other nodes, and (of course) to transmit packets, both own and relayed. Assuming that E_p, E_r, and E_t denote the energy expenditure for a receiving a single POLL packet, receiving a single data packet, and transmitting a single packet, respectively, the total energy expenditure of a node may be obtained as

$$E_i = m_1 E_p + n_R E_r + (n_R + 1) E_t \tag{7.2}$$

Nodes in the most distant zone n_z don't relay any packets so for them, the second component in the above expression is zero, $n_R = 0$.

More importantly, the energy needed by node i to transmit a packet depends on the distance $d_{i,j}$ to the recipient (i.e., relay node) j [4] as

$$E_t = \begin{cases} E_{t0} + E_{td} \left(\frac{d_{i,j}}{d_{max}} \right)^{\gamma}, & d_{i,j} \leq d_{max} \\ E_{t0} + E_{td}, & d_{i,j} > d_{max} \end{cases} \tag{7.3}$$

where γ is the path loss coefficient – 2 in free space, but as high as 4 or 5 in closed spaces [30].

All nodes begin with identical energy reserve E_{max}. When the energy level of the node drops below a predefined threshold E_{min}, the node will send its DATA or NULL packet with the HELP bit set, possibly using full power so that the master can receive it directly rather than through relaying.

Upon learning that recharge is needed, the master will announce the pending recharge in the next POLL packet, and then send a recharge pulse. Recharging occurs on the same RF frequency/band used for data communications. While this will temporarily disrupt regular communications, its hardware simplicity makes is preferable to the alternative in which separate RF bands are used [22, 27].

The energy increment received by node i through recharge can be calculated using the Friis' equation [6] as

$$\Delta E_i = t_r p_r \eta G_r G_t \left(\frac{\lambda_w}{4\pi d_i} \right)^{\gamma} \tag{7.4}$$

where t_r and P_r denote duration and power of the recharge pulse, respectively; η is the coefficient of efficiency of RF power conversion; G_r and G_t are the antenna gains at the receiver and transmitter, respectively; λ_w is the wavelength, and $d_i \gg \lambda_w$ is the distance to the master node.

It follows that recharge will be requested after the interval of

$$RI_x = \frac{\Delta_x}{E_x} \tag{7.5}$$

by the node x for which $d_x \geq d_i, i = 1 \,..\, N$. This time may also be expressed in polling cycles as $ri_x = \frac{\Delta_x}{E_x}/T_c$.

When recharge is requested, data communication is suspended for the duration of the recharge pulse. To minimize disruption, we might increase the power of the recharge pulse, which has its practical limits, or extend the duration of the recharge interval. Decreasing the recharge threshold is not a viable solution since it just increases the risk that the most distant node will completely exhaust its energy.

Performance of this approach can be evaluated using two main performance metrics:

first, the time interval between successive recharge requests, and second, the available bandwidth. For obvious reasons, both of these are crucially affected by the location of individual nodes, which we typically can't control, but also on the number of zones and the number of nodes in each zone, as well as the layout of the relay nodes, which can be controlled. As outlined above, reducing the distance to the next relay eases the burden for the source node but increases the number of packets that the relay node has to receive and subsequently re-send. At the same time, the relay node generally receives a larger energy increment with each recharge pulse due to it being closer to the master node. As the result, relaying may increase or decrease the recharge interval, depending on the actual distances and path losses.

A simple remedy for the problems above is to increase the power of the recharge pulse could improve the situation somewhat, but there are practical limits to this increase. A better solution is to increase the time interval between recharge pulses whilst making sure that all nodes, from the one closest to the master to the one farthest away, receive sufficient energy to continue operation. This solution is the focus of the work reported in this paper.

A better solution is to find the optimum number of zones and the optimum partitioning of nodes into disjoint zones $m_1, m_2, \ldots m_{nz}$, where $\sum_{i=1}^{n_z} m_i = M$, and the corresponding relay assignment. In this context, 'optimal' means 'maximum value of the shortest time interval between successive recharge requests.' Optionally, we may introduce the constraint that the resulting bandwidth does not drop below a predefined threshold; in the analysis that follows, we will just evaluate the resulting bandwidth.

7.3 Performance of the optimum solution

Optimal partitioning and relay assignment is obviously a combinatorial optimization problem which can be solved via exhaustive search. To investigate the range of improvements that can be obtained through zoning, we have performed the procedure of finding the best layout of zones and relays through extensive simulation. The network had 25 nodes

located at randomly chosen points (the distance and azimuth of each node location were chosen from a uniform distribution) in a circular field with 10 meter radius around the master node. Data for energy consumption of a node during receive and transmit operations were taken from the datasheets of a widely used Bluetooth LE chipset [2, 41]. We have then run an exhaustive search to find the optimum relay configuration in the setup with 2 to 6 zones. Each experiment was repeated 25 times for different randomly generated node topologies.

For simplicity, we have assumed that the network operates in saturation regime where each node has a packet to send in each polling cycle; the impact of packet errors is left as a topic for future work. We have assumed that the default layout in which all nodes communicate with the master directly uses one POLL packet per cycle, whereas multi-zone layouts use one POLL packet per sector. (Sectors correspond to nodes in zone one that communicate directly with the master.)

The performance results obtained in this setup are shown in Fig. 7.3; they can be summarized as follows. The zoning approach indeed leads in extension of the time interval between successive recharge requests, shown in Fig. 7.3(a). For the default single-zone scenario, the recharge is needed once every 37.3 polling cycles on the average, but only at every 56 and 61.9 polling cycles for 2 and 3 zones, respectively. Mean recharge interval is virtually stabilized at about 61.94 for the network with 4, 5, and 6 zones.

The polling cycle lengthens with the number of zones, as shown in Fig. 7.3(b). In the default case, the polling cycle takes 25.5 slots (one POLL packet and 25 DATA packets), but then increases nearly linearly to about 97.8 slots for zones 4 to 6.

As the result, the actual duration of the recharge interval expressed in slots increases considerably with the number of zones, as can be seen in Fig. 7.3(c) – from about 950 slots in the default single-zone scenario, to about 6057.6 slots in the scenarios with 4, 5, and 6 zones. Note that the actual duration of the recharge pulse is kept at the same value throughout. Therefore, increasing the number of zones leads to more efficient energy expenditure and makes recharge pulses less frequently needed; this may facilitate the construction of

the actual recharge pulse transmitter at the master node.

The price to be paid for zoning is the decrease in bandwidth: as each node is able to send only one data packet during a polling cycle, longer polling cycle means fewer data packets. The available bandwidth, shown in Fig. 7.3(d), drops from about 5056kBps in the default single-zone case to only about 1571kBps in the scenario with 4, 5, or 6 zones. Maximum number of hops also increases, as can be seen from Fig. 7.3(e), although its mean value increases slower than the number of zones which means that not all optimal solutions will actually use all possible zones. Consequently, packet delays also increase; the details are beyond the scope of this work.

For comparison purposes, the diagrams in Fig. 7.3 include a line (shown in red) corresponding to the minimum distance tree – the topology obtained by connecting each of the nodes to the nearest node closest to the master. The minimum distance tree has a fairly long recharge interval compared to one- and two zone solutions as well as to the heuristic solution. However, it also exhibits much higher maximum hop count and, consequently, much reduced bandwidth of only about 60% of the bandwidth of the optimal six-zone solution (982kBps vs. 1571kBps).

In practice, optimal partitioning and relay assignment would have to be performed by the master node. Master would need to learn about the location of each node, either accurately (in case nodes are equipped with GPS) or using a suitable approximate localization algorithm such as the one described in [18]. It would then perform the required search and then instruct the nodes about the relay assignment as well as about distance to the assigned relays so that they could adjust their transmission power.

The main obstacle to implementing this approach is, of course, the combinatorial explosion in the number of candidate topologies that need to be examined to find the optimal one. In the network of 25 nodes and up to 6 zones, the number of candidates rises very quickly, as can be seen in Fig. 7.4. Going through all of them for any number of zones beyond two or three is prohibitively expensive in terms of computation time, regardless of the actual computational capabilities of the master node. Furthermore, the actual node locations are

known only within a certain margin of error, which means that the optimum found in this manner may not be quite accurate. Therefore, a faster solution has to be found, but with as little performance deterioration as possible.

7.4 Heuristic algorithm

The key to such a solution can be found from the observation that the shortest recharge interval is often dictated by the nodes farthest away from the master. This is true by design in the single-zone solution, and generally (but not always) true in optimum solutions with two or more zones, as can be seen from Fig. 7.5. While these results are necessarily limited by the sample size of 25 topologies with 1 to 6 zones, they nevertheless provide good indication of the general trend.

The solution to our problem is, then, to focus on the most distant nodes, one by one, and gradually extend their lifetime until a solution of satisfactory performance is reached. This may be accomplished by the following heuristics.

1. In the beginning, the network operates in the default, flat single-zone mode. The master monitors network operation and performs recharge when requested.

2. After a certain number of recharge pulses, the master notes the critical node, i.e., the one which requests recharge most often, say N_1, and the node closest to it, say, N_{r1}. (Note that, in the first step, the critical node should be the most distant node in the network.) In the absence of noise and interference, a single polling cycle would suffice to establish the critical node in each round of the algorithm; in practice, several rounds may be needed.

3. The master then instructs the node N_1 to direct its packets to node N_{r1}, and instructs the latter to act as relay for the former.

4. The remaining nodes are instructed to adjust their transmission slots to accommodate

this change; this may be unnecessary if the relay node directly communicates with the master node.

5. The master continues to monitor the operation of the network. If the improvement in recharge interval is insufficient and the available bandwidth is above the required value, step 2 is repeated with the next critical node.

The important feature of the algorithm is that it can be applied without suspending normal operation of the network.

Performance of the heuristic algorithm described above, expressed through the same set of performance metrics as in the case of optimal zoning, is shown in Fig 7.6. The values were obtained from the same set of 25 randomly generated node topologies as above. In all the diagrams, the independent variable is the number of nodes re-connected through relays. For reference, we have added lines depicting the performance of default solution and optimal two zone solution, as found through exhaustive search.

The duration of the recharge interval expressed in polling cycles increases slowly with the number of re-connected nodes, as can be seen in Fig. 7.6(a). In fact, when only one or two most distant nodes are re-connected, recharge interval is even slightly smaller than in the default case. This is due to the variability of the random topologies used to obtain the results: the interval increases over the default value in some cases, but drops below them in others. However, the polling cycle increases, Fig. 7.6(b), hence the actual duration of the recharge expressed in slots increases, Fig. 7.6(c). The increase is gradual and tends to level off above 6 or 7 re-connected nodes.

At the same time, the available bandwidth of the heuristic solution is above that obtained with a two zone solution up to about five re-connected nodes, and its average is about the same or slightly lower than the value for the optimal two zone solution when more nodes are included in the process. Maximum number of hops also increases, but remains limited to about 4 or so which is comparable to the optimum solution.

Therefore, we can conclude that the proposed heuristic offers considerable improve-

ment in terms of extension of the time interval between successive recharges whilst achieving moderate reduction of available bandwidth. While these improvements do not seem like much, they are obtained at a much reduced cost, which was the original objective of the heuristic.

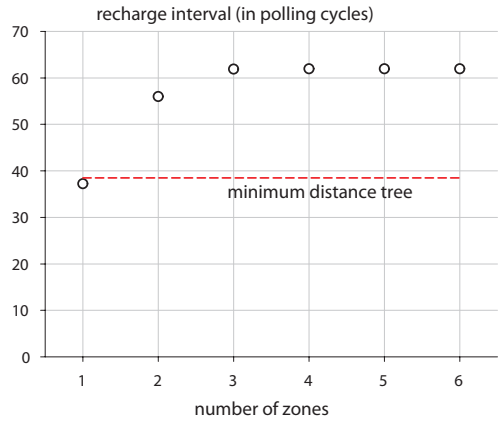

(a) Duration of recharge interval (in polling cycles).

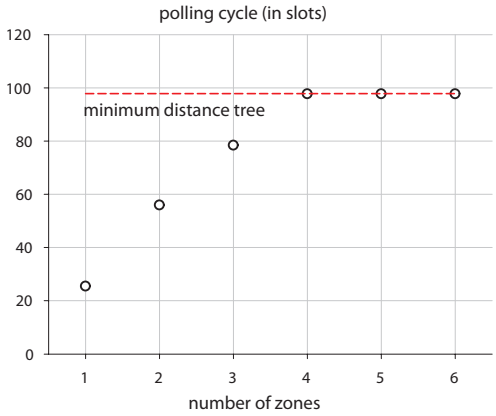

(b) Duration of polling cycle (in slots).

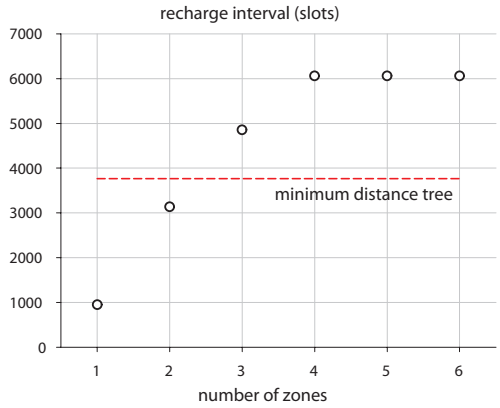

(c) Duration of recharge interval (in slots).

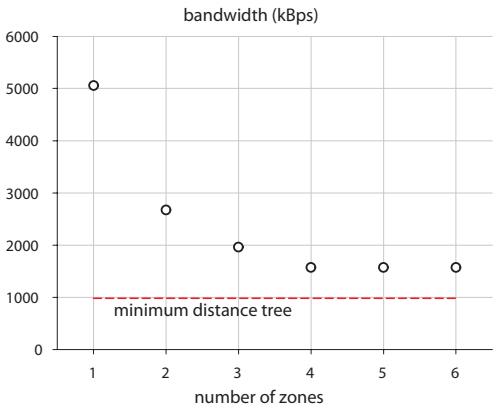

(d) Available bandwidth.

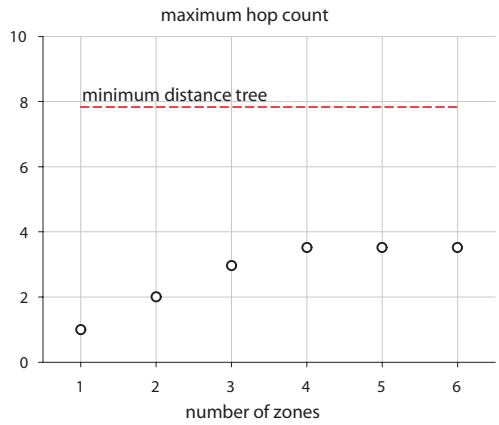

(e) Maximum number of hops.

Figure 7.3: Performance of optimum zoning approach vs. number of zones in the tree. All results obtained by averaging the results of 25 runs with different random topologies.

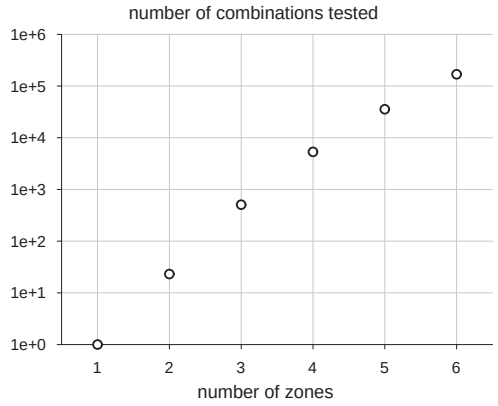

Figure 7.4: Number of topologies tested to find the optimum solution.

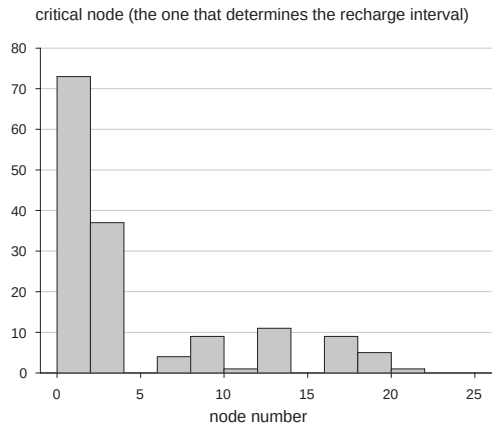

Figure 7.5: Number of times a particular node (value on the horizontal axis) shows up as the critical node (the one that determines the recharge interval) in the optimum solution (out of the total of $25 \times 6 = 150$).

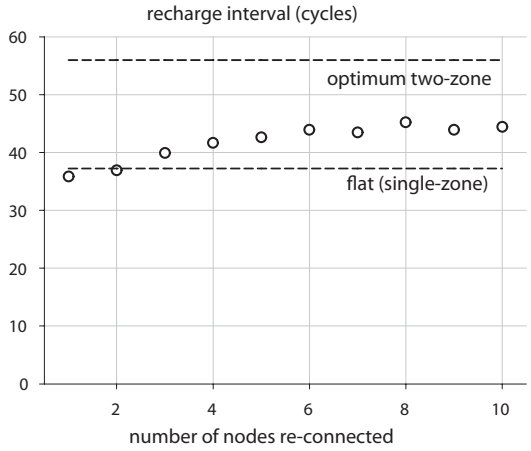

(a) Duration of recharge interval (in polling cycles).

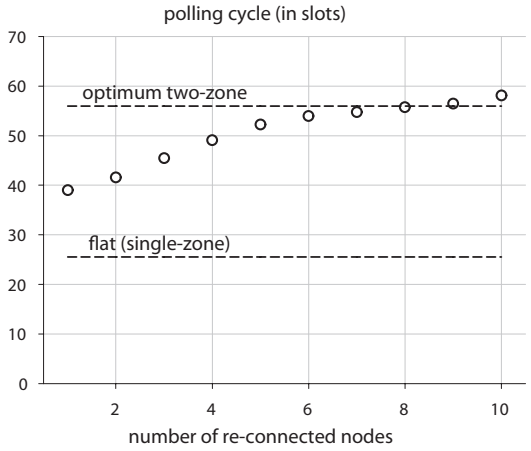

(b) Duration of polling cycle (in slots).

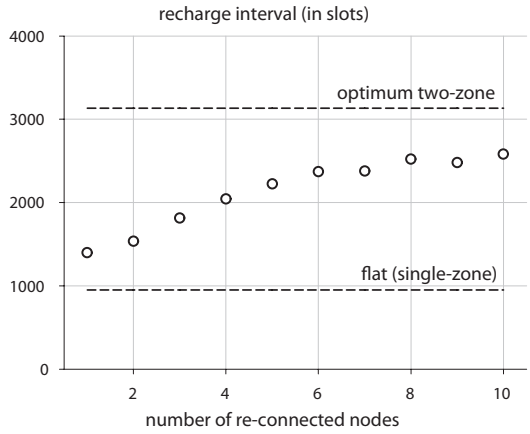

(c) Duration of recharge interval (in slots).

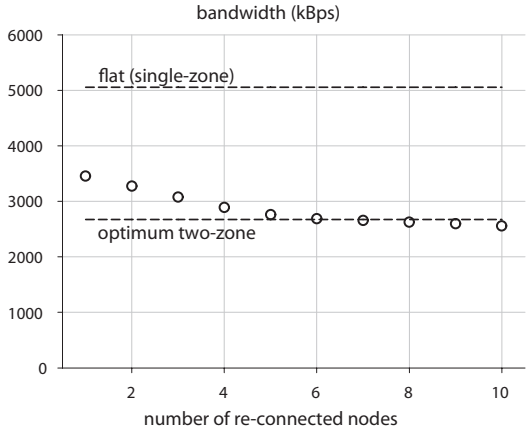

(d) Available bandwidth.

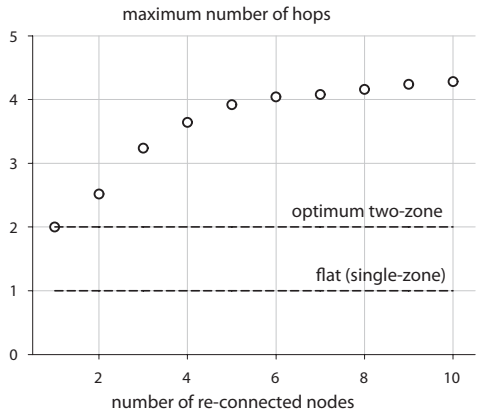

(e) Maximum number of hops.

Figure 7.6: Performance of optimum zoning approach.

Chapter 8

Conclusion

8.1 Conclusions

In this thesis we have analyzed the behavior and evaluated performance of a family of polling based MAC protocols that support in-band RF recharging in wireless sensor networks. We have investigated the interplay between recharging and performance of data communications, and proposed a number of techniques to extend the lifetime of such networks.

To evaluate the performance of such networks, we have developed a series of probabilistic models for cycle duration between two successive recharging events as well as queuing models for the node and packet waiting time. Our results indicate that network load and the parameters of recharging pulse have a major impact on the distribution of the waiting time of the packets, while the impact of noise and interference through bit error rate is of secondary importance. As the result, careful tuning of protocol parameters is required to achieve the desired performance levels and, in particular, to prevent longer access delays for data collected by the network.

Allowing nodes to send more than a single packet, which corresponds to non-gated E-limited service policy, has shown improvement in performance with respect to the default case in which each node can send only one packet at a time. Nonetheless, the basic behavior

of the network did not change much, and other means of extending the network lifetime have to be sought. Similar observations were made for the case where nodes can go to sleep, which does extend the network lifetime at the expense of complicated synchronization due to the fact that some nodes may miss the recharging pulse.

Further extension of network lifetime can be obtained through zoning with relaying, in which the network is partitioned into zones and sectors so that packets are forwarded within the sector to nodes that are closer to the master which acts as the network sink. This approach has been found to be capable of extending the recharging interval, as was the initial objective. At low traffic volume, recharging will be mainly determined by the nodes which are farthest away from the master (i.e., those in the highest numbered zone). As the traffic volume increases, variability of the recharging interval increases and nodes in closer zones may also generate recharging requests. At the same time, zoning tends to reduce the available bandwidth. In a network with more zones, high packet arrival rates are more likely to lead to saturation in which case packet delays increase and available bandwidth is drastically reduced. Therefore, the number of zones should be determined on the basis of desired throughput of sensed data (event sensing reliability), guided by the results of the analysis above.

We have also discussed the problem of relay assignment which can improve the performance of wireless sensor networks with RF recharging of node batteries. While the optimum partitioning requires exhaustive search which is computationally infeasible, an efficient heuristic was shown to offer comparable performance without the need for accurate localization of sensor nodes.

8.2 Future work

Our future work will focus on fine tuning of network parameters to optimize performance, in particular the choice of network parameters like recharging durations and power intensity values to find the values that lead to lowest packet waiting times and minimal

per bit power consumption in transferring data. We will also investigate the possibility of reducing the number of POLL packets in order to reduce the power consumption of the network, as well as the modifications to the MAC protocol that will improve the network lifetime through individual and/or joint scheduling of node transmissions. This approach appears promising in particular if packet arrival rates at individual nodes differ from one node to another.

A promising avenue for further research is the search for optimum characteristics of the recharging process and the possibility of extending the time interval between recharging pulses.

Finally, the zoning approach can be augmented by the optimization of the number of zones, in particular in cases where the spatial distribution of nodes is non-uniform, and further refinements of the MAC protocol. Our future work will focus on refining the heuristic as well as on investigating packet delays and the impact of varying traffic load on the performance of the proposed scheme.

My published papers related to this thesis

Journal papers

1. M. S. I. Khan, J. Mišić, and V. B. Mišić. "Zoning and relaying-based MAC protocol with RF recharging", *IEEE Transactions on Vehicular Technology*, 2016.

2. M. S. I. Khan, J. Mišić, and V. B. Mišić. "Performance of the MAC Protocol in Wireless Recharging under E-limited Scheduling", *Computer Communications* **73**(Part A):157-164, January 2016.

3. M. S. I. Khan, J. Mišić, and V. B. Mišić. "Modeling of RF recharging in a wireless sensor network with coordinated node sleep", *Journal of Communications* **10**(9):707–714, September 2015.

4. M. S. I. Khan, J. Mišić, and V. B. Mišić. "Impact of network load on the performance of a polling MAC with wireless recharging of nodes", *IEEE Transactions on Emerging Topics in Computing* **3**(3):307–316, September 2015.

5. V. B. Mišić, M. S. I. Khan, Md. M. Rahman, H. Khojasteh, and J. Mišić. "Simple Solutions May Still Be Best: On the Selection of Working Channels in a Channel-Hopping Cognitive Network", *Wireless Communications and Mobile Computing* **15**(6):1026-1036, April 2015.

Conference papers

1. J. Mišić, M. S. I. Khan, and V. B. Mišić. "Recharge interval and packet delay in wireless sensor network with RF recharging", *GlobeCom 2016*, Washington, DC, December 2016.

2. V. B. Mišić, J. Mišić, and M. S. I. Khan. "Optimum Zoning in RF-Recharged Sensor Networks", *Vehicular Technology Conference VTC-Fall 2016*, Montreal, QC, September 2016.

3. M. S. I. Khan, J. Mišić, and V. B. Mišić. "Zoning based MAC with support for recharging process in WSN", *IEEE GlobeCom 2015*, San Diego, CA, December 2015.

4. M. S. I. Khan, J. Mišić, and V. B. Mišić. "A Polling MAC with Reliable RF Recharging of Sensor Nodes", *2015 IEEE Wireless Communications and Networking Conference (WCNC)*, New Orleans, LA, March 2015.

5. M. S. I. Khan, J. Mišić, and V. B. Mišić. "MAC protocol for wireless sensor networks with on-demand RF recharging of sensor nodes", *2015 International Conference on Computing, Networking and Communications* (Invited Position Paper), Anaheim, CA, February 2015.

6. J. Mišić, M. S. I. Khan, and V. B. Mišić. "Performance of simple polling MAC with wireless re-charging in the presence of noise", *The 17th ACM Int. Conf. on Modeling, Analysis and Simulation of Wireless and Mobile Systems (MSWiM'14)*, Montreal, QC, Canada, September 2014.

Bibliography

[1] F. Barreras and O. Jimenez, "RF coupled, implantable medical device with rechargeable back-up power source," Mar. 31 1998, uS Patent 5,733,313. [Online]. Available: http://www.google.com/patents/US5733313

[2] B. Blum, "Bluetooth low energy, A Very Low Power Solution," Texas Instruments, Inc., Dallas, TX, Tech. Rep., 2012.

[3] A. Capone, R. Kapoor, and M. Gerla, "Efficient polling schemes for Bluetooth picocells," in *Proceedings of IEEE International Conference on Communications ICC 2001*, vol. 7, Helsinki, Finland, Jun. 2001, pp. 1990–1994.

[4] J. Deng, Y. S. Han, P.-N. Chen, and P. K. Varshney, "Optimal transmission range for wireless ad hoc networks based on energy efficiency," *IEEE Transactions on Communications*, vol. 55, no. 7, pp. 1439–1439, 2007.

[5] Z. A. Eu, H.-P. Tan, and W. K. Seah, "Design and performance analysis of MAC schemes for wireless sensor networks powered by ambient energy harvesting," *Ad Hoc Networks*, vol. 9, no. 3, pp. 300–323, May 2011.

[6] H. T. Friis, "A note on a simple transmission formula," *Proc. IRE*, vol. 34, no. 5, pp. 254–256, 1946.

[7] M. Gorlatova, A. Wallwater, and G. Zussman, "Networking low-power energy har-

vesting devices: Measurements and algorithms," *IEEE Transactions on Mobile Computing*, vol. 12, no. 9, pp. 1853–1865, 2013.

[8] C. K. Ho and R. Zhang, "Optimal energy allocation for wireless communications with energy harvesting constraints," *IEEE Transactions on Signal Processing*, vol. 60, no. 9, pp. 4808–4818, 2012.

[9] F. Iannello, O. Simeone, and U. Spagnolini, "Medium access control protocols for wireless sensor networks with energy harvesting," *IEEE Transactions on Communications*, vol. 60, no. 5, pp. 1381–1389, 2012.

[10] N. Jain, S. Das, and A. Nasipuri, "A multichannel CSMA MAC protocol with receiver-based channel selection for multihop wireless networks," in *Computer Communications and Networks, 2001. Proceedings. Tenth International Conference on*, 2001, pp. 432–439.

[11] V. Joseph, V. Sharma, and U. Mukherji, "Optimal sleep-wake policies for an energy harvesting sensor node," in *IEEE. Int. Conf. Communications (ICC 2009)*, Dresden, Germany, 2009, pp. 1–6.

[12] A. Kansal and M. B. Srivastava, "An environmental energy harvesting framework for sensor networks," in *Int. Symp. Low Power Electronics and Design (ISLPED 2003)*, 2003, pp. 481–486.

[13] M. S. I. Khan, J. Mišić, and V. B. Mišić, "Impact of network load on the performance of a polling MAC with wireless recharging of nodes," *Emerging Topics in Computing, IEEE Transactions on*, vol. 3, no. 3, pp. 307–316, Sep. 2015.

[14] V. Kumar, S. Jain, and S. Tiwari, "Energy efficient clustering algorithms in wireless sensor networks: A survey," *IJCSI International Journal of Computer Science Issues*, vol. 8, no. 5, 2011.

[15] J. Lei, R. Yates, and L. Greenstein, "A generic model for optimizing single-hop transmission policy of replenishable sensors," *IEEE Transactions on Wireless Communications*, vol. 8, no. 2, pp. 547–551, 2009.

[16] H. Levy and M. Sidi, "Polling systems: applications, modeling, and optimization," *Communications, IEEE Transactions on*, vol. 38, no. 10, pp. 1750–1760, Oct 1990.

[17] H. Levy, M. Sidi, and O. J. Boxma, "Dominance relations in polling systems," *Queueing Systems Theory and Applications*, vol. 6, no. 2, pp. 155–171, 1990.

[18] C. Liu, K. Wu, and T. He, "Sensor localization with ring overlapping based on comparison of received signal strength indicator," in *IEEE Int. Conf. Mobile Ad-hoc and Sensor Systems (MASS 2004)*, Fort Lauderdale, FL, 2004, pp. 516–518.

[19] Maplesoft, Inc., *Maple 16*, Waterloo, ON, Canada, 2013.

[20] J. Mišić and V. B. Mišić, *Performance Modeling and Analysis of Bluetooth Networks: Network Formation, Polling, Scheduling, and Traffic Control*. Boca Raton, FL: CRC Press, Jul. 2005.

[21] J. Mišić, S. Shafi, and V. B. Mišić, "Maintaining reliability through activity management in an 802.15.4 sensor cluster," vol. 55, no. 3, pp. 779–788, May 2006.

[22] V. B. Mišić and J. Mišić, "A polling MAC for wireless sensor networks with rf recharging of sensor nodes," in *27th Queen's Biennial Symposium on Communications*, Kingston, ON, Canada, 2014.

[23] J. Mišić, M. S. Khan, and V. B. Mišić, "Performance of simple polling mac with wireless re-charging in the presence of noise," in *Proceedings of the 17th ACM international conference on Modeling, analysis and simulation of wireless and mobile systems*. ACM, 2014, pp. 137–143.

[24] M. Naderi, P. Nintanavongsa, and K. Chowdhury, "RF-MAC: A medium access control protocol for re-chargeable sensor networks powered by wireless energy harvesting," *Wireless Communications, IEEE Transactions on*, vol. PP, no. 99, pp. 1–1, 2014.

[25] M. Y. Naderi, K. R. Chowdhury, S. Basagni, W. Heinzelman, S. De, and S. Jana, "Experimental study of concurrent data and wireless energy transfer for sensor networks," in *Proceedings of IEEE GLOBECOM*, 2014.

[26] P. Nintanavongsa, M. Y. Naderi, and K. R. Chowdhury, "Medium access control protocol design for sensors powered by wireless energy transfer," in *IEEE INFOCOM*, Apr. 2013, pp. 150–154.

[27] P. Nintanavongsa, M. Y. Naderi, and K. R. Chowdhury, "A dual-band wireless energy transfer protocol for heterogeneous sensor networks powered by RF energy harvesting," in *Int. Comp. Sci. Eng. Conf. (ICSEC 2013)*, Sep. 2013, pp. 387–392.

[28] S. Olariu and I. Stojmenović, "Design guidelines for maximizing lifetime and avoiding energy holes in sensor networks with uniform distribution and uniform reporting," in *Proc. INFOCOM*, Barcelona, Spain, 2006, pp. 1–12.

[29] J.-D. Park, H. Lee, and M. Bond, "Uninterrupted thermoelectric energy harvesting using temperature-sensor-based maximum power point tracking system," *Energy Conversion and Management*, vol. 86, pp. 233–240, 2014.

[30] T. S. Rappaport, *Wireless Communications: Principles and Practice*. Prentice Hall PTR, 1996.

[31] I. Stojmenović, *Handbook of sensor networks: algorithms and architectures*. John Wiley & Sons, 2005.

[32] H. Takagi, "Queuing analysis of polling models," *ACM Computing Surveys (CSUR)*, vol. 20, no. 1, pp. 5–28, 1988.

[33] H. Takagi, *Queueing Analysis*. Amsterdam, The Netherlands: North-Holland, 1991, vol. 1: Vacation and Priority Systems.

[34] H. Takagi, *Queueing Analysis*. Amsterdam, The Netherlands: North-Holland, 1993, vol. 2: Finite Systems.

[35] L. Xie, Y. Shi, Y. T. Hou, W. Lou, H. D. Sherali, and S. F. Midkiff, "On renewable sensor networks with wireless energy transfer: The multi-node case," in *9th Ann. IEEE Comm. Soc. Conf. Sensor, Mesh and Ad Hoc Communications and Networks (SECON 2012)*, Seoul, Korea, 2012, pp. 10–18.

[36] L. Xie, Y. Shi, Y. T. Hou, and H. D. Sherali, "Making sensor networks immortal: An energy-renewal approach with wireless power transfer," *IEEE/ACM Transactions on Networking*, vol. 20, no. 6, pp. 1748–1761, Dec. 2012.

[37] L. Xie, Y. Shi, Y. T. Hou, and A. Lou, "Wireless power transfer and applications to sensor networks," *IEEE Wireless Communications*, vol. 20, no. 4, pp. 140–145, 2013.

[38] W. Ye, J. Heidemann, and D. Estrin, "An energy-efficient mac protocol for wireless sensor networks," in *INFOCOM 2002. Twenty-First Annual Joint Conference of the IEEE Computer and Communications Societies. Proceedings. IEEE*, vol. 3, 2002, pp. 1567–1576 vol.3.

[39] W. Yue, Q. Sun, and S. Jin, "Performance analysis of sensor nodes in a wsn with sleep/wakeup protocol," in *Proc. Int. Symp. Operations Research and its Applications, Chengdu-Jiuzhaigou, China*, 2010, pp. 370–377.

[40] A. Willig, "Polling-based mac protocols for improving real-time performance in a wireless profibus," *Industrial Electronics, IEEE Transactions on*, vol. 50, no. 4, pp. 806–817, Aug 2003.

[41] "Measuring Bluetooth(r) Low Energy Power Consumption, Application Note AN092," Texas Instruments, Inc., Dallas, TX, Tech. Rep., 2012.